Response of a Parametrically-Excited System to a Nonstationary Excitation

by

Harold Lewis Neal, Jr.

Thesis submitted to the Faculty of the

Virginia Polytechnic Institute and State University

in partial fulfillment of the requirements for the degree of

Master of Science

in

Engineering Mechanics

APPROVED:

Ali H. Nayfeh

Dr. A. H. Nayfeh, Chairman

Dean T. Mook

Dr. D. T. Mook

L. Glenn Kraige

Dr. L. G. Kraige

December, 1992

Blacksburg, Virginia

C.2

Response of a Parametrically-Excited System to a Nonstationary Excitation

by

Harold Lewis Neal, Jr.

Dr. A. H. Nayfeh, Chairman

Engineering Science and Mechanics

(ABSTRACT)

The response of a parametrically-excited system to a deterministic nonstationary excitation is studied. The system, which has a cubic nonlinearity, has one focus and two saddle points and can be used as a simple model of a ship in head or follower seas. The method of multiple scales is applied to the governing equation to derive equations for the amplitude and phase of the response. These equations are used to find the stationary response of the system to stationary excitation. The stability of the stationary response is examined. The stability of stationary periodic solutions to the original governing equation is examined through a Floquet analysis. The response to a nonstationary excitation having (a) a frequency that varies linearly with time, or (b) an amplitude that varies linearly with time, is studied. The response is computed from digital computer integration of the equations found from the method of multiple scales and of the original governing equation. The response to nonstationary excitation has several unique characteristics, including penetration, jump-up, oscillation, and convergence to the stationary solution. The agreement between solutions found from the original governing

equation and the method-of-multiple-scales equations is good. For some sweeps of the excitation frequency or amplitude, the response to nonstationary excitation found from the original governing equation exhibits behavior which is analogous to symmetry-breaking bifurcations, period-doubling bifurcations, chaos, and unboundedness in the stationary solution. The maximum response amplitude and the excitation frequency or amplitude at which the response goes unbounded is found as a function of sweep rate. The effect of initial conditions and noise on the response to nonstationary excitation is considered. The results of the digital-computer simulations are verified with an analog computer.

Acknowledgements

I wish to thank my advisor, Dr. Ali H. Nayfeh, for his guidance, support, and unending patience both during the preparation of this work and throughout my college career.

I would also like to thank my committee members, Dr. Dean T. Mook and Dr. L. Glenn Kraige, for their encouragement and advice during my years here.

I would like to thank my parents, Harold and Loretta Neal, for instilling in me the desire for an education and for their support, advice, and love, and especially for sticking with me through the last few years.

I would like to thank the many graduate students, both past and present, that I have worked with for their camaraderie and help. Special thanks goes to Sally Shrader, who has saved me countless times by knowing what I needed to get things done and helping make it so.

Finally, I would like to thank my friends, Daryl, Anne, Jen, and especially James for their encouragement and help, and for the good times which made the burdens a little easier to bear.

This work was made possible by a Fellowship provided by the Office of Naval Research and administered by the American Society of Engineering Education.

Table of Contents

List of Figures

CHAPTER 1

Introduction

Many physical systems are *nonstationary*, which means they have components that vary with time (Evan-Iwanowski, 1969). For instance, such systems could have masses or damping forces that are time-dependent. Other types of nonstationary systems have time-dependent excitation amplitude or frequency. This type of excitation might occur, for example, when a motor is started up or shut down (Nayfeh and Asfar, 1988). One specific class of such systems has an excitation frequency or amplitude that varies linearly with time. In this thesis, we study this type of system.

Lewis (1932) performed one of the first investigations of nonstationary phenomena. He studied the case of an unbalanced linear rotor that was uniformly accelerated through its critical speed. Baker (1939) considered a similar nonstationary rotor problem, but also considered constant deceleration. Howitt (1961) produced simplified conclusions to the problem through

approximation. Extending the problem, Qazi and McFarlane (1967) controlled the passage through resonance using a feedback control system. Ishida, et. al. (1987, 1989) examined the maximum response amplitude and unboundedness of a nonlinear rotor passing through a critical speed.

Several researchers have considered the nonstationary behavior of other systems. Collinge and Ockendon (1979) considered the Duffing oscillator with slowly varying forcing frequency. Moslehy and Evan-Iwanowski (1991) considered linear variations of the frequency and amplitude as well as sinusoidal variations of the frequency for the Duffing oscillator. Hok (1948) used Laplace transforms to consider a linear system with linearly varying amplitude. McCann and Bennett (1949) used analog computers to examine a two-dimensional linear system with linearly varying frequency. Kevorkian (1971) used the method of matched asymptotic expansions to analyze passage through resonance for a system that had constant forcing frequency but slowly varying natural frequency. Arya, Bojadziev, and Farooqui (1975) used the method of averaging to study the van der Pol oscillator. Davies and Nandall (1990) also studied the van der Pol oscillator, but they used the method of multiple scales. Agrawal and Evan-Iwanowski (1973) used the method of averaging to study a gyroscopic system with varying frequency. Evan-Iwanowski (1969) provided an overview of the literature (especially the Russian literature) for many more nonstationary problems. Nayfeh and Mook (1979) also provided references to the literature of nonstationary problems.

We consider nonstationary excitation of a parametrically excited system. In a *parametrically excited system*, the excitation appears as a coefficient in the governing equations and boundary conditions (Nayfeh and Mook, 1979). For instance, ship motion is often parametrically excited (Sanchez and Nayfeh, 1990). A common model of a parametrically excited system is a slender beam excited parallel to its long axis and carrying a concentrated mass (Zavodney and Nayfeh, 1989). Parametrically excited systems pose special problems because they can have large responses to small excitations. The trivial solution always exists for these systems, although it is not always stable. Linear analysis of a parametrically excited system predicts that the stationary (steady-state) response is trivial below a critical value of the excitation amplitude, and that the response grows exponentially above this critical value. Exponential growth is unrealistic because all physical systems have inherent nonlinearities that will limit the response. Nonlinearities may result from (a) a system's geometry, such as large curvatures or rotations of structural elements; (b) a system's inertia, because of concentrated and distributed masses; and (c) material behavior, including nonlinear stress-strain relations, and friction effects, such as dry friction. Although nonlinearities are sometimes ignored in small-amplitude analysis, nonlinearities must be included to predict such behaviors as multiple solutions, chaotic motions, and subharmonic and superharmonic resonances (Nayfeh and Mook, 1979).

Specifically, we consider a simple one-degree-of-freedom parametrically

excited system governed by

$$\ddot{u}+2\bar{\mu}\dot{u}+\left(1-\bar{f}\cos\phi t\right)u-\bar{\alpha}u^3=0 \tag{1.1}$$

Here, $\bar{\mu}$ is the coefficient of damping, $\bar{f}$ is the excitation amplitude, and $\bar{\alpha}$ is the coefficient of cubic nonlinearity. When $\bar{\alpha}$ is negative, the nonlinearity is called a hardening nonlinearity, and when it is positive, the nonlinearity is called a softening nonlinearity. The variables have been non-dimensionalized so that the natural frequency of this system is one. This system is indeed parametrically excited because the time-varying excitation term $\bar{f}\cos\phi t$ appears as a coefficient of u. The frequency of excitation is ϕ.

Nonstationary excitation is introduced into the problem in two ways. First, we consider a nonstationary excitation in which the excitation frequency is a linear function of time. This condition is expressed by

$$\phi=\phi_0+\bar{r}t \tag{1.2}$$

Here, $\bar{r}$ is called the *sweep rate* and ϕ_0 is the initial frequency.

We will also consider a nonstationary excitation in which the excitation amplitude is a linear function of time. This condition is expressed by

$$f=f_0+\bar{s}t \tag{1.3}$$

Here, $\bar{s}$ is the sweep rate and $\bar{f}_0$ is the initial excitation amplitude.

Sweeps of the excitation frequency with this system have been considered previously by Neal and Nayfeh (1990) for the case of hardening nonlinearity ($\bar{\alpha} < 0$). The present work is unique in that we will consider

softening nonlinearity ($\bar{\alpha} > 0$). The case of softening nonlinearity is more interesting because the system is more robust—we encounter response behaviors such as symmetry-breaking bifurcations, period-doubling bifurcations, chaotic solutions, and unboundedness, which were not encountered in the previous work.

In this thesis, we seek to identify the characteristics of the nonstationary response to both frequency sweeps and amplitude sweeps. These characteristics will allow us to identify the differences between the response to stationary excitation and the response to nonstationary excitation. We will examine how the sweep rate and the initial conditions affect (a) the nonstationary response characteristics, (b) the maximum response of the system, and (c) the onset of unboundedness in the response. To examine the response to nonstationary excitation, we will use both digital and analog computers.

In order to understand the response to nonstationary excitation, we first need to understand the response to stationary excitation. Thus, in Chapter 2, we perform a method-of-multiple-scales analysis to find perturbation equations for the amplitude and phase of the response. We use the perturbation equations to find the stationary response of the system to stationary excitation. We perform a stability analysis on the solutions found from the perturbation equations, and we perform a Floquet analysis to determine the stability of stationary solutions of the original governing equation.

In Chapter 3, we consider sweeps of the excitation frequency. We use digital computer simulations of both the perturbation equations and the original governing equation.

In Chapter 4, we consider sweeps of the excitation amplitude. Again, we use digital computer simulations of both the perturbation equations and the original governing equation.

In Chapter 5, we use analog computer simulations to verify the results of the digital computer simulations for both frequency and amplitude sweeps. We also will consider the effect of the nonstationary response after a sweep has ended and the excitation becomes stationary.

In Chapter 6, we present our conclusions.

CHAPTER 2

Stationary Solutions

In order to understand the response to nonstationary excitation, we must first find the stationary response to stationary excitation. To find the stationary response, we will apply the method of multiple scales to the governing equation (1.1).

2.1 Method of Multiple Scales

We use the method of multiple scales (Nayfeh, 1973, 1981) to analyze our system. To motivate the use of this technique, we note that, in many physical systems, changes in the response of the system can be characterized in terms of many time scales. For instance, consider a simple linear oscillator with small damping μ governed by

$$\ddot{x}+2\mu\dot{x}+x=0 \tag{2.1}$$

A general solution to (2.1) can be expressed as

$$x=ae^{-\mu t}\cos\left(\sqrt{1-\mu^2}\,t+\beta\right) \tag{2.2}$$

where a and β are constants. Using the binomial theorem to approximate the radical for small μ, we have

$$\sqrt{1-\mu^2}\approx 1-\frac{1}{2}\mu^2 \tag{2.3}$$

Then, the solution (2.2) could be approximated by

$$x=\bar{a}(\mu t)\cos\left[t+\bar{\beta}(\mu^2 t)\right] \tag{2.4}$$

where

$$\bar{a}(\mu t)=ae^{-\mu t} \tag{2.5}$$

$$\bar{\beta}(\mu^2 t)=\beta-\frac{1}{2}\mu^2 t \tag{2.6}$$

Note that this solution contains three time scales. The oscillation itself varies on the time scale t. Changes in the amplitude $\bar{a}$ occur on the slow time scale μt. And the phase of the solution $\bar{\beta}$ (relative to an undamped oscillator) changes on an even slower time scale, $\mu^2 t$.

Since we also expect the solution of (1.1) to involve many time scales, we formulate them into the solution of the problem. To use the method of multiple time scales, we introduce a small dimensionless parameter ϵ, which is much less than one and is used as a bookkeeping device. In our problem, we consider systems that are weakly damped ($\bar{\mu} << 1$) and weakly nonlinear ($\bar{\alpha} << 1$). Also, we know that large responses occur for small excitation levels

($\bar{f} << 1$). To represent the smallness of these parameters, we replace each of them with a new parameter that is multiplied by the parameter ϵ which embodies the smallness. So, we rewrite (1.1) as

$$\ddot{u}+u=-\epsilon\left(2\mu\dot{u}-\alpha u^3-uf\cos\,\phi t\right) \tag{2.7}$$

where

$$\bar{f}=\epsilon f \qquad \bar{\mu}=\epsilon\mu \qquad \bar{\alpha}=\epsilon\alpha \tag{2.8}$$

At this point in our analysis, we introduce the detuning σ. The detuning relates the nearness of the excitation frequency to twice the natural frequency. The detuning can be introduced into the problem in many ways, so it must be chosen with care and with a knowledge of how the method of multiple scales works. In this analysis, we chose the detuning σ such that

$$1=\frac{1}{4}\phi^2+\epsilon\sigma \tag{2.9}$$

Note that since the detuning is multiplied by ϵ, we have already incorporated the nearness of the excitation frequency to two in the analysis. Multiplying (2.9) by u, we get

$$u=\frac{1}{4}\phi^2 u+\epsilon\sigma u \tag{2.10}$$

We use (2.10) to replace u on the left-hand side of (2.7), and obtain

$$\ddot{u}+\frac{1}{4}\phi^2 u=-\epsilon\left(2\mu\dot{u}-\alpha u^3-uf\cos\,\phi t+\sigma u\right) \tag{2.11}$$

Next, we use ϵ to set up multiple time scales. We define the time scales T_n by

$$T_0=t,\ T_1=\epsilon t,\ T_2=\epsilon^2 t,\ \ldots,\ T_n=\epsilon^n t \tag{2.12}$$

Now u will be a *function* of multiple time scales. Also u will depend on the *parameter* ϵ. So we expand u in a series of powers of ϵ, as

$$u(t;\epsilon)=u_0(T_0,T_1,\ldots)+\epsilon u_1(T_0,T_1,\ldots)+\ldots \tag{2.13}$$

Next, we express the time derivatives in (1.1) in terms of the multiple time scales. Using (2.12), we get

$$\frac{d}{dt}=\frac{\partial}{\partial T_0}\frac{\partial T_0}{\partial t}+\frac{\partial}{\partial T_1}\frac{\partial T_1}{\partial t}+\ldots=\frac{\partial}{\partial T_0}+\epsilon\frac{\partial}{\partial T_1}+\ldots=D_0+\epsilon D_1+\ldots \tag{2.14}$$

$$\frac{d^2}{dt^2}=D_0^2+2\epsilon D_0 D_1+\ldots \tag{2.15}$$

Here, we use the operator $D_n=\dfrac{d^n}{dt^n}$ for convenience. In this analysis, we will keep terms only up to order ϵ.

Substituting (2.13) - (2.15) into (2.11) and keeping only terms up to the first power of ϵ yields

$$\begin{aligned} D_0^2u_0+\epsilon D_0^2u_1+2\epsilon D_0D_1u_0+\frac{1}{4}\phi^2u_0+\frac{1}{4}\phi^2\epsilon u_1= \\ -2\epsilon\mu D_0u_0+\epsilon\alpha u_0^3+\epsilon fu\cos\phi T_0-\epsilon\sigma u_0 \end{aligned} \tag{2.16}$$

Note that this is a partial-differential equation rather than an ordinary-differential equation. The coefficients of each power of ϵ must be the same on both sides of (2.16). So from the coefficients of ϵ^0, we get

$$D_0^2u_0+\frac{1}{4}\phi^2u_0=0 \tag{2.17}$$

and from the coefficients of ϵ^1, we get

$$D_0^2 u_1 + \frac{1}{4}\phi^2 u_1 = -2D_0 D_1 u_0 - 2\mu D_0 u_0 + \alpha u_0^3 + f u_0 \cos \phi T_0 - \sigma u_0 \tag{2.18}$$

The solution of (2.17) can be expressed as

$$u_0 = A(T_1) e^{\frac{1}{2} i \phi T_0} + cc \tag{2.19}$$

In (2.19) and in what follows, the notation *cc* refers to the complex conjugate of the preceding terms. We write the solution (which is sinusoidal) in polar form so that we can manipulate it more easily in what follows. Note also that $A(T_1)$, which contains the amplitude and phase of the sinusoid, depends on the time scale T_1 since equation (2.17) is a partial-differential equation. Substituting (2.19) into (2.18) and converting the cosine term to polar form, we get

$$D_0^2 u_1 + \frac{1}{4}\phi^2 u_1 = -i\phi D_1 A e^{\frac{1}{2} i \phi T_0} - i\phi \mu A e^{\frac{1}{2} i \phi T_0} + \alpha A^3 e^{\frac{3}{2} i \phi T_0} + 3\alpha A^2 \bar{A} e^{\frac{1}{2} i \phi T_0}$$

$$+ \frac{1}{2} f A e^{\frac{3}{2} i \phi T_0} + \frac{1}{2} f \bar{A} e^{\frac{1}{2} i \phi T_0} - \sigma A e^{\frac{1}{2} i \phi T_0} + cc \tag{2.20}$$

Here, the overbar denotes the complex conjugate.

Consider those terms in (2.20) that contain $e^{\pm \frac{1}{2} i \phi T_0}$. Such terms produce so-called *secular* terms. The particular solution u_1 corresponding to such terms will be proportional to $T_0 e^{\pm \frac{1}{2} i \phi T_0}$, which grows with time. This would invalidate our analysis, since we implicitly assumed that the term ϵu_1 is a small correction to the term u_0. (If ϵu_1 becomes the same order as u_0, we cannot separate the

terms with different powers of ϵ in (2.16) to form (2.17) and (2.18).) So the coefficients of $e^{\pm\frac{1}{2}i\phi T_0}$ must be zero. Therefore, we must have

$$i\phi D_1 A + i\phi\mu A - 3\alpha A^2\bar{A} - \frac{1}{2}f\bar{A} + \sigma A = 0 \tag{2.21}$$

Then, the particular solution to (2.20) is

$$u_1 = -\frac{2\alpha A^3 + fA}{4\phi^2} e^{\frac{3}{2}i\phi T_0} + cc \tag{2.22}$$

Now, we find the equations governing the amplitude and phase of the response from (2.21). First, we express $A(T_1)$ in the polar form

$$A(T_1) = \frac{1}{2}a(T_1)e^{i\beta(T_1)} \tag{2.23}$$

Substituting (2.23) into (2.21) and collecting the real and imaginary parts, we get

$$\sigma a - a\phi\beta' - \frac{3}{4}\alpha a^3 - \frac{1}{2}fa\cos 2\beta = 0 \tag{2.24}$$

$$\phi a' + \mu\phi a + \frac{1}{2}fa\sin 2\beta = 0 \tag{2.25}$$

Solving (2.24) and (2.25) for the derivatives, we get

$$a' = -\mu a - \frac{fa}{2\phi}\sin 2\beta \tag{2.26}$$

$$a\beta' = \frac{\sigma a}{\phi} - \frac{fa}{2\phi}\cos 2\beta - \frac{3\alpha}{4\phi}a^3 \tag{2.27}$$

Note that (2.26) and (2.27) are ordinary differential equations in the slow time scale T_1 for the amplitude and phase of the response to either stationary

or nonstationary excitations.

We now find the solution for the amplitude and phase by substituting (2.19), (2.22) and (2.23) into (2.13) and using the Euler formula to get

$$u=a\cos\left[\frac{1}{2}\phi t+\beta\right]-\epsilon\left[\frac{fa}{4\phi^2}\cos\left[\frac{3}{2}\phi t+\beta\right]+\frac{\alpha a^3}{8\phi^2}\cos\left[\frac{3}{2}\phi t+3\beta\right]\right]+\ldots \qquad (2.28)$$

where the amplitude a and phase β are governed by the ordinary-differential equations (2.26) and (2.27).

2.2 Fixed-Point Solutions

Before considering responses to nonstationary excitation, we first need to consider the stationary responses to stationary excitations. By definition, the amplitude and phase are constant for the stationary solutions, so we set $a'=\beta'=0$ in (2.26) and (2.27) and obtain

$$a\sin 2\beta=-\frac{2\mu\phi a}{f} \qquad (2.29)$$

$$a\cos 2\beta=\frac{2\sigma a}{f}-\frac{3\alpha a^3}{2f} \qquad (2.30)$$

These equations are algebraic. Solutions to these equations are called *fixed-points* of the system (2.26) and (2.27). Therefore, a fixed-point solution corresponds to an oscillatory solution of (2.11) that has constant amplitude and

phase. One solution to these equations is the trivial solution $a = 0$. Through manipulation of (2.29) and (2.30), we also find the following two nontrivial solutions for the amplitude:

$$a^2 = \frac{4\sigma}{3\alpha} + \frac{4}{3\alpha}\sqrt{\frac{f^2}{4} + 4\mu^2(\epsilon\sigma - 1)} \tag{2.31a}$$

$$a^2 = \frac{4\sigma}{3\alpha} - \frac{4}{3\alpha}\sqrt{\frac{f^2}{4} + 4\mu^2(\epsilon\sigma - 1)} \tag{2.31b}$$

Depending on the values of the parameters, there are either zero, one, or two possible nontrivial solutions. If we fix the values of all the parameters but one (for instance σ), then each of (2.31a) and (2.31b) yields a *solution curve* in the σ - a space. Every point on these curves is a fixed-point solution of (2.26) and (2.27) and corresponds to an oscillatory solution of (2.11) with constant amplitude and phase. Note that given a set of parameters for which real solutions to (2.31a) and (2.31b) exist, the solution corresponding to (2.31a) is always larger than that corresponding to (2.31b) when $\alpha > 0$ (the reverse is true when $\alpha < 0$); so we refer to the solution curves as the larger and smaller solution curves, respectively. In Figure 2.1, we plot the *frequency-response* curves. For these curves, μ, α, and f are constants and the ordinate axis is ϕ. For each value of ϕ, we plot all of the possible solutions for the response amplitude. For all values of ϕ, the trivial solution is possible. For $\phi > 2.21$, there are no nontrivial solutions for a. For $1.75 < \phi < 2.21$, one

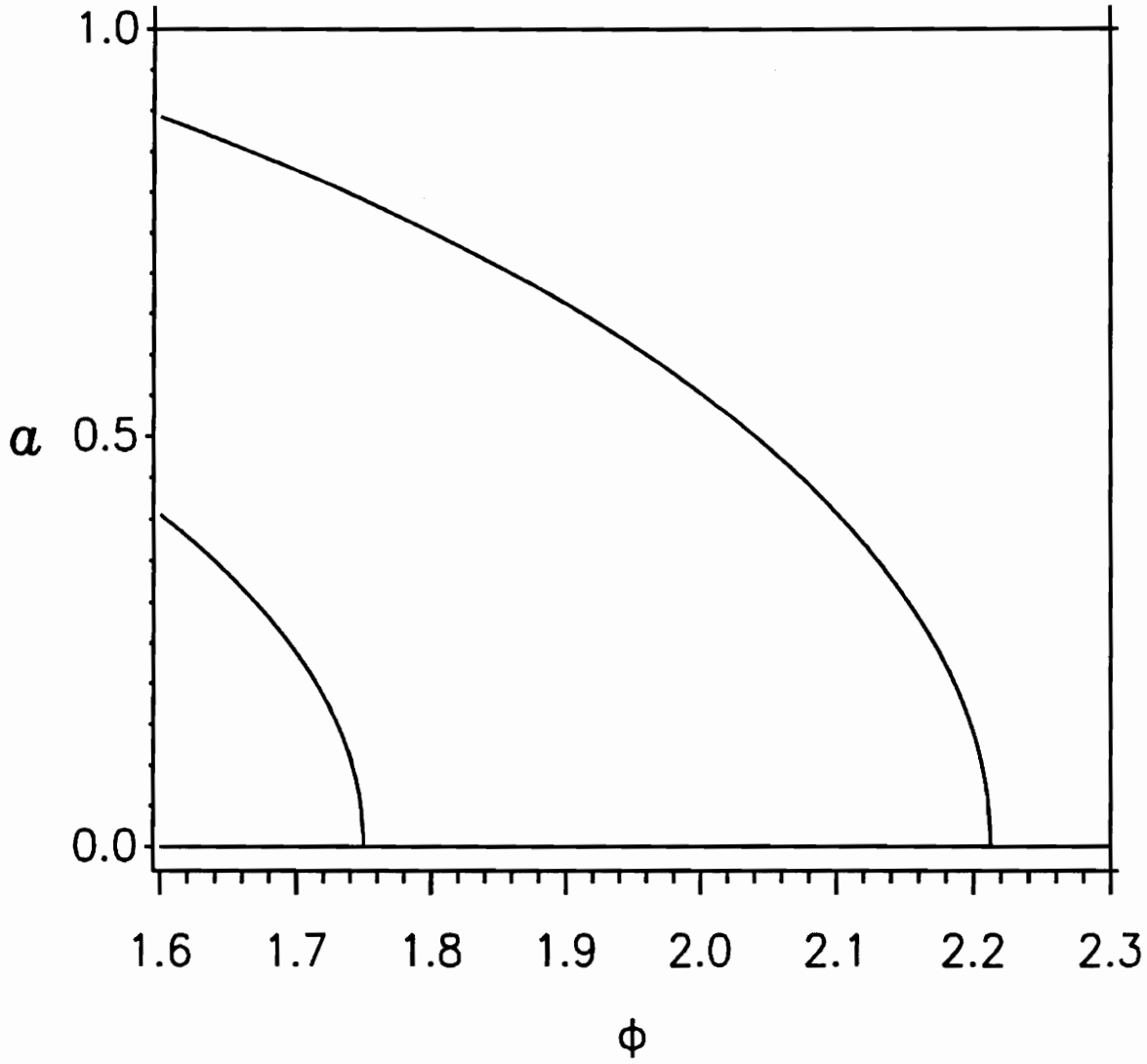

Figure 2.1 Frequency-response curves. Two, one, or zero nontrivial solutions exist depending on the value of ϕ. The trivial solution exists for all ϕ.
$\alpha = 1.0$, $\mu = 0.05$, $\epsilon = 1.0$, and $f = 0.5$.

nontrivial solution exists. And for $\phi < 1.75$, two nontrivial solutions exist. Note that if α were negative, these solution curves would be bent in the opposite direction, with no nontrivial solutions for $\phi < 1.75$ and two nontrivial solution for $\phi > 2.21$.

Because we will be considering sweeps of the excitation amplitude f, we need to consider *force-response* curves also. For these curves, α, μ, and ϕ are constants, and the ordinate axis is the excitation amplitude f. Again, each value on this curve represents a fixed-point solution to (2.26) and (2.27) and an oscillatory solution of (2.11) with constant amplitude and phase. The force-response curve can take one of two shapes, depending on the constant value of ϕ at which it occurs.

Figure 2.2 is an example of the force-response curve when $\phi \geq 2$. Moving from left to right as f increases, we see that only the trivial solution exists up to the critical value $f = 0.474$. Above this critical value, a single nontrivial solution coexists with the trivial solution. The nontrivial solution curve intersects the f axis at the critical value.

When $\phi < 2$, the force-response curve has a shape similar to that in Figure 2.3. Again, the trivial solution exists for all values of f. For $f < 0.190$, the trivial solution is the only solution. But unlike the previous case, in the range $0.190 < f < 0.272$ there are *two* nontrivial solutions along with the trivial solution. These two solutions intersect at $f = 0.190$. The smaller

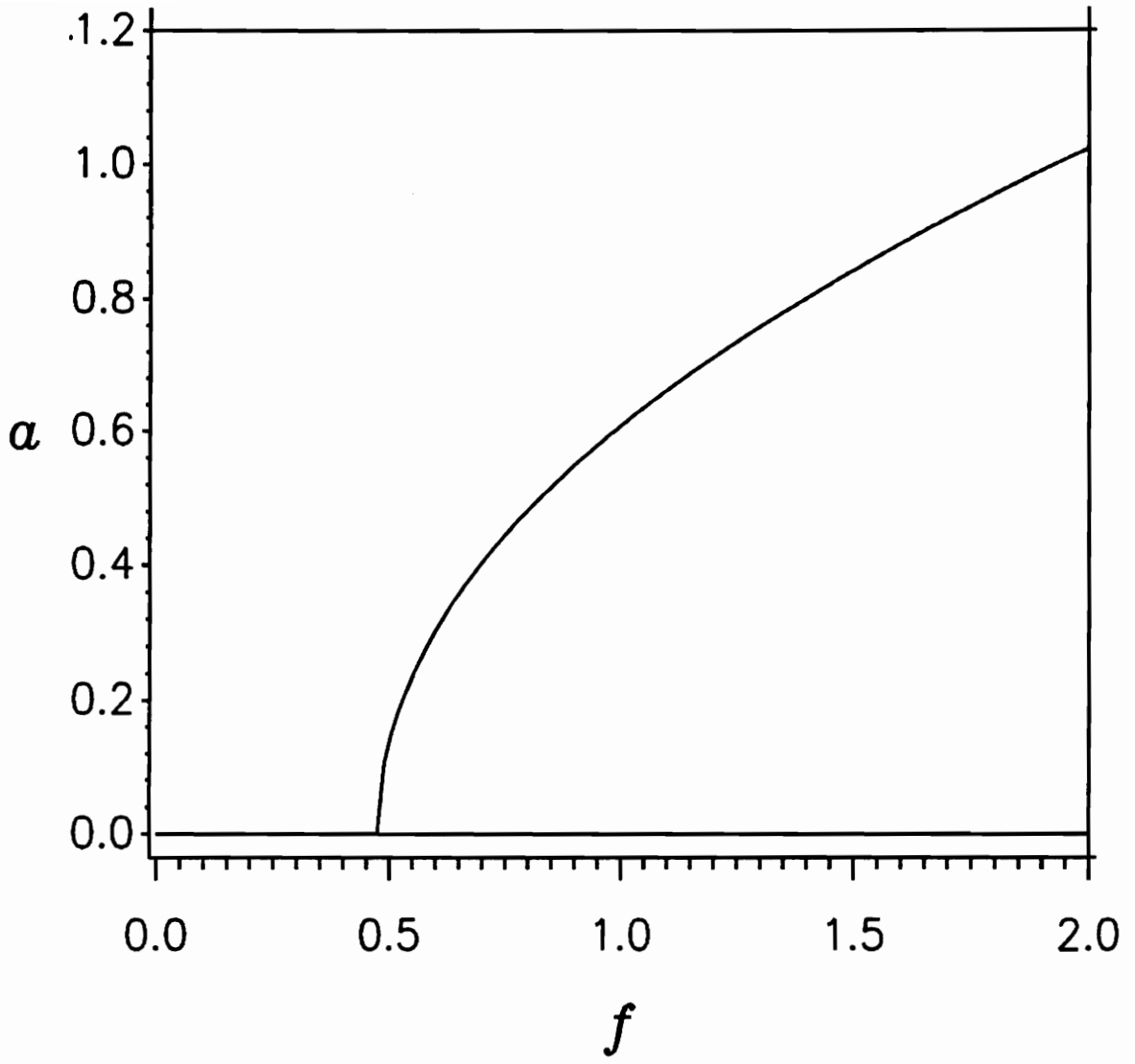

Figure 2.2 Force-response curves. One nontrivial solution exists depending on the value of f. The trivial solution exists for all f. $\alpha = 1.0$, $\mu = 0.05$, $\epsilon = 1.0$, and $\phi = 2.2$.

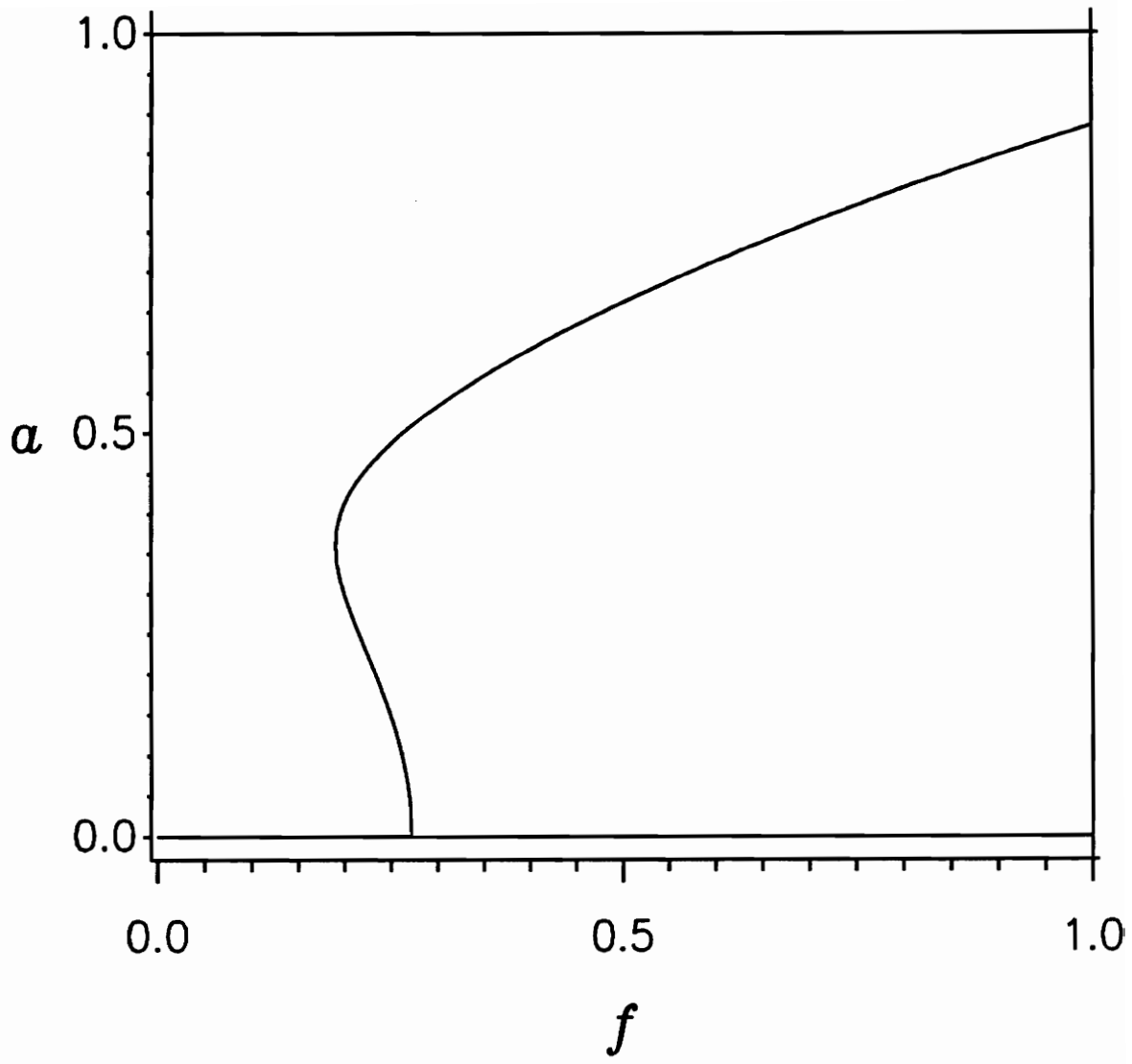

Figure 2.3 Force-response curves. One or two nontrivial solutions exist depending on the value of f. The trivial solution exists for all f.
$\alpha = 1.0$, $\mu = 0.05$, $\epsilon = 1.0$, and $\phi = 1.9$.

solution tends to zero as f tends to 0.272. The larger solution increases as f increases, and for $f > 0.272$, the larger solution is the only nontrivial solution.

In preparation to study nonstationary responses to nonstationary excitation, we have first sought to understand stationary responses. Although each point on the response curves of Figure 2.1 - 2.3 is a fixed-point solution to (2.26) and (2.27) and represents an oscillatory solution to (2.11) with constant amplitude and phase, some of these solutions are not stable. Such unstable solutions are not realized physically because all systems are subject to disturbances. So, to find stationary responses, we must understand stability, which we consider next.

2.3 Stability of a Fixed-Point

A solution is *asymptotically stable* if the system's response returns to it after the system is perturbed by a small disturbance. If the system diverges from the solution after a small disturbance, the solution is *unstable* (Nayfeh and Mook, 1979).

To begin our examination of the stability, we will use the variational equations (2.26) and (2.27) obtained from the method of multiple scales to find the stability of a fixed-point solution.

In order to find the stability of a fixed point, we first consider a general

system governed by n equations of the form

$$\mathbf{x}'=\mathbf{f}(\mathbf{x}) \tag{2.32}$$

where $\mathbf{x}$ and $\mathbf{f}$ are n dimensional vectors. A fixed point $\mathbf{x}_0$ of the system is defined by

$$\mathbf{x}_0'=\mathbf{0}=\mathbf{f}(\mathbf{x}_0) \tag{2.33}$$

We perturb the system from the fixed point with a small time-varying disturbance $\mathbf{v}(T_1)$ and obtain

$$\mathbf{x}=\mathbf{x}_0+\mathbf{v}(T_1) \tag{2.34}$$

Note that the disturbance varies on the time scale T_1 because the variational equations (2.26) and (2.27) depend on this time scale. After we substitute (2.34) into (2.32), expand $\mathbf{f}$ in a Taylor series, and linearize the result, we get

$$\mathbf{v}'(T_1)=\nabla\mathbf{f}(\mathbf{x}_0)\mathbf{v}(T_1) \tag{2.35}$$

where $\nabla\mathbf{f}$ is the Jacobian of $\mathbf{f}$ at $\mathbf{x}_0$. But since (2.35) is a system of ordinary-differential equations with constant coefficients, it possesses solutions of the form

$$\mathbf{v}(T_1)=\mathbf{c}e^{\lambda T_1} \tag{2.36}$$

Substituting (2.36) into (2.35), we find there are nontrivial solutions if and only if

$$\left| \nabla\mathbf{f}(\mathbf{x}_0)-\lambda\mathbf{I} \right| =0 \tag{2.37}$$

If the real part of *any* of the roots λ of (2.37) is positive, $\mathbf{v}$ will grow

exponentially, thus the fixed point is unstable. If the real part of *each* of the roots is negative, the fixed point is stable. If the real parts of some of the roots are zero and the real parts of the rest of the roots are negative, the stability cannot be determined from this analysis alone.

As noted, the disturbance in this analysis is slowly varying; it varies on the same time scale T_1 as the equations we are analyzing. Since this analysis excludes fast varying disturbances, a periodic solution of (2.11) may be stable to slowly varying disturbances but may be unstable if perturbed by a general disturbance. A periodic solution that is unstable to a slowly varying disturbance will, of course, be unstable when perturbed by a general disturbance. This analysis is useful, though, because it is easy to get closed-form solutions without computer integration, and its results are valid for a large range of parameters. Later, we will consider a more general stability analysis.

To apply this method we substitute our system, (2.26) and (2.27), into (2.37) to get

$$\begin{vmatrix} -\mu-\frac{f}{2\phi}\sin 2\beta-\lambda & -\frac{fa}{\phi}\cos 2\beta \\ -\frac{3\alpha a}{2\phi} & \frac{f}{\phi}\sin 2\beta-\lambda \end{vmatrix} =0 \qquad (2.38)$$

Expanding this determinant and using (2.29) and (2.30), we get

$$\lambda^2+2\mu\lambda+\frac{3\alpha a^2}{4\phi^2}\left(\frac{3\alpha a^2}{4}-\sigma\right)=0 \qquad (2.39)$$

as the general equation for λ. Substituting the solution (2.31a) into (2.39), we

get

$$\lambda^2+2\mu\lambda+\eta=0 \tag{2.40}$$

where

$$\eta=\frac{3\alpha a^2}{4\phi^2}\sqrt{\frac{f^2}{4}+4\mu^2(\epsilon\sigma-1)} \tag{2.41}$$

When α is positive, η is also positive as long as a and f are nontrivial. Solving for λ, we get

$$\lambda=-\mu\pm\sqrt{\mu^2-\eta} \tag{2.42}$$

Since η is positive, the real parts of both roots are negative. Therefore, the solution (2.31a) is stable when $\alpha > 0$. When $\alpha < 0$, $\eta < 0$ and (2.31a) is unstable.

Substituting the solution (2.31b) into (2.39), we get

$$\lambda^2+2\mu\lambda-\eta=0 \tag{2.43}$$

The roots λ of (2.43) are given by

$$\lambda=-\mu\pm\sqrt{\mu^2+\eta} \tag{2.44}$$

When $\alpha > 0$, η is positive, and one root is always positive. So the solution (2.31b) is unstable. When $\alpha < 0$, the solution (2.31b) is stable.

To study the stability of the trivial solution, we find it convenient to use (2.21) and express A in the Cartesian form

$$A(T_1)=\frac{1}{2}\left[p(T_1)-iq(T_1)\right] \tag{2.45}$$

Substituting (2.45) into (2.21) and separating the real and imaginary parts, we

get

$$\frac{1}{2}\phi q' + \frac{1}{2}\phi\mu q - \frac{3}{8}\alpha\left(p^3+pq^2\right) - \frac{1}{4}fp + \frac{1}{2}\sigma p = 0 \tag{2.46}$$

$$\frac{1}{2}\phi p' + \frac{1}{2}\phi\mu p + \frac{3}{8}\alpha\left(p^2q+q^3\right) - \frac{1}{4}fq - \frac{1}{2}\sigma q = 0 \tag{2.47}$$

Solving for p' and q', we get

$$p' = -\mu p - \frac{3\alpha}{4\phi}\left(p^2q+q^3\right) + \frac{fq}{2\phi} + \frac{\sigma q}{\phi} \tag{2.48}$$

$$q' = -\mu q + \frac{3\alpha}{4\phi}\left(p^3+pq^2\right) + \frac{fp}{2\phi} - \frac{\sigma p}{\phi} \tag{2.49}$$

So, upon substituting the right-hand sides of (2.48) and (2.49) into (2.37) and setting $p = q = 0$ for the trivial solution, we get

$$\lambda^2 + 2\mu\lambda + \mu^2 + \frac{4\sigma^2 - f^2}{4\phi^2} = 0 \tag{2.50}$$

The roots λ of (2.50) are given by

$$\lambda = -\mu \pm \sqrt{\frac{f^2 - 4\sigma^2}{4\phi^2}} \tag{2.51}$$

The trivial solution is unstable when the real part of either of the roots is positive, which occurs when

$$f_c > 2\sqrt{\sigma^2 + \mu^2\phi^2} \tag{2.52}$$

In Figure 2.4, we repeat the frequency-response curves of Figure 2.1, but now we plot stable solutions with solid lines and unstable solutions with dashed lines. As noted, the solutions on the larger branch are stable, while

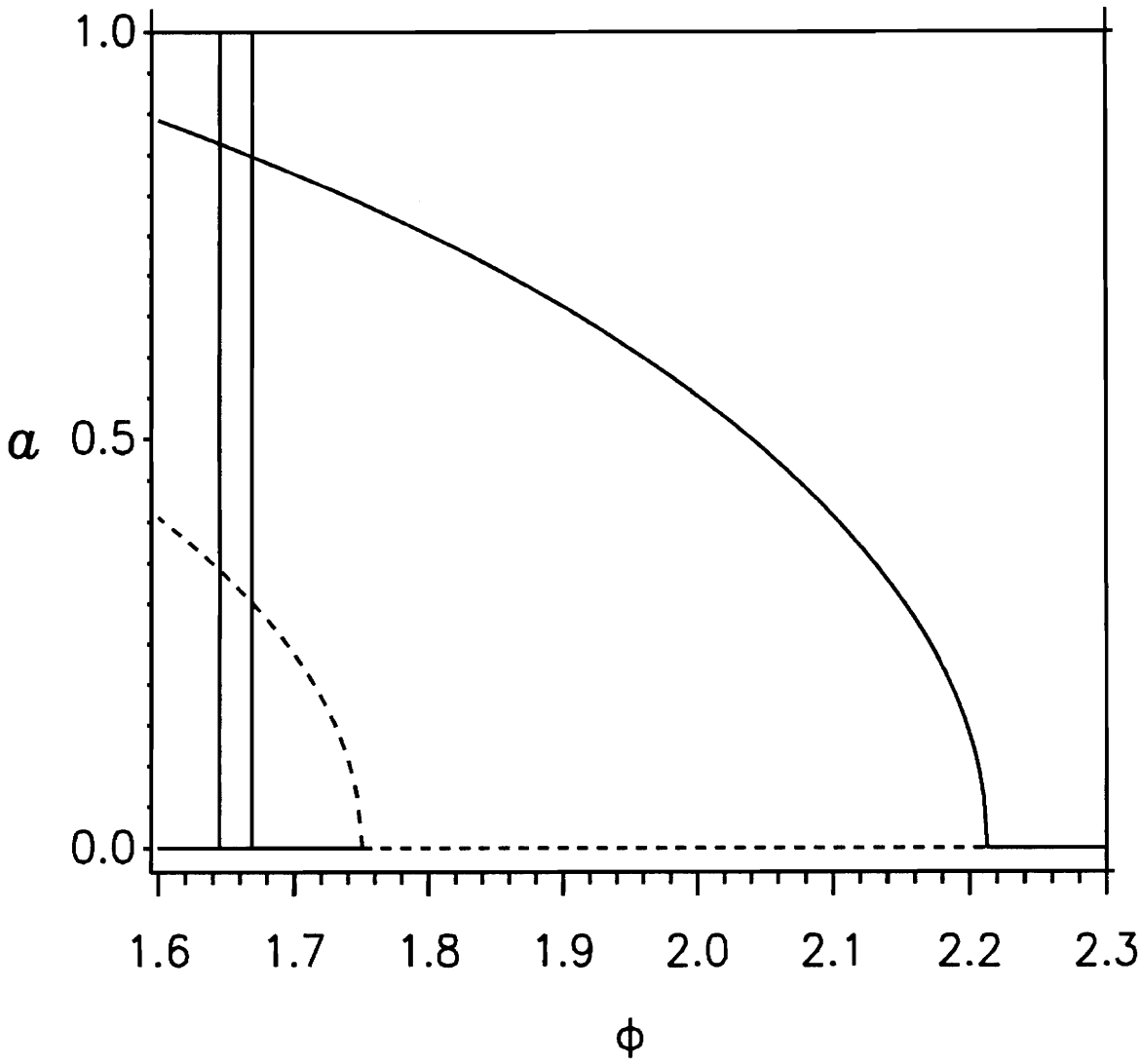

Figure 2.4 Stability of the frequency-response curves of Figure 1.1. Solid lines represent stable solutions. Dashed lines represent unstable solutions.
$\alpha = 1.0$, $\mu = 0.05$, $\epsilon = 1.0$, and $f = 0.5$.

those on the smaller branch are unstable. Note that the trivial solution is stable for all ϕ except in the interval $1.75 < \phi < 2.21$. This region is bounded by the intersections of the nontrivial frequency-response curves with the ϕ axis.

In Figure 2.5, we show the stability characteristics of the force-response curve of Figure 2.2. Again, we plot stable solutions as solid lines and unstable solutions as dashed lines. Although the trivial solution exists for all values of f, it is stable only up to the critical value f_c and unstable for all larger values. For this case with the constant value of $\phi \geq 2$, a single nontrivial solution that is stable exists above the critical value of f.

In Figure 2.6, we show the stability characteristics of the force-response curve corresponding to Figure 2.3 for a system with a value of ϕ less than two. Like the previous case, the trivial solution is stable up to the critical value f_c and unstable above it. For the range of f where two nontrivial solutions exist, the large solution is stable and the small solution is unstable. In this range of f, the response may be trivial or nontrivial, depending on the initial conditions. Because the response may be nontrivial in this range of f that is less than f_c, the system is said to have a *subcritical instability*. Above f_c, the response is given by the only nontrivial solution, which is stable.

We note that the stability analysis based on the variational equations (2.26) and (2.27) is limited to slowly varying disturbances and that a solution may be stable to a slowly varying disturbance but not to a general disturbance. Next, we consider a more general stability analysis based on Floquet theory.

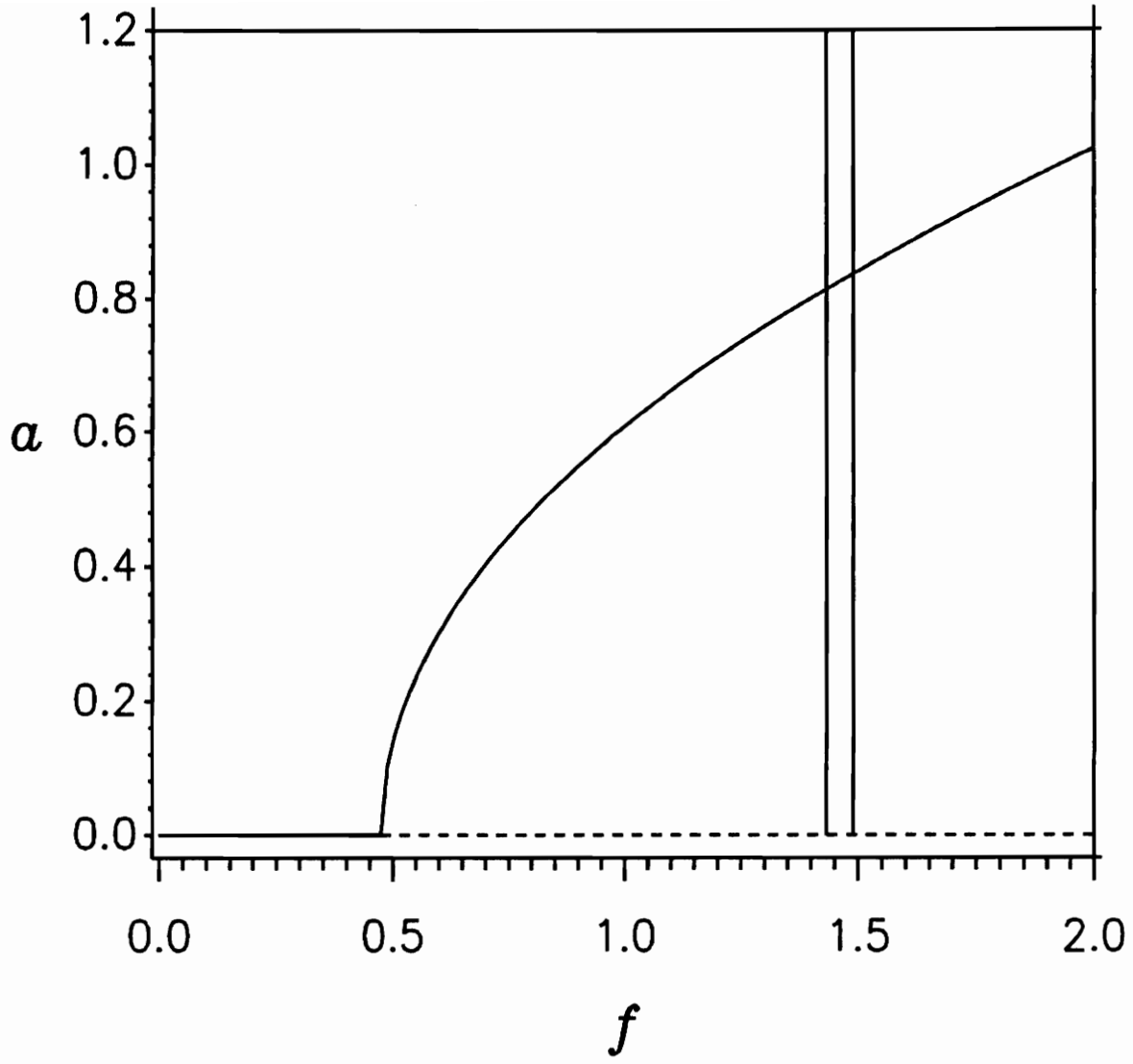

Figure 2.5 Stability of the force-response curves of Figure 1.2. Solid lines represent stable solutions. Dashed lines represent unstable solutions.
$\alpha = 1.0$, $\mu = 0.05$, $\epsilon = 1.0$, and $\phi = 2.2$.

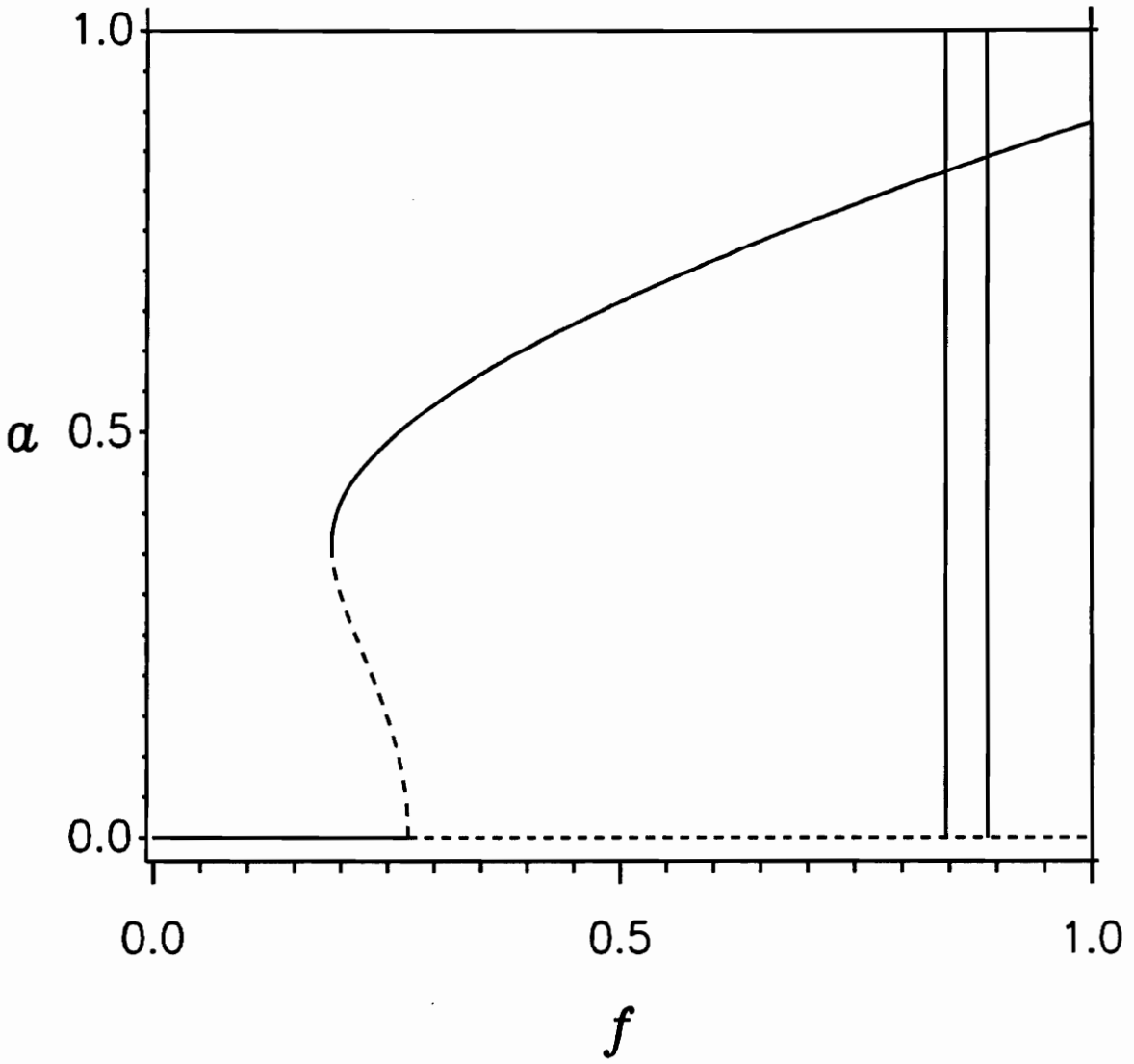

Figure 2.6 Stability of the force-response curves of Figure 1.3. Solid lines represent stable solutions. Dashed lines represent unstable solutions.
$\alpha = 1.0$, $\mu = 0.05$, $\epsilon = 1.0$, and $\phi = 1.9$.

This analysis, which we apply to the governing equation (2.11) rather than the variational equations, is not limited to slowly varying disturbances.

2.4 Floquet Theory Stability Analysis

To describe this analysis, we consider the general system

$$\dot{\mathbf{u}}(t)=\mathbf{f}(\mathbf{u}(t)) \tag{2.53}$$

In this analysis, we are not considering the stability of a fixed point solution ($\mathbf{f}(\mathbf{x}_0)=0$) of the variational equations (2.26) and (2.27). Instead, we are considering the stability of the corresponding solution of (2.11) in the original time scale, which is a periodic oscillation. To the periodic solution $\mathbf{U}$, where $\mathbf{U}(t+\tau)=\mathbf{U}(t)$, we add a small disturbance $\mathbf{x}$ and obtain

$$\mathbf{u}(t)=\mathbf{U}(t)+\mathbf{x}(t) \tag{2.54}$$

Substituting (2.54) into (2.53), expanding $\mathbf{f}$ in a Taylor series, and keeping linear terms in $\mathbf{x}$, we get

$$\dot{\mathbf{x}}(t)=\nabla\mathbf{f}(t)\mathbf{x}(t) \tag{2.55}$$

We note that (2.55) is a set of n linear equations with *periodic* coefficients having a period commensurate with τ. There are n linearly independent solutions to these equations, with each solution being a column vector. These n solutions can be combined to form an n x n matrix known as the *fundamental solution matrix* $\mathbf{X}$(t). This matrix satisfies

$$\dot{\mathbf{X}}(t)=\nabla\mathbf{f}(t)\mathbf{X}(t) \tag{2.56}$$

If $\mathbf{X}(t)$ is a solution matrix of (2.56), then $\mathbf{X}(t+\tau)$ is also a solution matrix, because $\nabla\mathbf{f}$ is periodic with period τ. Since there are only n linearly independent solutions to (2.55), the n solutions represented by $\mathbf{X}(t+\tau)$ must be linear combinations of the n linearly independent solutions represented by $\mathbf{X}(t)$; that is,

$$\mathbf{X}(t+\tau)=\mathbf{X}(t)\mathbf{A} \tag{2.57}$$

where $\mathbf{A}$ is an n x n constant matrix. Next, we introduce the linear transformation

$$\mathbf{X}(t)=\mathbf{v}(t)\mathbf{P} \tag{2.58}$$

where $\mathbf{P}$ is nonsingular. Substituting (2.58) into (2.57), we get

$$\mathbf{v}(t+\tau)=\mathbf{v}(t)\mathbf{J} \tag{2.59}$$

where

$$\mathbf{J}=\mathbf{PAP}^{-1} \tag{2.60}$$

We can choose $\mathbf{P}$ such that $\mathbf{J}$ assumes the *Jordan canonical form*

$$\mathbf{J}=\begin{bmatrix} \lambda_1 & 0 & \cdots & 0 \\ 0 & \lambda_2 & \cdots & 0 \\ \vdots & \vdots & \ddots & \vdots \\ 0 & 0 & \cdots & \lambda_n \end{bmatrix} \tag{2.61}$$

if all of the eigenvalues λ_i are distinct, or a more complicated form when they are not distinct. Substituting (2.61) into (2.59), we get

$$v_i(t+\tau)=\lambda_i v_i(t) \tag{2.62}$$

Therefore, we have

$$v_i(t+m\tau)=\lambda_i^m v_i(t) \tag{2.63}$$

Clearly, for the disturbance to decay, the magnitude of each eigenvalue λ_i must be less than one. If the magnitude of any of the λ_i is greater than one, the solution is unstable.

In order to find the eigenvalues, we note from (2.60) that $\mathbf{J}$ and $\mathbf{A}$ have the same eigenvalues. Setting $t = 0$ in (2.57), we get

$$\mathbf{X}(\tau)=\mathbf{X}(0)\mathbf{A} \tag{2.64}$$

If we choose the initial condition $\mathbf{X}(0) = \mathbf{I}$, where $\mathbf{I}$ is the identity matrix, we can find the matrix $\mathbf{A}$ simply by integrating (2.56) for one period τ. This integration can be done on a digital computer, if necessary. Once we find $\mathbf{A}$, we can compute the eigenvalues (with a digital computer if we choose).

To apply this analysis to our system, we first convert (2.7) from a second-order equation to a system of two first-order equations using

$$u_1(t)=u(t) \qquad\qquad u_2(t)=\dot{u}(t) \tag{2.65}$$

Using (2.65), we rewrite the governing equation as

$$\dot{u}_1=u_2 \tag{2.66a}$$

$$\dot{u}_2=-u_1-2\epsilon\mu u_2+\epsilon\alpha u_1^3+\epsilon u_1 f\cos\,\phi t \tag{2.66b}$$

The right-hand side of (2.66) now corresponds to $\mathbf{f}$ in (2.53). Substituting (2.66) into (2.55), we get the following equations for the disturbance $\mathbf{x}$:

$$\begin{bmatrix}\dot{x}_1\\ \dot{x}_2\end{bmatrix}=\begin{bmatrix}0 & 1\\ -1+3\epsilon\alpha u_1^2+\epsilon f\cos\,\phi t & -2\epsilon\mu\end{bmatrix}\begin{bmatrix}x_1\\ x_2\end{bmatrix} \tag{2.67}$$

The computational method to find $\mathbf{A}$ involves six equations. We integrate the two equations (2.66) to find $\mathbf{U}$. (Since we wish to find the stability of periodic solutions, we must have a method to guarantee that the initial conditions we choose are on a solution trajectory that closes. We discuss a method for this in the Appendix.) We also integrate equations (2.67) twice; once with the initial conditions $x_1(0) = 1$ and $x_2(0) = 0$ and once with the initial conditions $x_1(0) = 0$ and $x_2(0) = 1$. These initial conditions correspond to setting $\mathbf{X}(0) = \mathbf{I}$ in (2.64). Therefore, after integrating for one period τ, we have the matrix $\mathbf{A}$ for our system, and we can determine the stability of $\mathbf{U}(t)$ by examining the magnitudes of the eigenvalues of $\mathbf{A}$.

To use this analysis, we choose a value of ϕ (or f) and perform the calculations. If the magnitudes of both λ are less than one, the solution is stable, so we increment ϕ (or f) and repeat the calculations. We continue this until we find the value of ϕ (or f) at which the magnitude of one of the λ's passes through one. This gives us the value of ϕ (or f) at which the solution becomes unstable. If we wish, we can search for a new stable solution at this value of ϕ (or f) and repeat the analysis for this new solution.

Sanchez and Nayfeh (1990) applied the Floquet analysis to a system similar to the one considered here. The results are similar to the analysis performed here.

We consider the stability of solutions along the frequency-response curves. The larger solution, which the variational stability analysis predicts to

be always stable, is also stable according to the Floquet analysis for a large range of ϕ. However, as ϕ decreases or f increases, one floquet multiplier λ passes through one. The value of ϕ or f at which the solution becomes unstable is marked in Figures 2.4 - 2.6 with a vertical line. To predict the subsequent response, we recall that the period of the response $\mathbf{U}$ is $\tilde{T} = 4\pi/\phi$. Therefore, u_1^2, as well as $\epsilon f \cos \phi t$, the time-varying terms in (2.67), has a period $\frac{1}{2}\tilde{T}$ because $\mathbf{U}$ is symmetric. Since λ passes through positive one, the disturbance $\mathbf{x}$ will also have the period $\frac{1}{2}\tilde{T}$. Because $\mathbf{U}$ has the period $\tilde{T}$, the disturbance will cause $\mathbf{u}$ to be asymmetric. This is called a *symmetry-breaking bifurcation*. According to the Floquet analysis, this new asymmetric solution is stable, but only for a small range of ϕ. As we decrease ϕ further, one Floquet multiplier for the asymmetric solution passes though negative one. Again, $\mathbf{U}$ has period $\tilde{T}$. But since $\mathbf{U}$ is now asymmetric, the u_1^2 term in (2.67) has the period $\tilde{T}$. Since λ passes through negative one, it takes two cycles for the disturbance $\mathbf{x}$ to repeat, so $\mathbf{x}$ has the period $2\tilde{T}$. Therefore, the new solution $\mathbf{u}$ has a period of $2\tilde{T}$. This is called a *period-doubling bifurcation*. The Floquet analysis predicts that this new solution is stable. However, the range of ϕ for which the period-doubled solution is stable is smaller than the range of ϕ for which the asymmetric solution is stable. If we decrease ϕ further, the solution undergoes successive period doublings; each is stable over an even smaller range of ϕ. Then, a chaotic solution appears for a small range of ϕ, and

finally the solution becomes unbounded. Because the successive period doublings, chaos, and unboundedness occur in such small ranges of ϕ, we will later use the values of ϕ at which the asymmetric solution becomes unstable as an estimate of the value of ϕ at which unboundedness occurs in the stationary solution. This value of ϕ or f is also marked in Figures 2.4 - 2.6 with a vertical line. We would find a similar sequence of bifurcations (i.e., symmetry breaking, period doublings, chaos, and unboundedness) if we repeat the analysis using the excitation amplitude f as the control parameter.

CHAPTER 3

Frequency Sweeps

Now that we understand the stationary response of our system, we can examine the nonstationary behavior. In this chapter we explore the response to an excitation whose frequency varies linearly with time.

We find the response by numerically integrating the equations derived by using the method of multiple scales in Chapter 2. For chosen constants f, μ, α, and r, we use a digital computer to integrate the Cartesian form (2.48) and (2.49). (We do not use the polar form (2.26) and (2.27) because we would have to divide (2.27) by a factor a to get it in a digitally integrable form. This division would not be valid when a is trivial. Furthermore, Nayfeh and Asfar (1988) found that the integration of (2.26) and the integrable form of (2.27) yields incorrect results when the response was trivial or nearly trivial.) We also will integrate the governing equations (2.66) of the system. We integrate both sets of equations on an IBM 3090 digital computer. The integrations are

carried out in a Fortran program using the IMSL routine DVERK, which is a differential equation solver that uses fifth- and sixth-order Rungé-Kutta-Verner solution schemes.

The linear variation with time of the excitation frequency is given by (1.2), or by

$$\phi=\phi_0+r\epsilon^2 t \tag{3.1}$$

Here, we call r the *sweep rate* since its magnitude and sign determine how fast we "sweep" through a range of excitation frequencies. Since we implicitly assume that the detuning σ is a slowly varying function of time (that is, it varies on the time scale ϵt), we note from (2.9) that we need to use the ordering ϵ^2 in (3.1). The parameter ϵ can be set to equal one at this point since its purpose was to serve as a representation of the smallness in the multiple-scales analysis.

In order to determine the effect of sweep rates on the response, we need to limit the effect of other factors. For instance, we need to use the same initial conditions for all sweeps so that we can examine the effect of sweep rate independent of the initial conditions. Trivial initial conditions would be a convenient choice. However, if we use trivial initial conditions, we encounter a problem inherent in the use of a digital computer to model a physical system. With trivial initial conditions, the solution would balance exactly on the trivial solution—even when it is unstable. The system must be perturbed before the

response will diverge from an unstable solution. In a physical system, there are always slight disturbances from wind, geometrical imperfections, etc. that will perturb a system and prevent it from balancing on an unstable solution. For our analysis, we perturb the system with initial conditions which are small but non-zero. Because of this initial disturbance, the response does not become exactly trivial during the sweep; therefore, it cannot balance on the trivial solution when it is unstable.

After we have completed an analysis of the effect of sweep rate on the response with one set of initial conditions, we will repeat the analysis with a different set of small but nontrivial initial conditions. In this way, we can determine the effect of initial conditions on the response. This is also a preliminary step in determining the effect of the noise level on the response because the nontrivial initial conditions are a simple representation of the noise affecting the system.

To examine the nonstationary behavior, we plot the response amplitude against the frequency. However, since ϕ varies linearly with time, the ϕ axis is also a time axis. For reference, we also plot the stationary response curves so that the nonstationary response can be compared to the stationary response at the same values of ϕ. We plot the stationary response curves as dashed lines. Recall that only solutions on the upper curve are stable. Also recall that the trivial solution is stable except in the region around $\phi = 2$ bounded by the intersections of the stationary solution curves with the ϕ axis. For the

integration of equations (2.48) and (2.49) obtained by the method of multiple scales, we plot the response amplitude a that is given by

$$a=\sqrt{p^2+q^2} \tag{3.2}$$

For the integration of the governing equations (2.66), we plot the envelope of the response; that is, the absolute values of the positive and negative peaks for each cycle of the response. Due to the variation with time of the phase and amplitude of the response, these two measures would look slightly different even if the actual response given by both sets of equations were exactly the same. We should keep this in mind when comparing results from the two methods, but since the difference in the measures is small, we will not attempt to convert both results to one measure.

3.1 Forward Frequency Sweep

First, we consider a forward sweep—the excitation frequency increases linearly so that r is positive. In Figure 3.1, we plot the response envelope found by integrating the perturbation equations. We see several unique characteristics of the nonstationary response. First, we note that the response remains trivial even after the excitation frequency has reached values of ϕ at which the stationary trivial response is unstable. This phenomenon is called *penetration*. Next, the response amplitude *jumps* up from the trivial solution

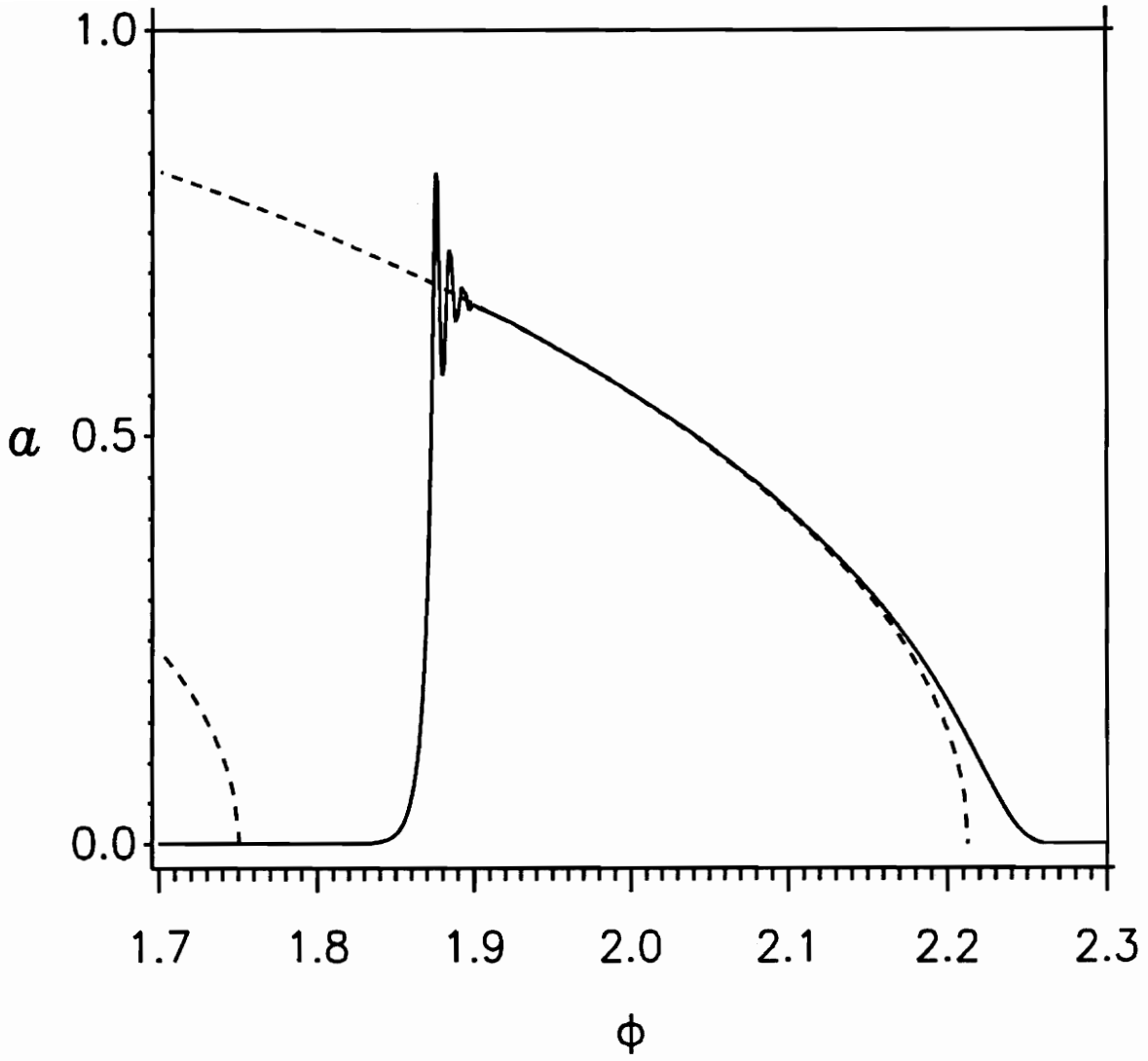

Figure 3.1 Forward frequency sweep. Solid line—nonstationary response found from perturbation equations. Dashed lines—stationary frequency-response curves.
$\alpha = 1.0$, $\mu = 0.05$, $\epsilon = 1.0$, $f = 0.5$, $r = 0.0004$, $p(0) = 0.001$, $q(0) = 0$, and $\phi_0 = 1.7$.

and *overshoots* the stationary frequency-response curve. The response amplitude then *oscillates* about the frequency-response curve. Note that since this oscillation occurs in the envelope of the response, the actual time trace of the response is undergoing a beating phenomenon. As the excitation frequency increases further, the size of the oscillations about the frequency-response curve decreases. This continues until the nonstationary amplitude *converges* to the frequency-response curve. When the response amplitudes become small, the nonstationary response *separates* from the stationary curve and remains nontrivial where the only stationary response is trivial. This is called *lingering* or *drag-out*. Finally, the nonstationary solution converges to the trivial solution. Sometimes, the nonstationary amplitude oscillates about the trivial solution before converging to it.

In Figure 3.2, we again plot the response from the perturbation equations (2.48) and (2.49) as a solid line so that we may compare it to the response found from integration of the original governing equations (2.66), which we plot as a dashed line. Both integrations qualitatively show the same nonstationary phenomena discussed above, and there is only a small quantitative discrepancy between the two. When nonstationary behaviors, such as the jump after penetration, occur, the nontrivial response obtained from the original governing equations occurs slightly after that obtained from the perturbation equations. As discussed previously, part of the discrepancy is due to the difference in amplitude measures. Some of the discrepancy is also due

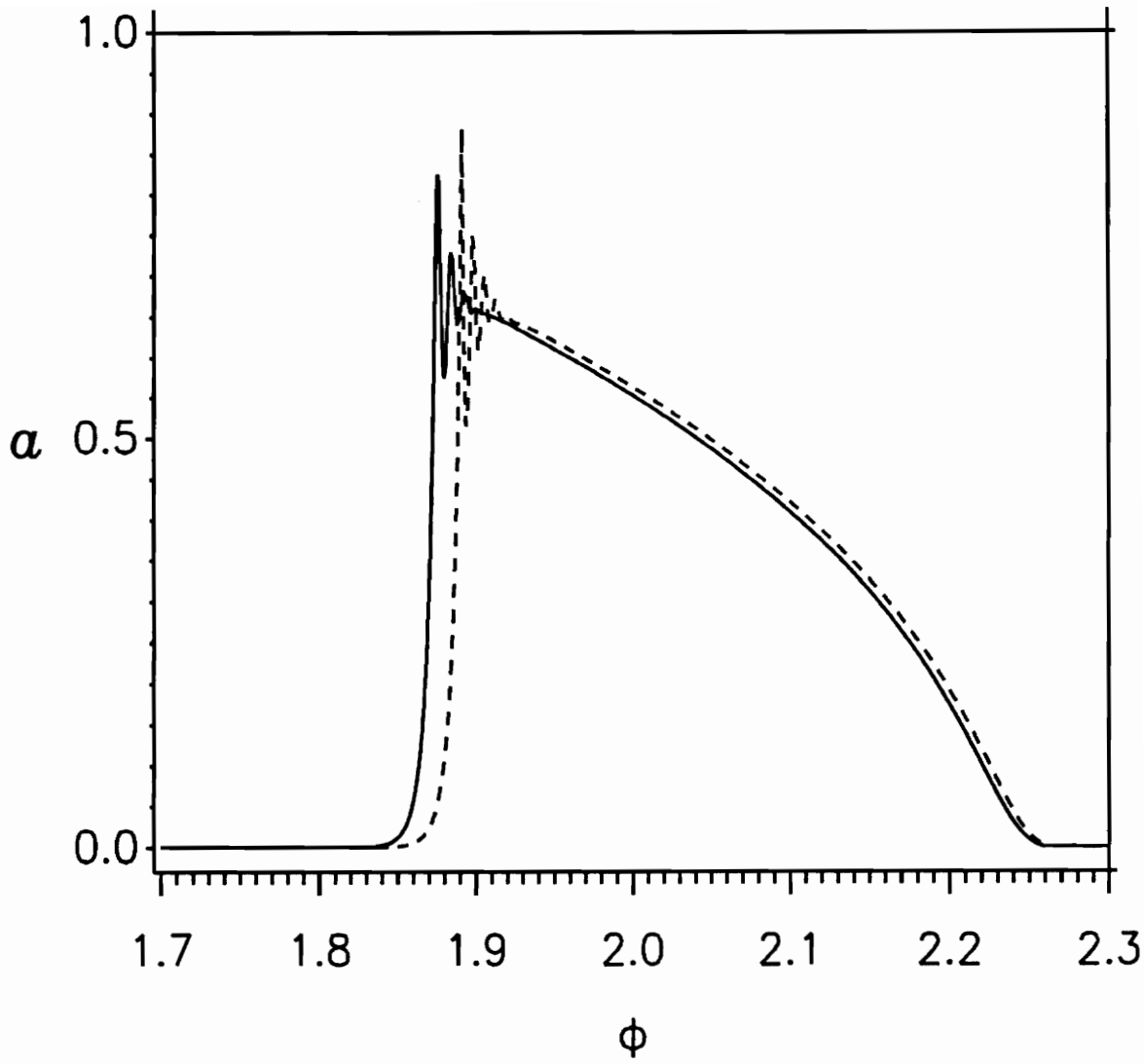

Figure 3.2 Forward frequency sweep. Solid line—nonstationary response found from perturbation equations. Dashed lines—nonstationary response found from original governing equations. $\alpha = 1.0$, $\mu = 0.05$, $\epsilon = 1.0$, $f = 0.5$, $r = 0.0004$, $p(0) = y_1(0) = 0.001$, $q(0) = y_2(0) = 0$, and $\phi_0 = 1.7$.

to approximations that we made when using the method of multiple scales. These approximations cause the perturbation response to shift in time with respect to the actual response.

In Figure 3.3, we plot the maximum amplitude of the response as a function of the sweep rate r. Here, we use the maximum amplitude determined from integrating the original governing equation. Responses are calculated at sweep rates which are multiples of 0.00002. All sweeps are started at the value of ϕ at which the trivial solution changes from stable to unstable, so that all sweeps have the same initial response as they enter this region. The maximum amplitude of the response tends to be smaller for larger sweep rates; however, this relationship is not strictly true for small sweep rates. For small values of r, there is a trend toward smaller maximum amplitudes for larger sweep rates, but the data is scattered. For some sweep rates in this range, a small increase or a small decrease in sweep rate might result in a significant increase in the maximum response amplitude. A series of humps develops in the data for larger sweep rates before the maximum response amplitude becomes a strictly decreasing function of sweep rate. For very slow sweep rates, another behavior is possible. The slow sweep rate can result in little penetration so that the nonstationary solution jumps at a small value of ϕ. The stationary solution is large at the point of jump so that the jump has a large overshoot. Because unbounded solutions exist for the system at this excitation frequency, the large overshoot carries the nonstationary solution to

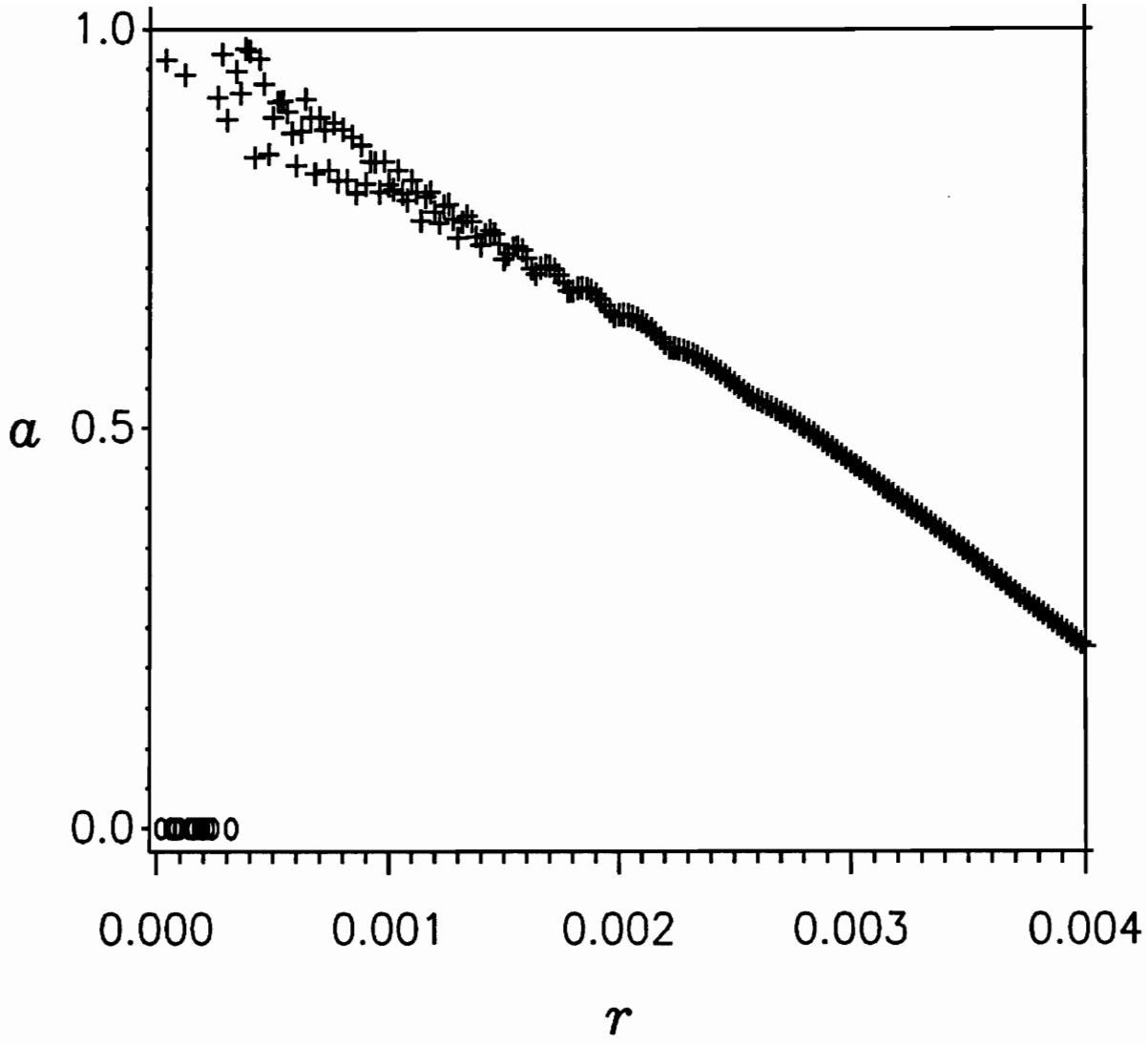

Figure 3.3 Maximum response amplitude versus sweep rate: + denotes maximum response amplitude and 0 denotes a sweep rate for which the response became unbounded.
$\alpha = 1.0$, $\mu = 0.05$, $\epsilon = 1.0$, $f = 0.5$, $\phi_0 = 1.751$, $y_1(0) = 0.001$, and $y_2(0) = 0$.

unboundedness. Sweep rates at which this occurs are denoted with an o in Figure 3.3. Note that when this situation occurs, the response changes from being trivial to unbounded directly or after only one or two cycles. This is a particularly dangerous situation for a physical system since the system goes from rest to failure with almost no warning. The sweep rates for which unboundedness occur are scattered among the sweep rates for which bounded solutions occur. For some small sweep rates that yield a bounded response, both a small increase or a small decrease in the sweep rate will yield an unbounded response.

In Figure 3.4, we again plot maximum response amplitude as a function of sweep rate. However, the set of initial conditions used for all of these sweeps is smaller than the set used for the sweeps of Figure 3.3. For most sweep rates, the smaller initial conditions result in a smaller maximum amplitude, although this is not always true for small sweep rates. With smaller initial conditions, there are fewer sweep rates at which unboundedness occur, although unboundedness does occur at some sweep rates for which a bounded response occurs with larger initial conditions. With these initial conditions and large sweep rates, note that the response *sweeps through*, barely growing from the initial conditions and having an essentially trivial maximum response amplitude.

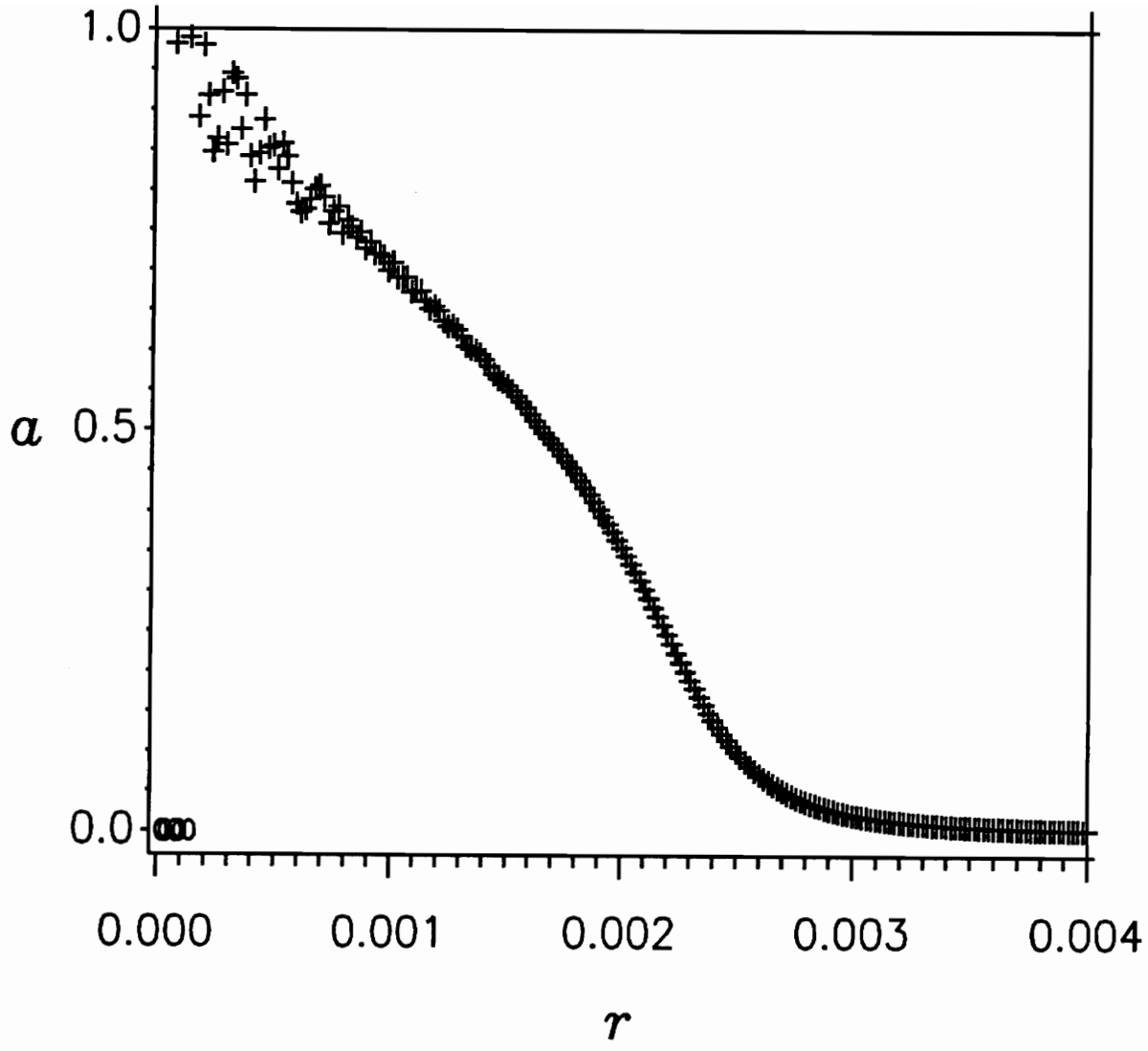

Figure 3.4 Maximum response amplitude versus sweep rate: + denotes maximum response amplitude and o denotes a sweep rate for which the response became unbounded.
$\alpha = 1.0$, $\mu = 0.05$, $\epsilon = 1.0$, $f = 0.5$, $\phi_0 = 1.751$,
$y_1(0) = 0.00001$, and $y_2(0) = 0$.

3.2 Reverse Frequency Sweep

Now we consider a reverse sweep in which the excitation frequency decreases, that is, r is negative. In Figure 3.5, we again plot the stationary frequency-response curves as dashed lines for reference, and we plot the nonstationary response found from the perturbation equations (2.48) and (2.49) as a solid line. Note, however, that time increases from *right to left* in this figure since ϕ is a linearly decreasing function of time. The same nonstationary characteristics that appear in the forward sweep are again evident in the response. The nonstationary response penetrates into the region where the stationary trivial solution is unstable. Then the nonstationary response jumps up and overshoots the frequency-response curve. The overshoot is very small for this sweep rate, and the convergence to the frequency-response curve occurs very quickly. There is no lingering here since the solutions do not become trivial again. In Figure 3.6, we show the response obtained from integrating the perturbation equations as a solid line and the response obtained from integrating the original governing equations (2.66) as a dashed line. Again, agreement between the two methods is good, but only up to a certain value of ϕ. Beyond this value, a qualitative change occurs in the response obtained from integrating the original governing equations, and then that solution goes unbounded.

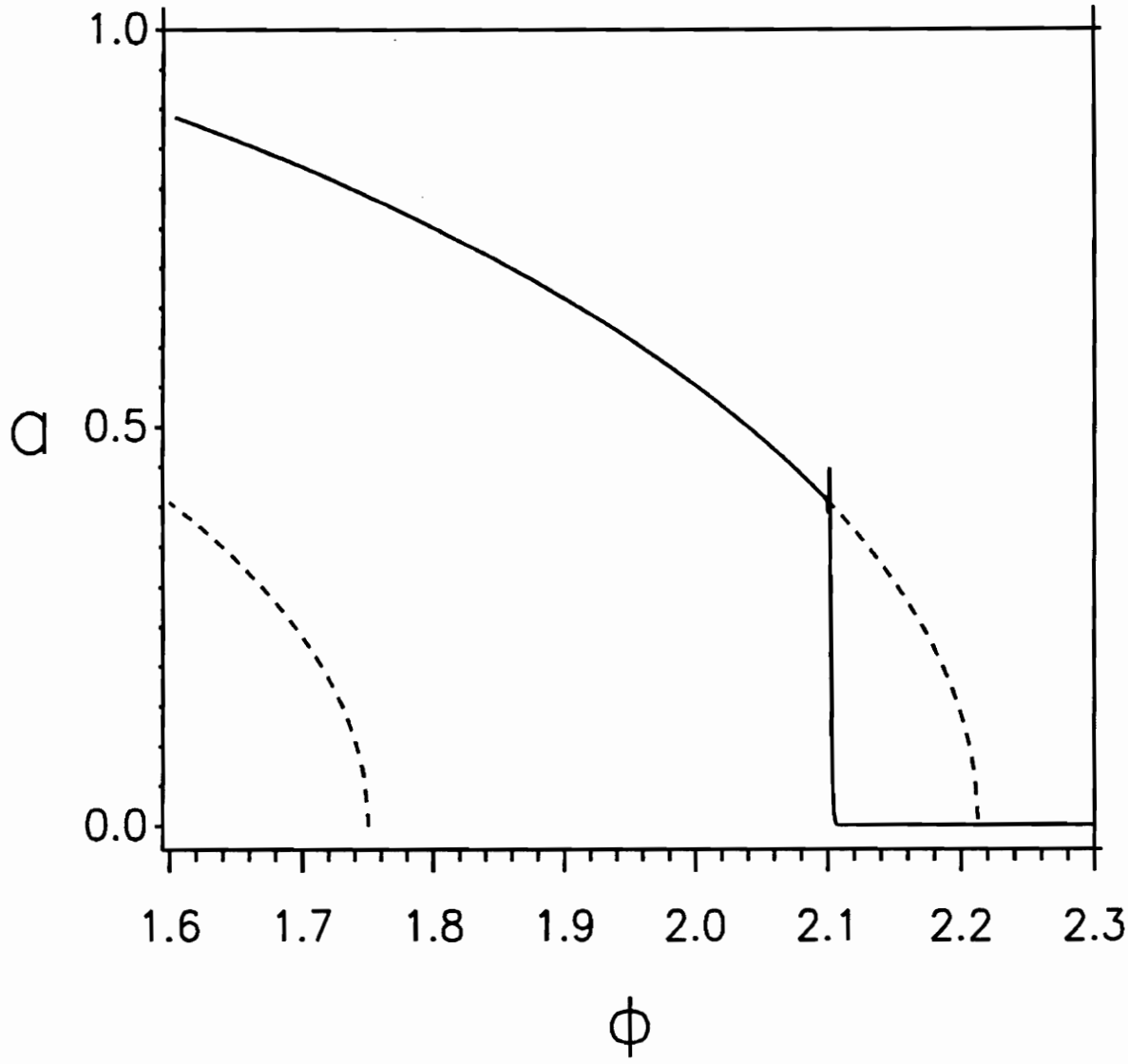

Figure 3.5 Reverse frequency sweep. Solid line—nonstationary response found from perturbation equations. Dashed lines—stationary frequency-response curves.
$\alpha = 1.0$, $\mu = 0.05$, $\epsilon = 1.0$, $f = 0.5$, $r = -0.00005$, $p(0) = 0.001$, $q(0) = 0$, and $\phi_0 = 2.3$.

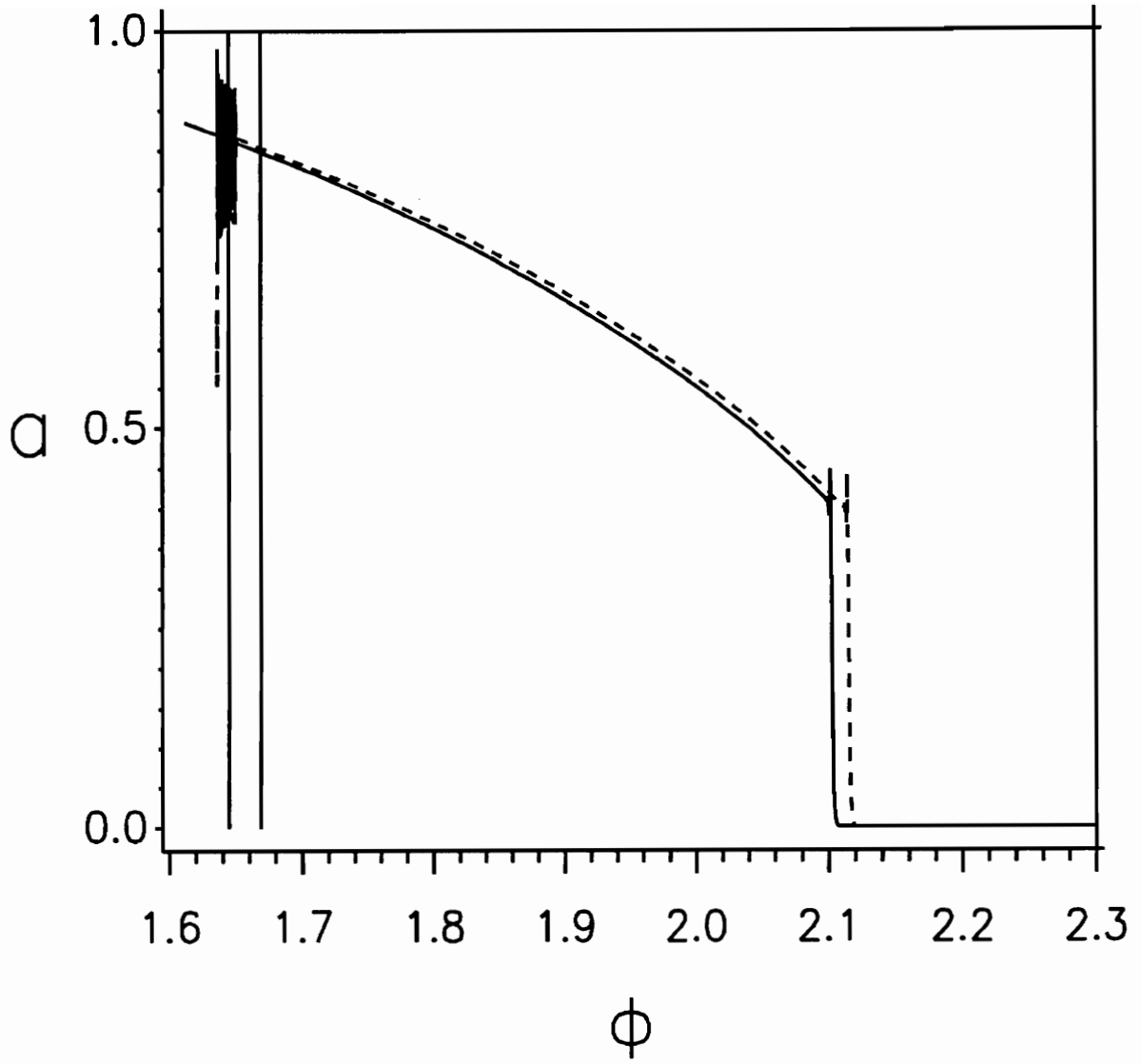

Figure 3.6 Reverse frequency sweep. Solid line—nonstationary response found from perturbation equations. Dashed lines—nonstationary response found from original governing equations. $\alpha = 1.0$, $\mu = 0.05$, $\epsilon = 1.0$, $f = 0.5$, $r = -0.00005$, $p(0) = y_1(0) = 0.001$, $q(0) = y_2(0) = 0$, and $\phi_0 = 2.3$.

To understand this behavior, we recall the Floquet analysis of the stationary solution performed in the last chapter. As ϕ decreases, the stationary solution undergoes a symmetry-breaking bifurcation, followed by a sequence of period doublings, and chaos before going unbounded. We have seen a correspondence between the stationary and nonstationary behaviors thus far in our work; therefore, we might expect the nonstationary solution to have some correspondence to these behaviors occurring in the stationary solution. Keeping this in mind to help us interpret the nonstationary response, we see behaviors analogous to symmetry breaking and period doubling in the nonstationary response before it becomes unbounded.

Because we plot the envelope of the response from the original governing equations (that is, we plot the absolute value of every extremum of the response, both maximum and minimum), when symmetry breaking occurs, two distinct points are generated for each cycle. Therefore, symmetry breaking appears as a short wedge, as shown in Figure 3.6. Note that as ϕ decreases, the distance between the maximum and minimum tends to increase. Note also that when symmetry breaking appears, the difference between the absolute values of the maximum and minimum is already large; this suggests the response jumps to the asymmetric solution rather than evolving from the symmetric solution with a slowly increasing asymmetry. From the Floquet analysis, the stationary symmetric response becomes unstable at $\phi = 1.669$, at which point symmetry breaking occurs. We mark this value in Figure 3.6

with a vertical line. In the nonstationary response, the onset of symmetry breaking is delayed to a lower value of ϕ. This suggests that the nonstationary response remains symmetric in a region where the stationary symmetric response is unstable. The first cycles after symmetry breaking occurs have a greater difference between the absolute values of the maximum and minimum than the immediate succeeding cycles. This suggests that, as in the previously studied nonstationary behavior, there is a penetration, jump, and overshoot behavior associated with symmetry breaking. After several cycles of growing difference between the absolute values of the maximum and minimum, the response begins to change again and then quickly becomes unbounded.

We see the last stages of the response in the time trace plotted in Figure 3.7, generated by integrating the original governing equation. Note that time increases as ϕ decreases from left to right in this figure. In the leftmost portion of this figure, the response is symmetric. Around $\phi = 1.650$, the response suddenly becomes asymmetric. At first, the size of the asymmetry changes substantially from cycle to cycle (suggesting a nonstationary overshoot and oscillation behavior in the size of the asymmetry), but around $\phi = 1.645$, the size of the asymmetry only grows slightly from cycle to cycle. At around $\phi = 1.642$, the response changes and begins to resemble that of a system which has undergone a period-doubling bifurcation. (We refer to this change in the nonstationary response as a *quasi*-period-doubling bifurcation because the nonstationary response has an infinite period.) Finally, the response

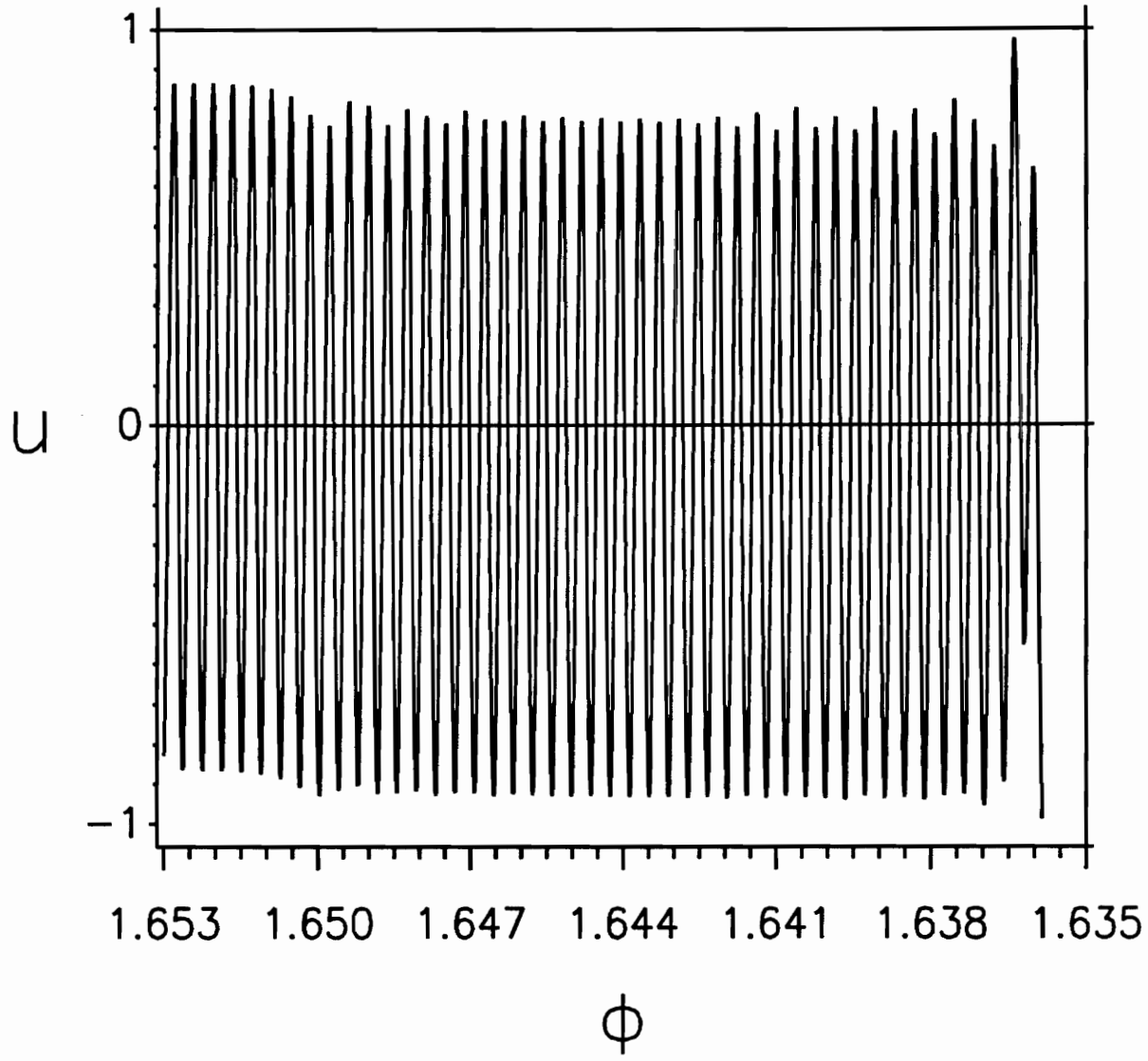

Figure 3.7 Time trace of a reverse frequency sweep. $\alpha = 1.0$, $\mu = 0.05$, $\epsilon = 1.0$, $f = 0.5$, $r = -0.00005$, $y_1(0) = 0.001$, $y_2(0) = 0$, and $\phi_0 = 2.3$.

changes rapidly in the last cycles before going unbounded. Because of the nonstationary nature of the response, it is difficult to identify and distinguish these behaviors. For faster sweep rates, this would be more difficult, as both the asymmetry and the quasi-period-doubling bifurcation occur for only a few cycles before the solution goes unbounded.

Floquet theory predicts that the asymmetric stationary solution becomes unstable at $\phi = 1.645$, at which point period doubling occurs. (We mark this value in Figure 3.6 with a vertical line.) As with symmetry breaking, the quasi-period-doubling bifurcation is delayed in the nonstationary response, occurring at a value of ϕ smaller than that in the case of the stationary response. This is another example of a nonstationary behavior, in this case the asymmetric solution, penetrating into a region where the corresponding stationary response is unstable.

In Figure 3.8, we plot ϕ_∞ versus the sweep rate r for reverse sweeps, where ϕ_∞ is the value of ϕ at which the response exceeds some large chosen value as it goes unbounded. All sweeps are started at the value of ϕ at which the trivial solution changes from stable to unstable, so that all sweeps have the same initial response as they enter this region. For reference, we mark $\phi = 1.645$, the value of ϕ at which period doubling is predicted to occur in the stationary solution, with a horizontal line and use it as an estimate of the value of ϕ at which the stationary solution becomes unbounded. For slow sweeps, ϕ_∞ tends to decrease as the absolute sweep rate $|r|$ increases. For sweeps in

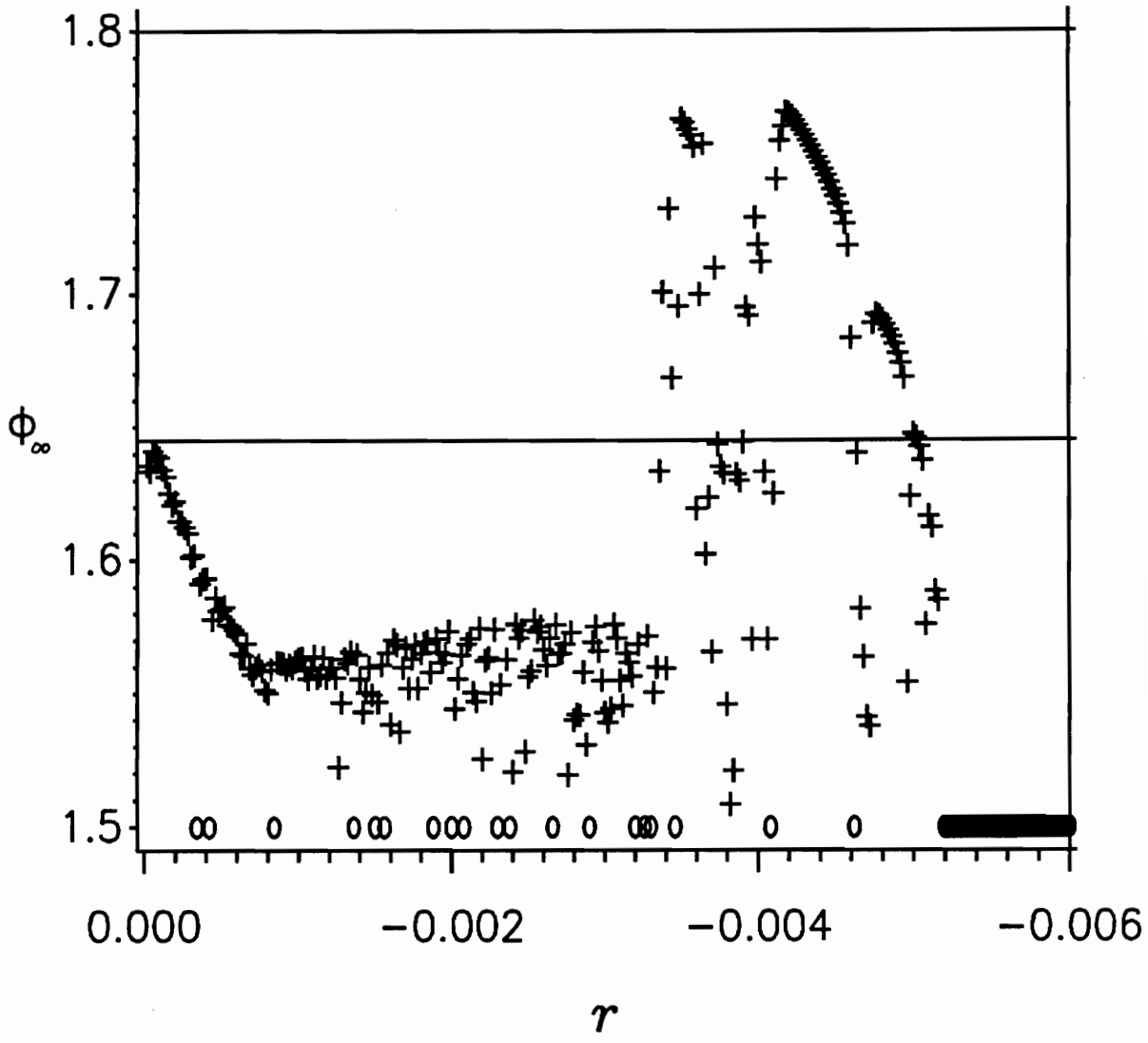

Figure 3.8 ϕ_∞ versus sweep rate: + denotes value of ϕ at which the response magnitude exceeded 4 as the response became unbounded and o denotes a sweep rate for which the response remained bounded.
$\alpha = 1.0$, $\mu = 0.05$, $\epsilon = 1.0$, $f = 0.5$, $\phi_0 = 2.212$,
$y_1(0) = 0.001$, and $y_2(0) = 0$.

this range of r, unboundedness is delayed to a value of ϕ less than that at which unboundedness occurs in the stationary case. Considering faster sweeps, in the succeeding range of sweep rates, the data is more scattered. There is no definite trend for increasing or decreasing ϕ_∞ as $|r|$ is increased. For even faster sweep rates in the next range of r, ϕ_∞ is generally larger than in the previous ranges of r. In this range, ϕ_∞ tends to decrease for larger $|r|$, and for some sweep rates, ϕ_∞ is significantly smaller than for similar sweep rates. But for most of the sweep rates in this region, the response becomes unbounded at a value of ϕ *larger* than that at which the stationary response is unbounded. This would be an important consideration in the design of a system subjected to nonstationary excitations because an analysis that assumes a stationary excitation would predict the response to be bounded for values of ϕ where the nonstationary response is unbounded.

For many sweep rates, the response remains bounded. We mark these sweep rates with an o in Figure 3.8. For all sweep rates faster than a certain value of r, the response sweeps through—the response never jumps up to the stationary frequency-response curve; instead it remains small throughout the sweep.

For some slow sweep rates, the response remains bounded, although it does not sweep through. For these sweep rates, the response penetrates, jumps up, oscillates about (and, for slow sweep rates, converges to) the stationary frequency-response curve. When ϕ reaches the range of values for

which the response to similar sweep rates becomes unbounded, the response to these sweep rates jumps down and converges to the trivial solution, which is stable for this range of ϕ. We plot the envelope of the amplitude of the response, found from integration of the original governing equations, for one such sweep in Figure 3.9. In this figure, time increases right to left. We plot the stationary frequency-response curves as dashed lines in this figure for reference. The values of ϕ at which the stationary solution becomes asymmetric and undergoes period doubling are marked with vertical lines, as in Figure 3.6. This type of response is very sensitive to changes in the sweep rate. A small increase or decrease in the sweep rate can change this type of response from bounded to unbounded. Note that the sweep rates for which this behavior occurs are scattered among those for which unboundedness occurs. Therefore, it is not safe to find a sweep rate that results in a bounded response and then assume that all faster sweep rates also will result in a bounded response.

In Figure 3.10, we repeat the sweep-rate analysis using a smaller set of initial conditions than we used for the sweeps of Figure 3.8. The first range of r, in which ϕ_∞ decreased for larger $|r|$, is very similar to that in Figure 3.8. The second range of r, in which there was no definite trend in ϕ_∞, and the third range of r, in which ϕ_∞ was much larger, are both smaller than the corresponding ranges in Figure 3.8. With smaller initial conditions, sweep through occurs at slower sweep rates.

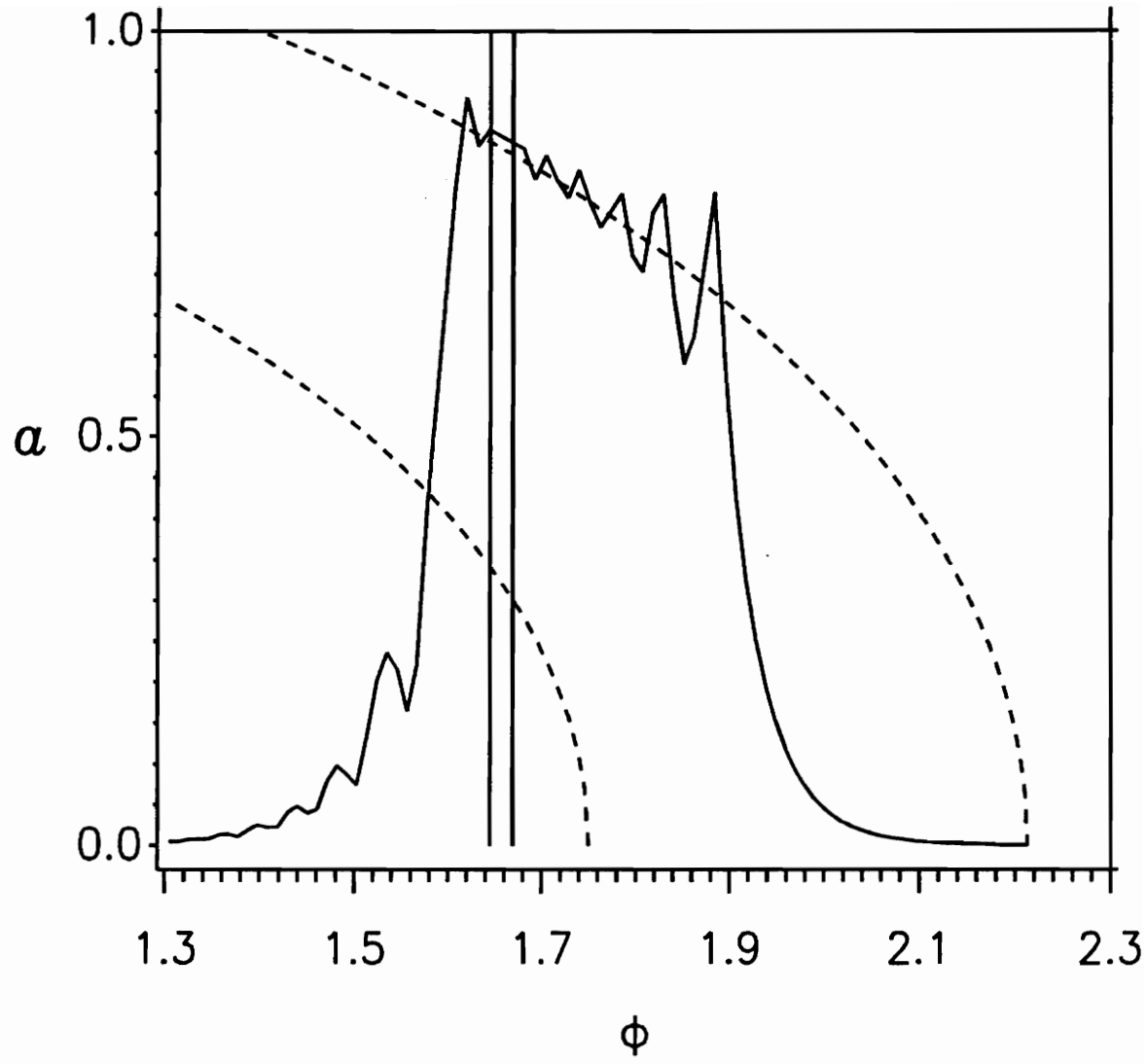

Figure 3.9 Reverse frequency sweep. Solid line—nonstationary response found from original governing equations. Dashed lines—stationary frequency-response curves.
$\alpha = 1.0$, $\mu = 0.05$, $\epsilon = 1.0$, $f = 0.5$, $r = -0.00084$, $y_1(0) = 0.001$, $y_2(0) = 0$, and $\phi_0 = 2.212$.

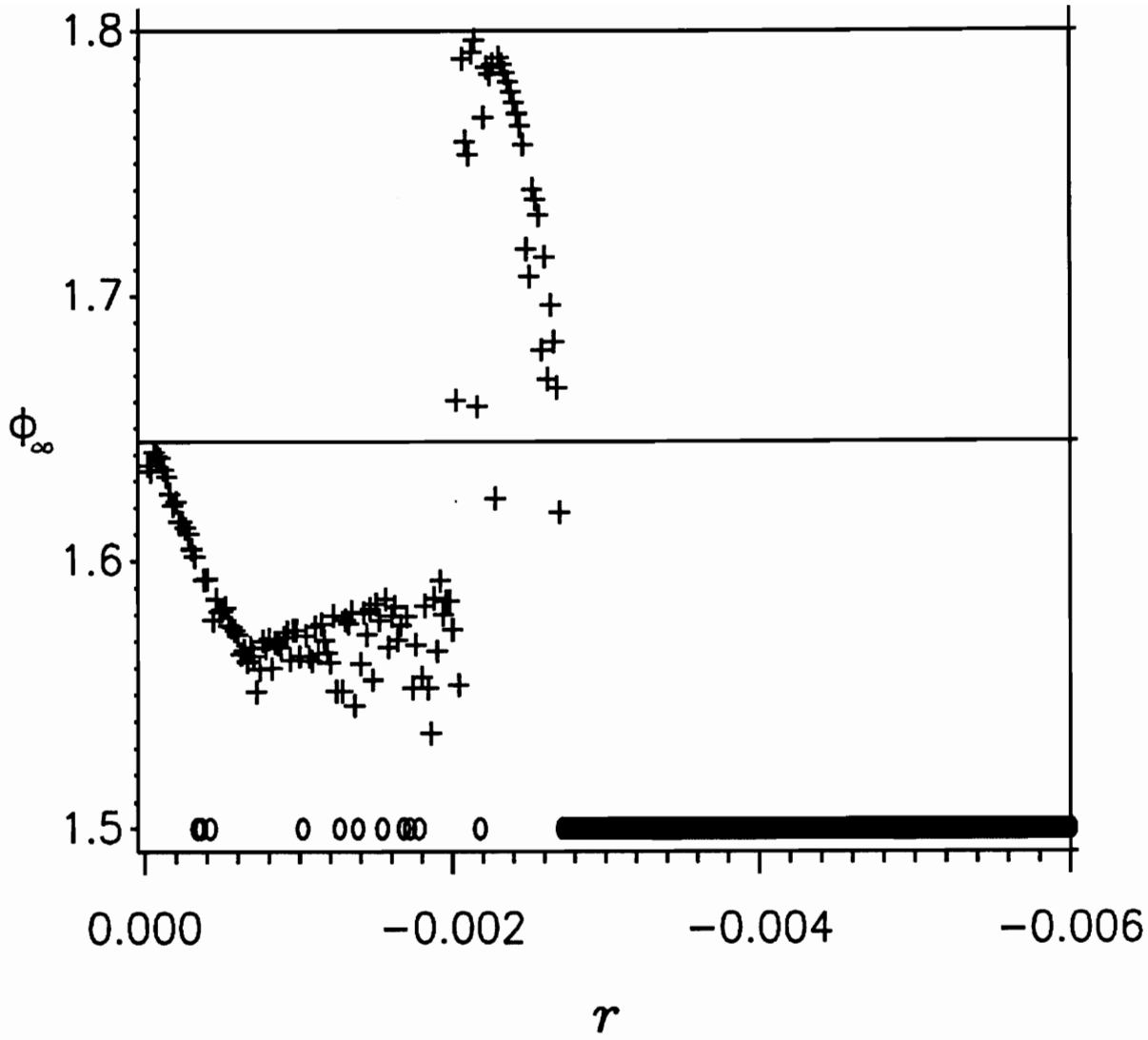

Figure 3.10 ϕ_∞ versus sweep rate: + denotes value of ϕ at which the response magnitude exceeded 4 as the response became unbounded and 0 denotes a sweep rate for which the response remained bounded.
$\alpha = 1.0$, $\mu = 0.05$, $\epsilon = 1.0$, $f = 0.5$, $\phi_0 = 2.212$,
$y_1(0) = 0.00001$, and $y_2(0) = 0$.

In general, for both forward and reverse sweeps, larger sweep rates result in increased penetration of the trivial solution. The size of the overshoot and the size of the oscillations about the stationary frequency-response curve increase in proportion to the magnitude of the stationary frequency-response curve at the jump point. For forward sweeps and softening nonlinearity, the magnitude of the stationary response at the jump point will be smaller for larger r because faster sweeps have larger penetrations. Analogously, for reverse sweeps, the magnitude of the stationary response at the jump point will be larger with increasing $|r|$.

The nonstationary response will not converge to the frequency-response curve if $|r|$ is large. Instead, the solution changes directly from being trivial or from oscillating about the stationary frequency-response curve to lingering or unboundedness. The amount of lingering, which depends on the size and rate of change of the response when lingering begins, varies in a complicated manner with r. These nonstationary behaviors can vary widely, quantitatively and qualitatively, for only small changes in r.

Although we have noted some general effects of the sweep rate on penetration, lingering, overshoot etc., we must remember that the effect of the sweep rate on the nonstationary behavior is very complex, as shown in Figures 3.3, 3.4, 3.8, and 3.10.

CHAPTER 4

Amplitude Sweeps

Now we turn our attention from frequency sweeps to sweeps of the excitation amplitude. The procedure is similar to that carried out in Chapter 3, except now ϕ is a constant, and the excitation amplitude f is a linear function of time given by (1.3), or by

$$f=f_0+s\epsilon^2 t \tag{4.1}$$

where s is the sweep rate. The scaling of f is consistent with (3.1). Again, we set ϵ equal to unity because it was used only as a bookkeeping device in the perturbation analysis.

We integrate the Cartesian form of the perturbation equations (2.48) and (2.49) using a digital computer to generate force-response curves. We also integrate the original governing equations (2.66) and plot the envelope of the response. For amplitude sweeps, the f axis is also a time axis because f varies linearly with time. As with frequency sweeps, we perturb the system with

small nontrivial initial conditions to prevent the response from balancing on the trivial solution when it is unstable.

The nonstationary response to amplitude sweeps can be divided into two cases, depending on the excitation frequency: ϕ greater than or equal to two and ϕ less than two. For each case, we consider forward ($s > 0$) and reverse ($s < 0$) sweeps.

4.1 Excitation Frequency Greater than Two

In this case, the stationary force-response curve consists of only one branch, which is stable, as shown in Figure 2.5. We plot this curve for reference as a dashed line. We also recall that the trivial solution is stable up to the intersection of this curve with the f axis and is unstable for all larger values of f. In Figure 4.1, we plot as a solid line the nonstationary response found from integration of the perturbation equations (2.48) and (2.49) for a forward sweep ($s > 0$). The same nonstationary behaviors that occur in frequency sweeps are present in the nonstationary responses to amplitude sweeps. First, the nonstationary response remains trivial and penetrates into the range of f where the stationary trivial solution is unstable. Then, the nonstationary amplitude jumps up, overshoots the stationary force-response curve, and oscillates about it so that the time trace of u would have a beating

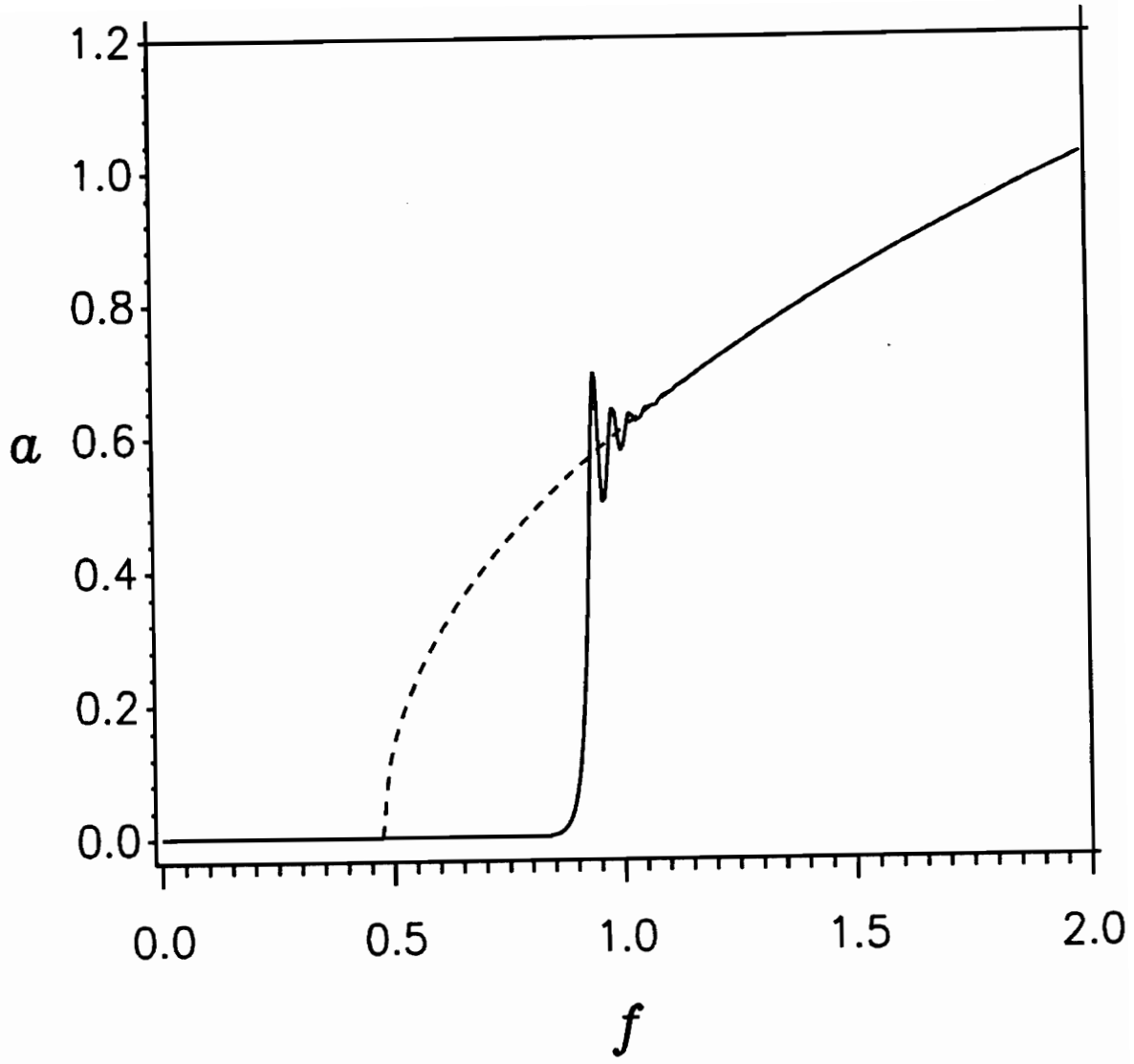

Figure 4.1 Forward amplitude sweep. Solid line—nonstationary response found from perturbation equations. Dashed lines—stationary frequency-response curves.
$\alpha = 1.0$, $\mu = 0.05$, $\epsilon = 1.0$, $\phi = 2.2$, $s = 0.002$,
$p(0) = 0.001$, $q(0) = 0$, and $f_0 = 0.0$.

nature. As f increases further, the size of the oscillations diminishes, and the nonstationary amplitude converges to the stationary force-response curve. There is no lingering here because the solutions do not become trivial again. For forward sweeps, penetration tends to increase for larger values of s. This results in larger jumps, larger oscillations of the response amplitude, and a longer time interval for convergence to the stationary force-response curve.

In Figure 4.2, we repeat the nonstationary response obtained from the perturbation equations as a solid line and plot the nonstationary response found from integrating the original governing equations (2.66) as a dashed line. There is good agreement up to a certain value of f, but the discrepancy between the solutions grows as f gets larger. (Recall that in the method-of-multiple-scales analysis, we assumed that f was small.) Then the response obtained from the original governing equations appears to undergo a symmetry-breaking bifurcation and then quasi-period-doubling bifurcations all within a few cycles before going unbounded. This is better seen in the time trace found from the original governing equations that we plot in Figure 4.3. It is difficult to identify these behaviors because they are short-lived. For a slower sweep rate, the asymmetry would extend for several cycles as it did in the frequency sweep of Figure 3.7. Floquet theory predicts that symmetry breaking occurs in the stationary solution at $f = 1.433$, and that the asymmetric stationary solution becomes unstable at $f = 1.490$. (Again we use the value of f at which the asymmetric stationary solution becomes unstable as an estimate of the value

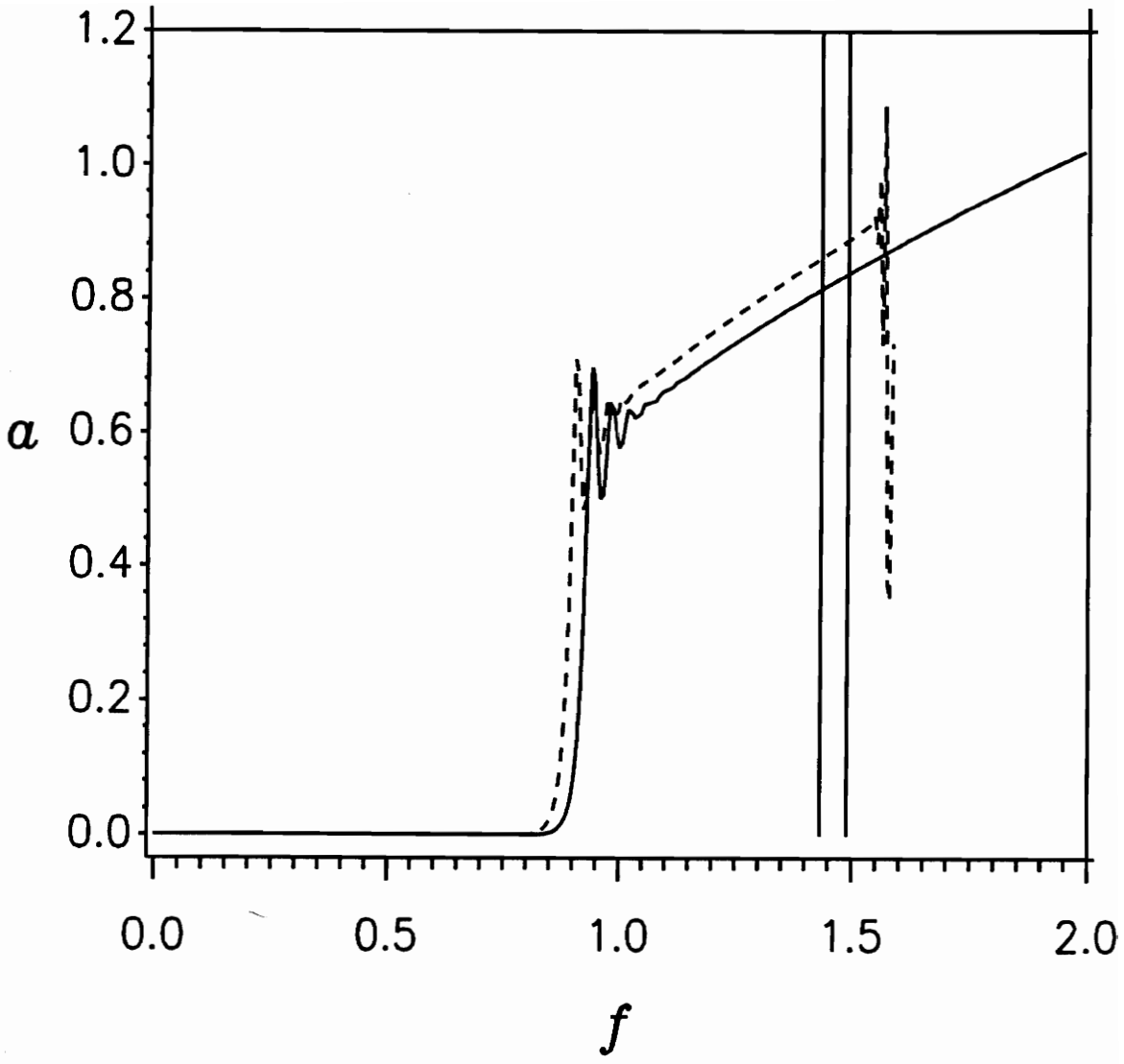

Figure 4.2 Forward amplitude sweep. Solid line—nonstationary response found from perturbation equations. Dashed lines—nonstationary response found from original governing equations. $\alpha = 1.0$, $\mu = 0.05$, $\epsilon = 1.0$, $\phi = 2.2$, $s = 0.002$, $p(0) = y_1(0) = 0.001$, $q(0) = y_2(0) = 0$, and $f_0 = 0.0$.

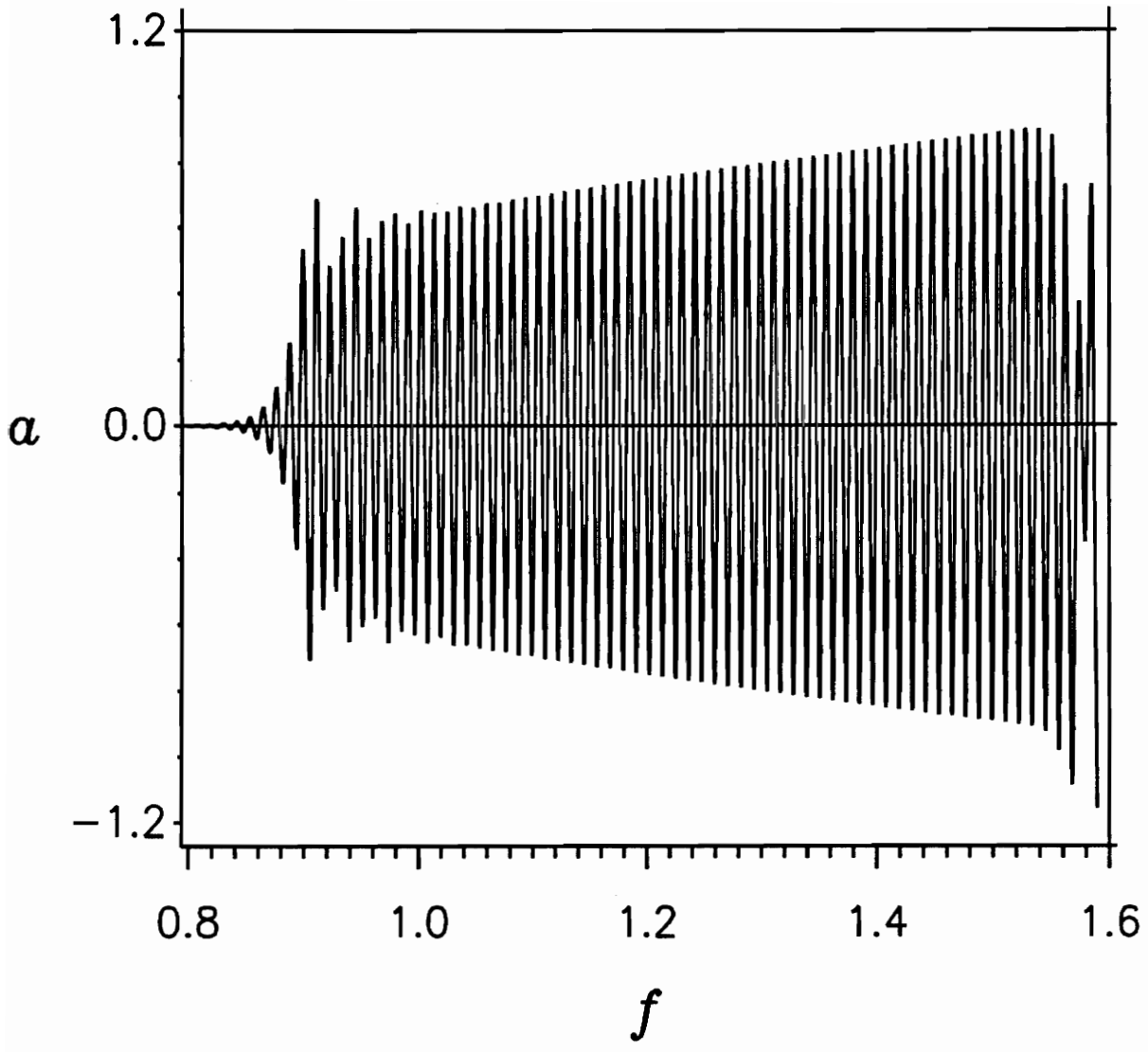

Figure 4.3 Time trace of a forward amplitude sweep. $\alpha = 1.0$, $\mu = 0.05$, $\epsilon = 1.0$, $\phi = 2.2$, $s = 0.002$, $y_1(0) = 0.001$, $y_2(0) = 0$, and $f_0 = 0.0$.

of f at which the solution becomes unbounded.) We mark these values by vertical lines in Figure 4.2. Note that both symmetry breaking and unboundedness occur at values of f higher than those in the case of the stationary response.

In Figure 4.4, we plot f_∞ as a function of the sweep rate s for forward sweeps, where f_∞ is the value of f at which the response exceeds some chosen value as it becomes unbounded. We mark the value of f at which period doubling occurs in the stationary solution with a horizontal line in Figure 4.4 and use it as an estimate of the value of f at which unboundedness occurs in the stationary solution. Responses are calculated at sweep rates which are multiple of 0.0002. All sweeps are started at the value of f at which the trivial solution changes from stable to unstable, so that all sweeps have the same response as they enter this region. For a range of small values of s, the response jumps up and *converges* to the stationary curve *before* it undergoes a symmetry-breaking bifurcation, quasi-period-doubling bifurcations, and chaos, on its way to becoming unbounded. The nonstationary solution has no wide amplitude swings that might carry it to unboundedness prematurely. This allows the nonstationary response to penetrate into the region of f where the stationary solution is unbounded. This type of response occurs for the leftmost part of Figure 4.4, where the data points lie above the horizontal line. The sweeps of Figures 4.2 and 4.3 are examples of this type of behavior. Considering faster sweeps, in the next range of sweep rates, the size of the

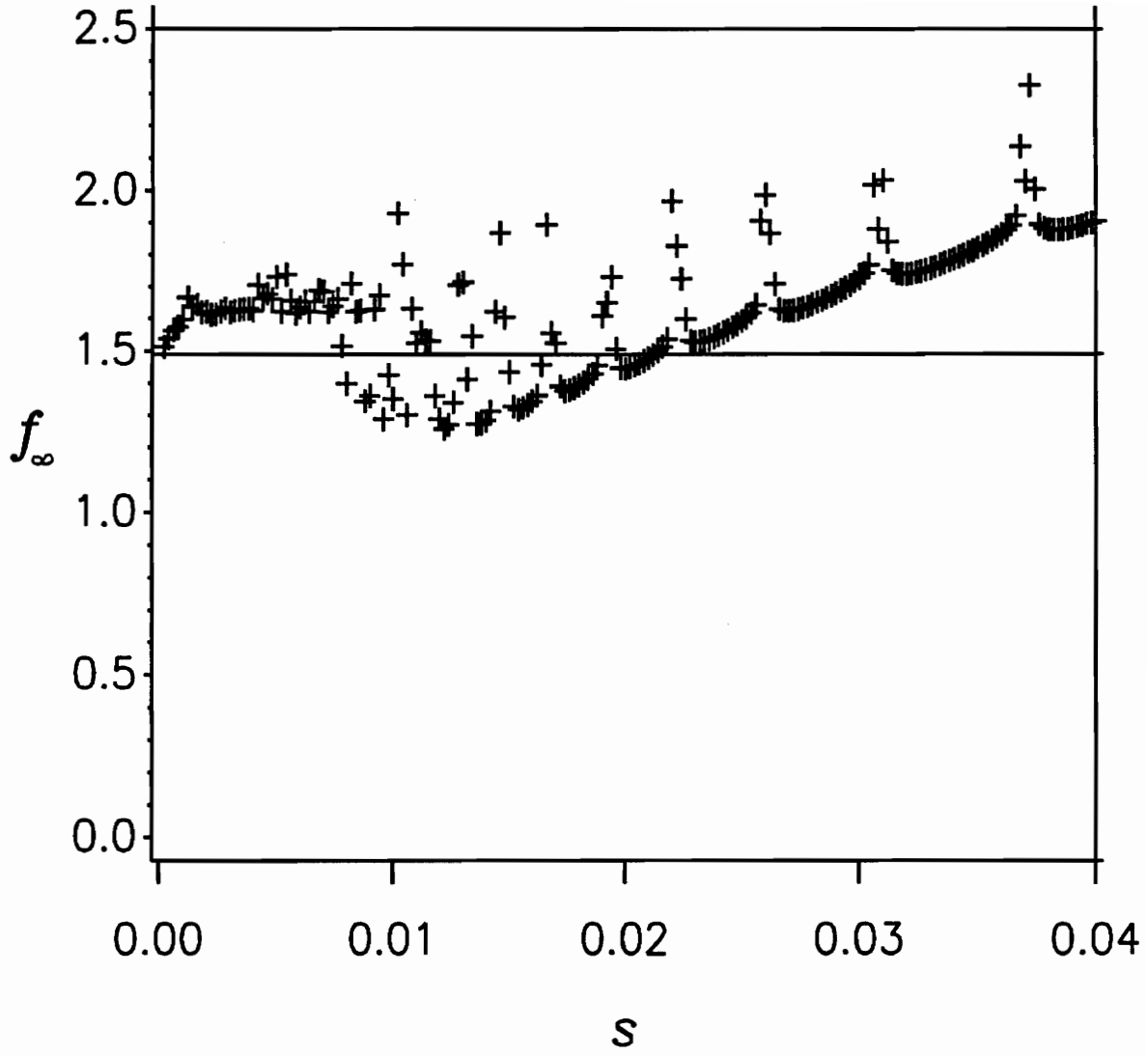

Figure 4.4 f_∞ versus sweep rate: + denotes value of f at which the response magnitude exceeded 3 as the response became unbounded. $\alpha = 1.0$, $\mu = 0.05$, $\epsilon = 1.0$, $\phi = 2.2$, $f_0 = 0.475$, $y_1(0) = 0.001$, and $y_2(0) = 0$.

jump or of the oscillations about the stationary force-response curve can carry the response to unboundedness. For many of these sweep rates, the nonstationary response becomes unbounded at values of f smaller than those at which unboundedness occurs in the stationary case, and f_∞ drops below the horizontal line. For a system undergoing sweeps with these sweep rates, it is dangerous to use the value of f at which the stationary solution becomes unbounded as a design estimate. However, for larger sweep rates, f_∞ always exceeds the value of f at which the stationary solution goes unbounded. In this range of s, the nonstationary response penetrates greatly before changing from trivial to unbounded in only a few cycles. In general for large s, f_∞ tends to increase with s because the penetration increases with s. Note, however, the existence of values of s that have much larger values of f_∞ than the surrounding smaller or larger sweep rates. Thus, f_∞ is very sensitive to the sweep rate.

In Figure 4.5, we repeat the sweep rate analysis using a set of initial conditions smaller than those used for the sweeps of Figure 4.4. The range of small sweep rates, for which f_∞ exceeds the value of f at which the stationary solution goes unbounded, is smaller in this case, although the values of f_∞ are similar. The sweep rate for which all faster sweeps yield points above the horizontal line is smaller than in Figure 4.4. For a given sweep rate, f_∞ tends to be larger in this case because the smaller initial conditions allow greater penetration of the trivial solution.

Now we consider reverse amplitude sweeps (i.e., negative s). Since

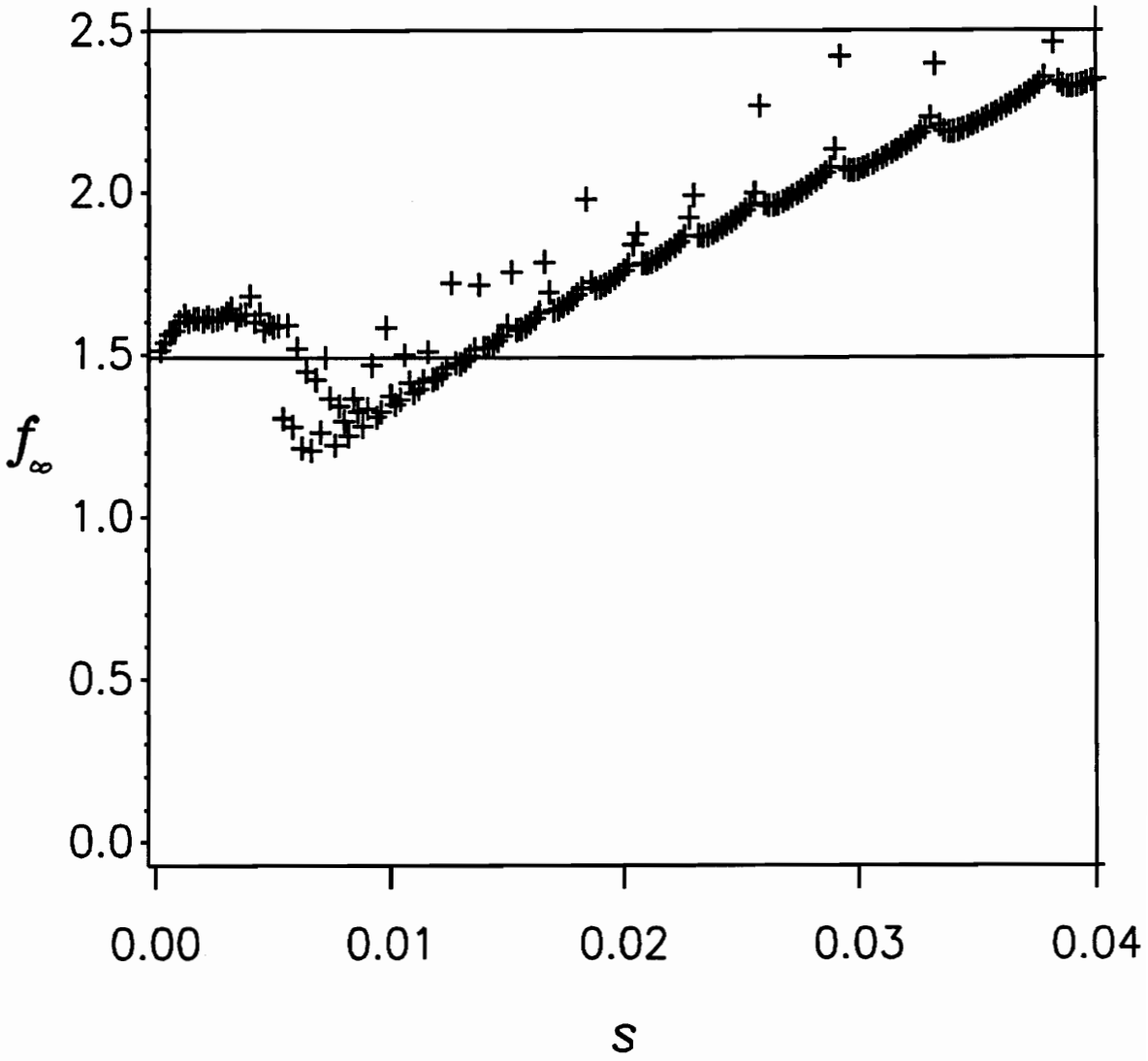

Figure 4.5 f_∞ versus sweep rate: + denotes value of f at which the response magnitude exceeded 3 as the response became unbounded. $\alpha = 1.0$, $\mu = 0.05$, $\epsilon = 1.0$, $\phi = 2.2$, $f_0 = 0.475$, $y_1(0) = 0.00001$, and $y_2(0) = 0$.

these sweeps begin where the trivial solution is unstable, the nonstationary response jumps soon after the sweep begins. The sizes of the jump and overshoot depend on the value of f at which the sweep begins; the sizes tend to be larger for larger starting values of f. The initial jump is large enough to take the solution directly to unboundedness in many circumstances. In other cases, the response jumps up, oscillates about, and converges to the stationary force-response curve. When the response becomes small, it separates from this curve and lingers. In Figure 4.6, we plot the result of integrating the perturbation equations for such a sweep as a solid line and plot the stationary force-response curve as a dashed line for reference. Remember that since this is a reverse sweep, time increases from right to left. In Figure 4.7, we repeat the perturbation result as a solid line, and plot the result of integrating the original governing equations as a dashed line. The agreement between the two methods is good and gets better as f gets smaller. For faster sweep rates, the nonstationary response may never converge to any nontrivial stationary solution; instead it goes directly from an oscillation about the stationary force-response curve to lingering. For some reverse sweeps, the nonstationary solution continues lingering so long that it is nontrivial even after the excitation amplitude has reached zero.

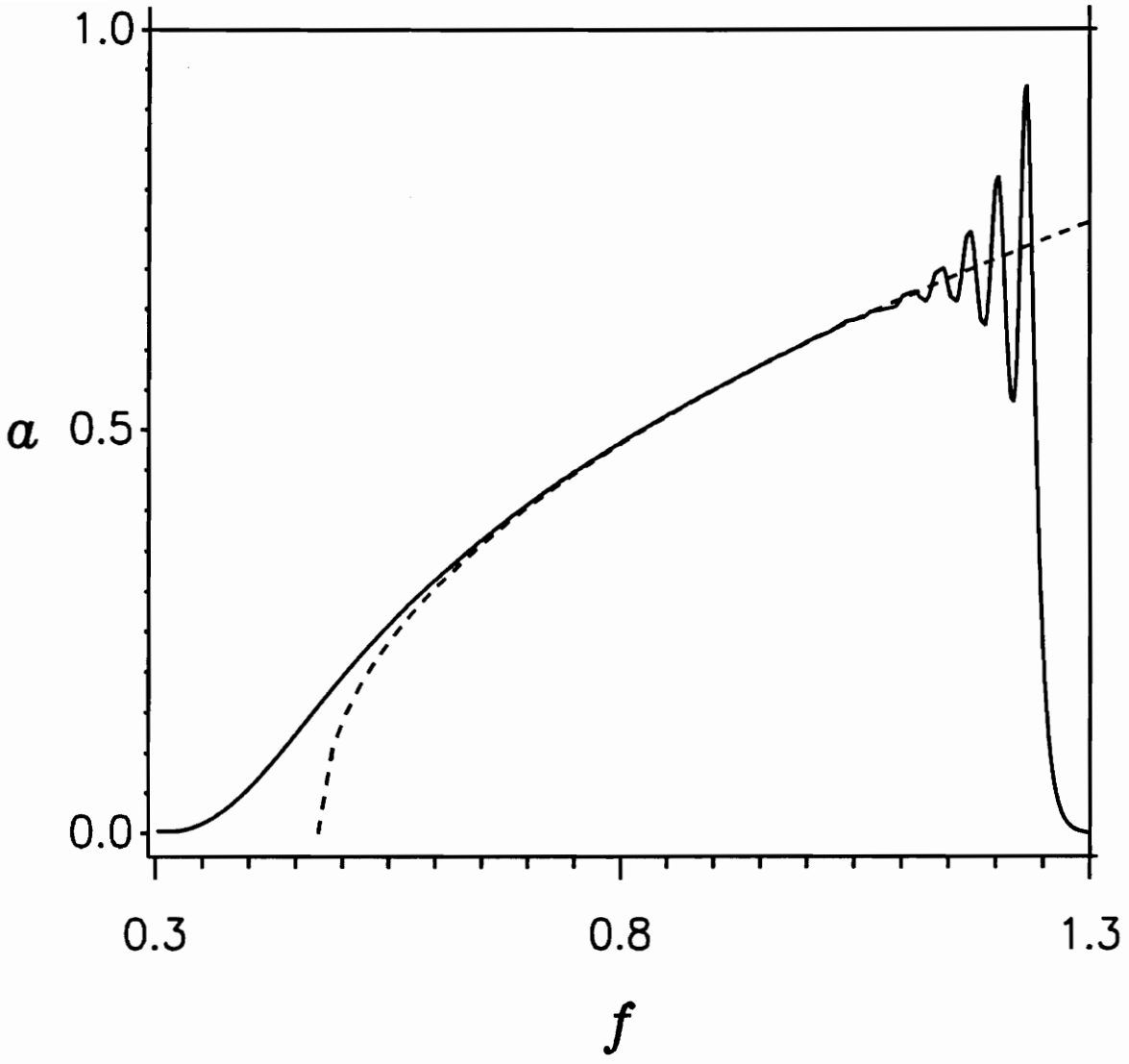

Figure 4.6 Reverse amplitude sweep. Solid line—nonstationary response found from perturbation equations. Dashed lines—stationary frequency-response curves.
$\alpha = 1.0$, $\mu = 0.05$, $\epsilon = 1.0$, $\phi = 2.2$, $s = -0.002$,
$p(0) = 0.001$, $q(0) = 0$, and $f_0 = 1.3$.

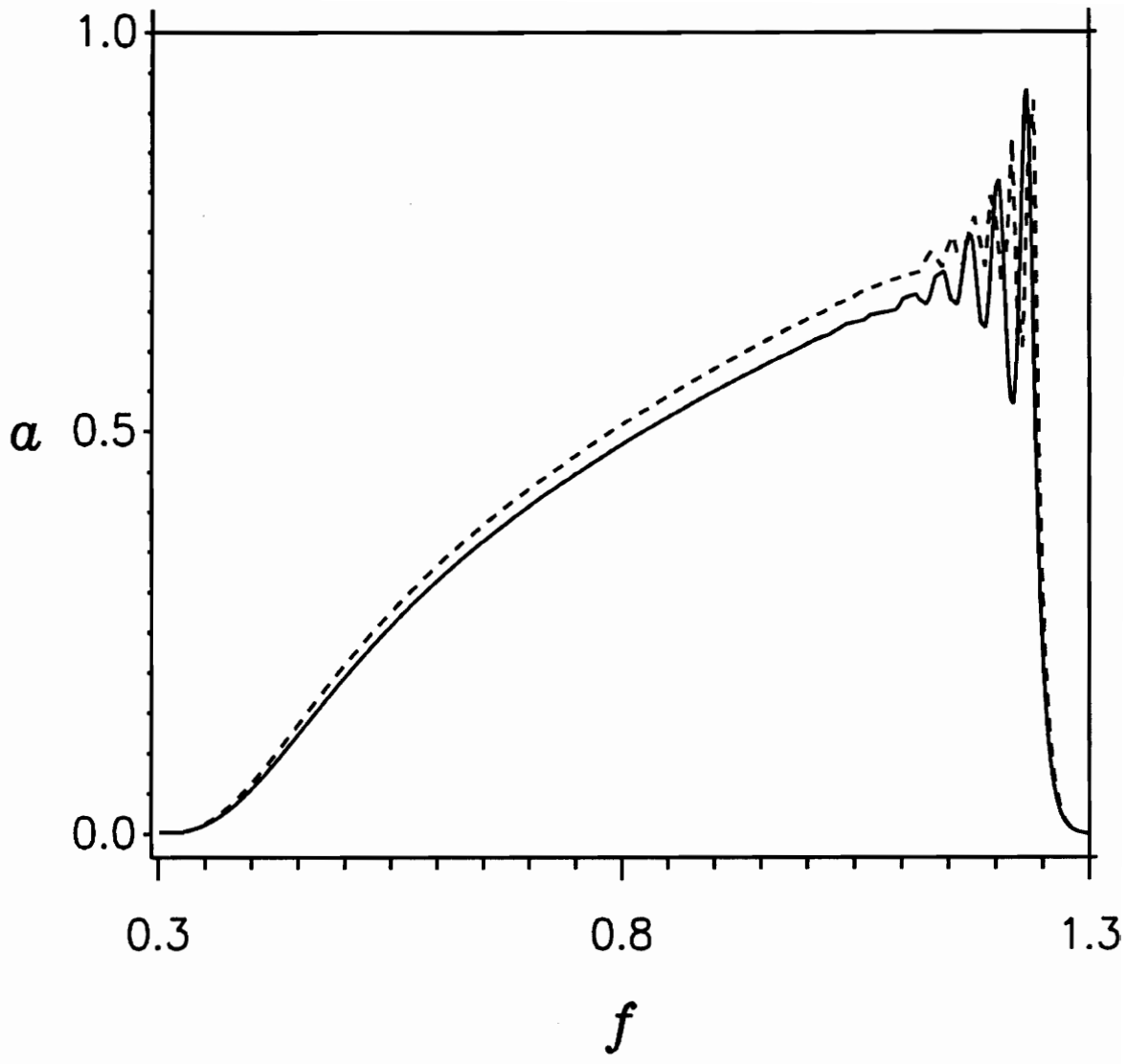

Figure 4.7 Reverse amplitude sweep. Solid line—nonstationary response found from perturbation equations. Dashed lines—nonstationary response found from original governing equations. $\alpha = 1.0$, $\mu = 0.05$, $\epsilon = 1.0$, $\phi = 2.2$, $s = -0.002$, $p(0) = y_1(0) = 0.001$, $q(0) = y_2(0) = 0$, and $f_0 = 1.3$.

4.2 Excitation Frequency Less than Two

In this case, the stationary force-response curve bends back on itself, as in Figure 2.6. All of the solutions on this curve are stable except those on the part which lies below the larger part of the curve. The trivial solution is stable up to the intersection of the force-response curve with the f axis and is unstable for larger values of f.

For a forward sweep of the amplitude ($s > 0$), the nonstationary behavior is similar to that in the case of $\phi \geq 2$. Again there is penetration, jump up, overshoot of, oscillation about, and convergence to the stationary force-response curve, followed (when we integrate the original governing equations) by a symmetry-breaking bifurcation, quasi-period doublings, and unboundedness. The primary difference between this case and the case of $\phi \geq 2$ is the shape of the stationary force-response curve about which the nonstationary behaviors take place. We show a forward sweep in Figure 4.8, with the nonstationary response found from integrating the perturbation equations being plotted as a solid line and the stationary force-response curve being plotted as a dashed line. In Figure 4.9, we repeat the solution for the nonstationary amplitude found from integrating the perturbation equations as a dashed line, and plot the *time trace* of the response found from integrating the original governing equations as a solid line. We see agreement between the

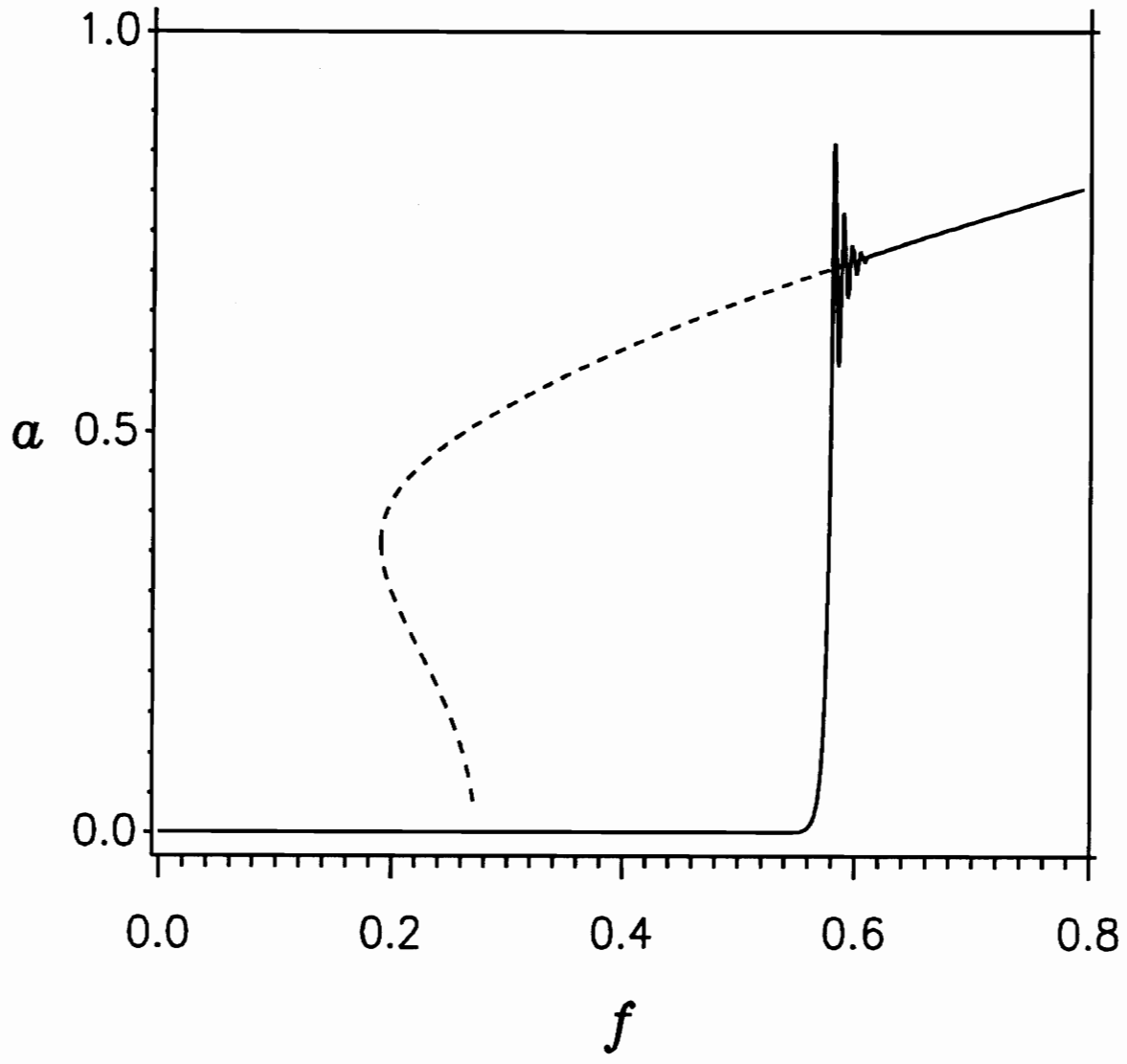

Figure 4.8 Forward amplitude sweep. Solid line—nonstationary response found from perturbation equations. Dashed lines—stationary frequency-response curves.
$\alpha = 1.0$, $\mu = 0.05$, $\epsilon = 1.0$, $\phi = 1.9$, $s = 0.0004$, $p(0) = 0.001$, $q(0) = 0$, and $f_0 = 0.0$.

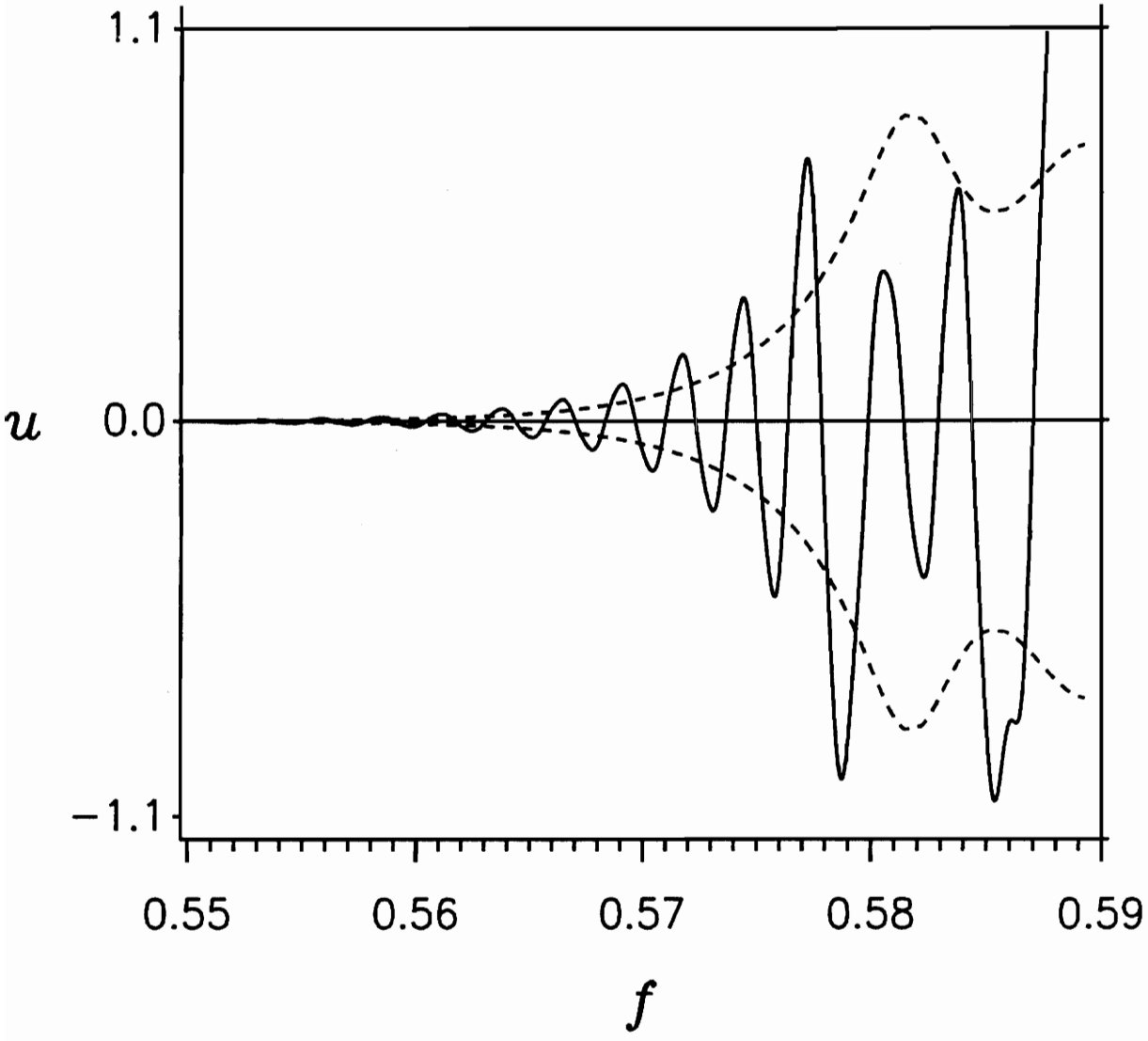

Figure 4.9 Forward amplitude sweep. Solid line—time trace of nonstationary response found from original governing equations. Dashed lines—amplitude of nonstationary response found from perturbation equations.
$\alpha = 1.0$, $\mu = 0.05$, $\epsilon = 1.0$, $\phi = 1.9$, $s = 0.0004$,
$p(0) = y_1(0) = 0.001$, $q(0) = y_2(0) = 0$, and $f_0 = 0.0$.

methods, particularly as to the location of the beginning of the jump up from the trivial solution. But at $f = 0.58$, the response found from the original governing equations begins to differ qualitatively from the response found from the perturbation equations, and it quickly goes unbounded. For this sweep, the oscillations of the amplitude about the stationary force-response curve are large enough to carry the response to unboundedness. For the case of stationary excitation, Floquet theory predicts that the asymmetric solution becomes unstable at $f = 0.890$. Using this last value as an estimate of the value of f at which unboundedness occurs in the stationary solution, we note that in this sweep, unboundedness occurs at a value of f smaller than in the case of the stationary response.

In Figure 4.10, we plot f_∞ as a function of the sweep rate s for forward sweeps, where f_∞ is the value of f at which the response exceeds some large value as it becomes unbounded. The variation of f_∞ with the sweep rate is much like that for the case $\phi \geq 2$. We mark the value $f = 0.890$ with a horizontal line in Figure 4.10 and use it as an estimate of the value of f at which the stationary solution becomes unbounded. Responses are calculated at sweep rates which are multiple of 0.0002. All sweeps are started at the value of f at which the trivial solution changes from stable to unstable, so that all sweeps have the same response as they enter this region. As in Figure 4.4, there is a range of small values of s for which f_∞ lies above the horizontal line. This is followed by a range of values of s in which f_∞ is below the line—the

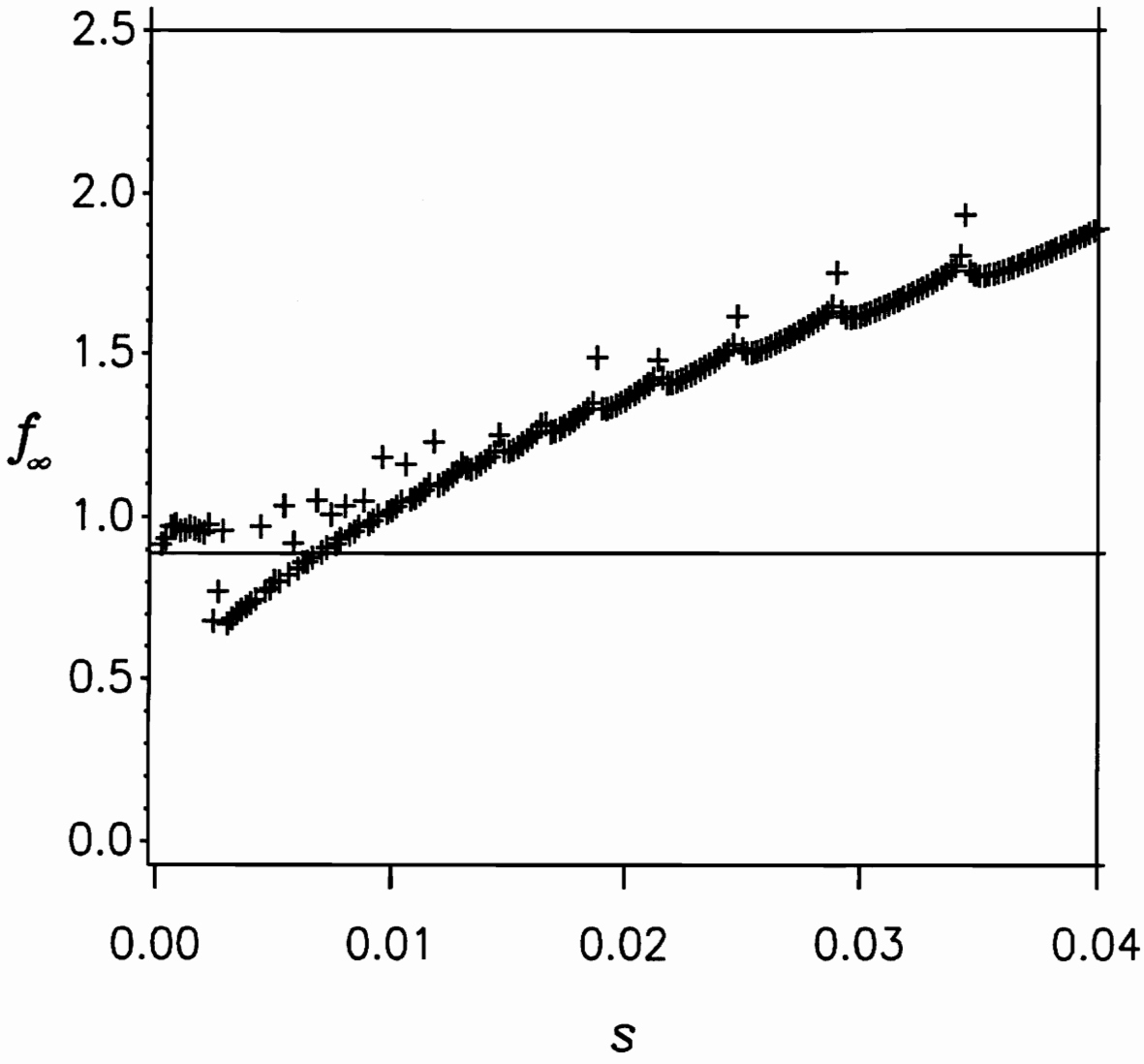

Figure 4.10 f_∞ versus sweep rate: + denotes value of f at which the response magnitude exceeded 3 as the response became unbounded. $\alpha = 1.0$, $\mu = 0.05$, $\epsilon = 1.0$, $\phi = 1.9$, $f_0 = 0.273$, $y_1(0) = 0.001$, and $y_2(0) = 0$.

response goes unbounded at a value of f at which the stationary response is bounded. The sweep rate used in the sweeps of Figures 4.8 and 4.9 lies in this region. For even larger values of s, f_∞ exceeds the horizontal line again. As in Figure 4.4, there are several sweep rates for which f_∞ is significantly larger than for surrounding sweep rates.

In Figure 4.11, we repeat the sweep rate analysis using a set of initial conditions smaller than those used for the sweep of Figure 4.10. The relationship between Figures 4.10 and 4.11 is analogous to that between Figures 4.4 and 4.5—the first range of small sweep rates for which f_∞ surpasses the horizontal line is smaller for smaller initial conditions; the sweep rate for which all faster sweeps have f_∞ above the horizontal line is smaller for smaller initial conditions; and f_∞ tends to be larger for smaller initial conditions.

As we consider smaller and smaller values of ϕ, the first range of sweep rates in which f_∞ lies above the horizontal line gets smaller until it essentially disappears. We illustrate this situation in Figure 4.12. We mark the value $f = 0.722$ at which period doubling occurs in the stationary solution with a horizontal line in Figure 4.12 and use it as an estimate of the value of f at which unboundedness occurs in the stationary solution. Except for extremely slow sweep rates, the response will not converge to the stationary response curve. Since there is no convergence to that curve, the oscillations of the nonstationary response amplitude are large enough to carry the response to unboundedness. Thus, the response changes quickly over a few cycles from

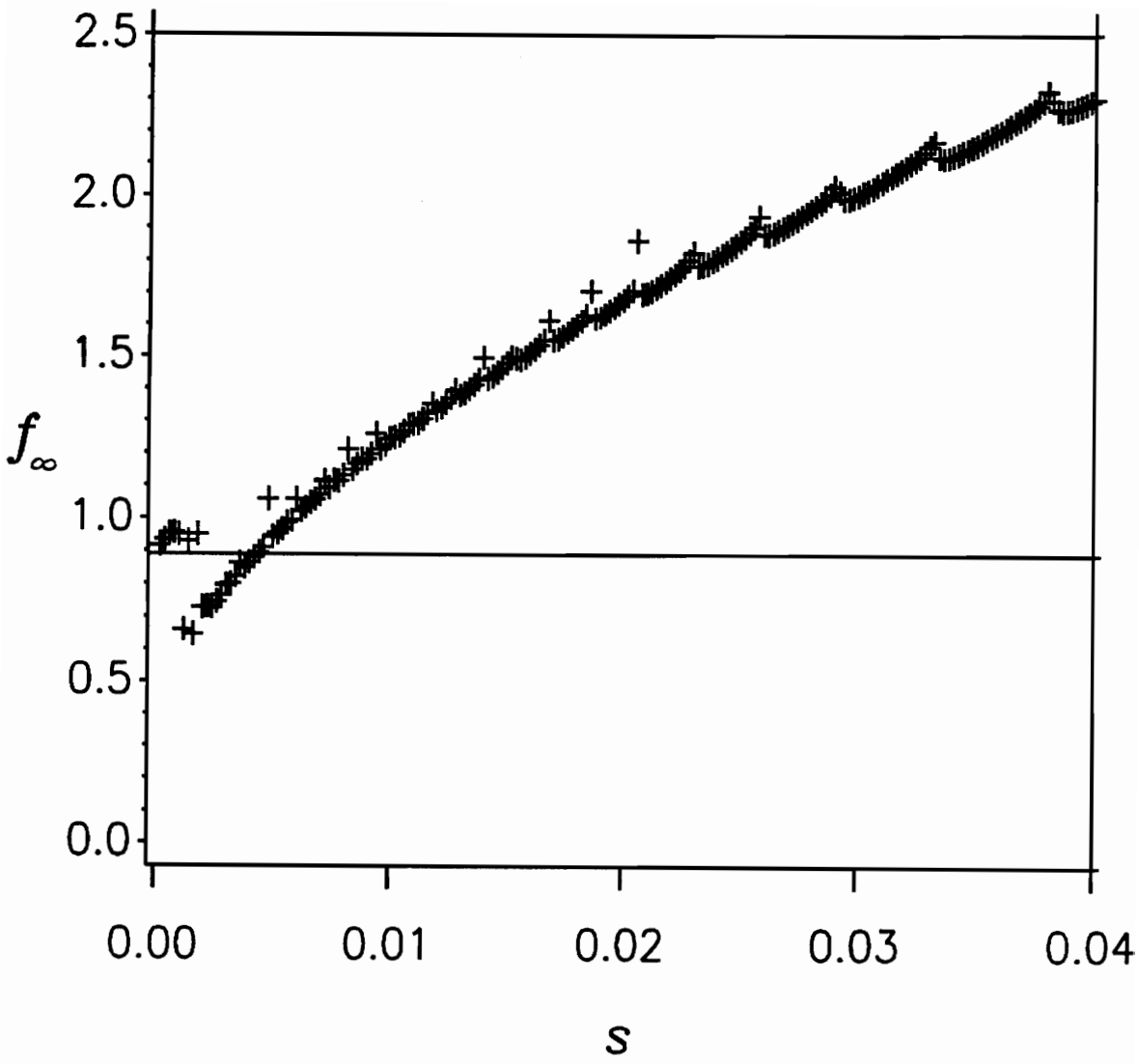

Figure 4.11 f_∞ versus sweep rate: + denotes value of f at which the response magnitude exceeded 3 as the response became unbounded. $\alpha = 1.0$, $\mu = 0.05$, $\epsilon = 1.0$, $\phi = 1.9$, $f_0 = 0.273$, $y_1(0) = 0.00001$, and $y_2(0) = 0$.

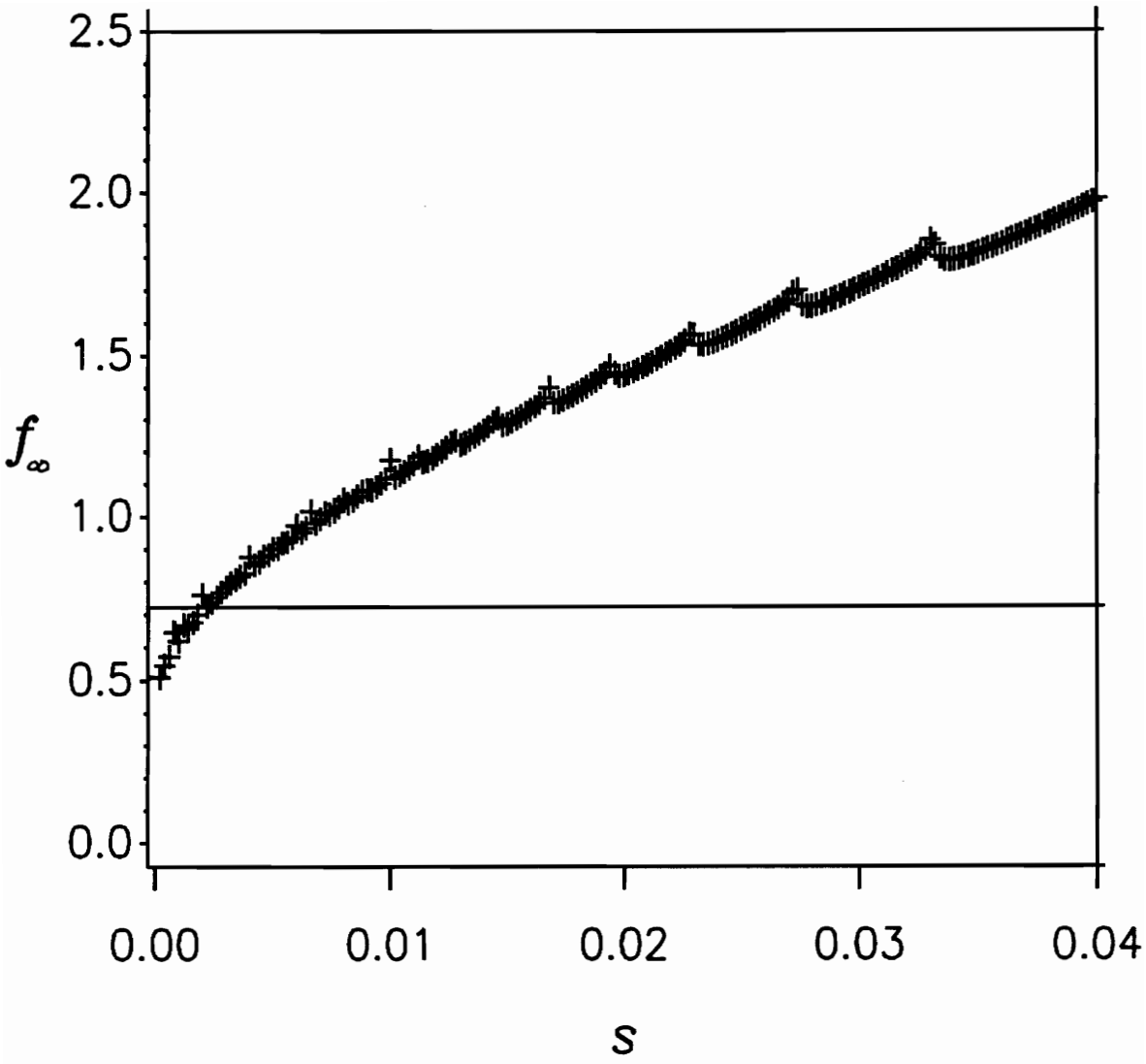

Figure 4.12 f_∞ versus sweep rate: + denotes value of f at which the response magnitude exceeded 3 as the response became unbounded. $\alpha = 1.0$, $\mu = 0.05$, $\epsilon = 1.0$, $\phi = 1.8$, $f_0 = 0.421$, $y_1(0) = 0.001$, and $y_2(0) = 0$.

being trivial to being unbounded at a value of f where the stationary response is bounded. For faster sweep rates, the penetration of the trivial solution is large enough so that f_∞ exceeds the horizontal line.

As with forward sweeps, the nonstationary response characteristics for reverse sweeps when ϕ is less than two is similar to those when ϕ is greater than two. Again, the response jumps quickly because the sweep begins at a value of f where the trivial solution is unstable. The initial jump can carry the response to unboundedness, or to an asymmetric solution, or to a response that oscillates about the stationary response curve, depending on f_0. In Figure 4.13, we plot the nonstationary response found from integrating the perturbation equations as a solid line and the stationary force-response curve as a dashed line. Recall that time increases from right to left in this figure because this is a reverse sweep. In this case, the nonstationary response does not converge to the stationary force-response curve, instead going directly from oscillation about this curve to lingering. There is much lingering here because the stable part of the stationary force-response curve is elevated above the f axis for $\phi < 2$. In fact, the response remains nontrivial even after f has become trivial.

In Figure 4.14, we compare the nonstationary response obtained by integrating the perturbation equations (solid line) with that obtained by integrating the original governing equations (dashed line). The agreement is good, although there is some discrepancy between the results of the two

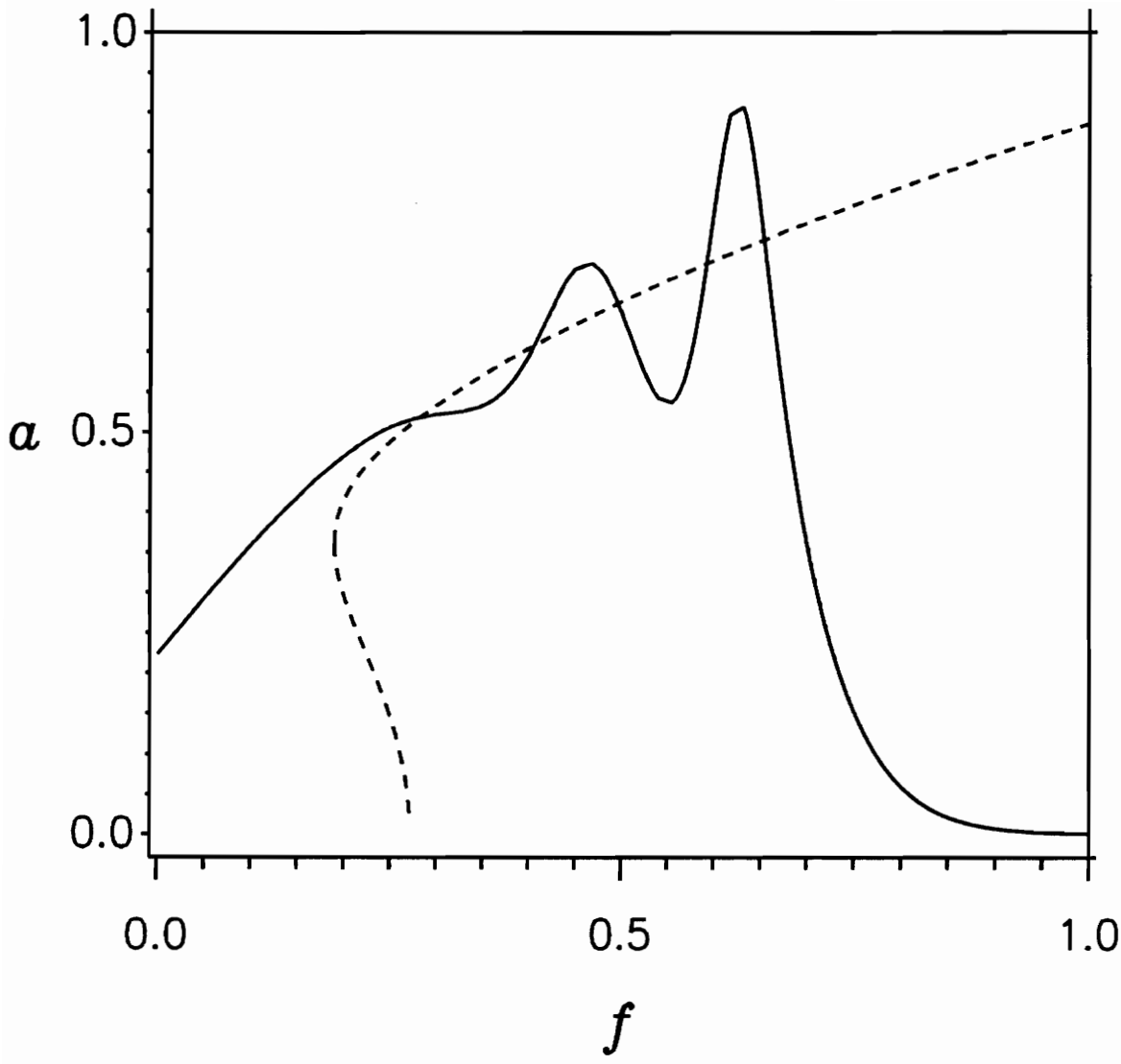

Figure 4.13 Reverse amplitude sweep. Solid line—nonstationary response found from perturbation equations. Dashed lines—stationary frequency-response curves.
$\alpha = 1.0$, $\mu = 0.05$, $\epsilon = 1.0$, $\phi = 1.9$, $s = -0.008$,
$p(0) = 0.001$, $q(0) = 0$, and $f_0 = 1.0$.

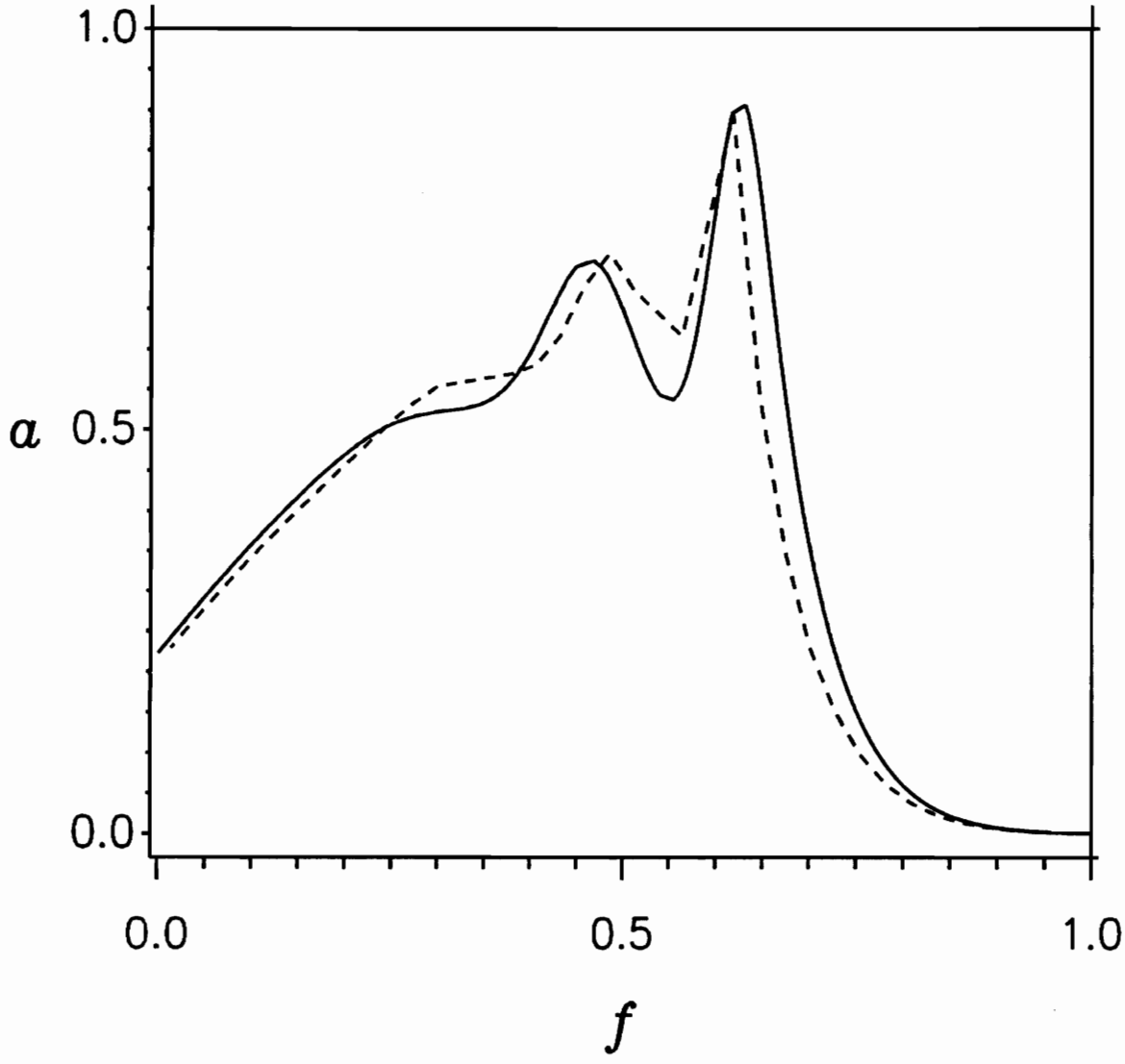

Figure 4.14 Reverse amplitude sweep. Solid line—nonstationary response found from perturbation equations. Dashed lines—nonstationary response found from original governing equations. $\alpha = 1.0$, $\mu = 0.05$, $\epsilon = 1.0$, $\phi = 1.9$, $s = -0.008$, $p(0) = y_1(0) = 0.001$, $q(0) = y_2(0) = 0$, and $f_0 = 1.0$.

methods. The discrepancy, as before, results from differences in the measures of the amplitudes and from approximations used in the analysis.

For smaller values of ϕ, meaningful reverse sweeps are not possible because the solution either remains trivial or immediately becomes unbounded, depending on the initial value of f.

CHAPTER 5

Analog-Computer Simulations

In this chapter, we use an analog computer to verify the conclusions of the digital-computer results of the previous chapters. We also consider the behavior of the response after a sweep is stopped and the excitation frequency and amplitude are held constant.

An analog computer is an actual physical system which can be programmed to model the system being studied. Because it produces a solution that is continuous in time, an analog computer yields a valuable verification of the digital-computer results. A digital computer must approximate the solution at discrete points in time, and the discretization of the solution can sometimes cause incorrect results.

However, an analog computer is subject to noise and other inaccuracies. The noise prevents an accurate control of the initial conditions. Thus, the same initial conditions cannot be duplicated in all sweeps when using an analog

computer, and one cannot analyze the effect of initial conditions on the response. Because of the noise and the inaccuracies in such systems, the analog computer does not produce the same accuracy as a digital computer. Therefore, we use the analog computer for a qualitative check of the characteristics of the nonstationary response, rather than as a quantitative check.

We use a Comdyna GP-10 analog computer in the slow (real time) integration mode. The excitation signal is generated using a Wavetek 650 Signal Generator. We sweep the excitation frequency by using the Wavetek's internal sweeping programs. We sweep the amplitude by using a PC program which I wrote that controls the signal generator through a General Purpose Interface Bus (GPIB).

5.1 Frequency Sweeps

In Figure 5.1, we show the results of a forward frequency sweep with $r = 0.001$. As with the digital-computer results, we see penetration, jump up, and then oscillation of the response amplitude. As the sweep continues, the amplitude converges to the stationary solution. Towards the end of the sweep, we see lingering in the response because the amplitude of the response does not become trivial in the abrupt manner the stationary solution amplitude does.

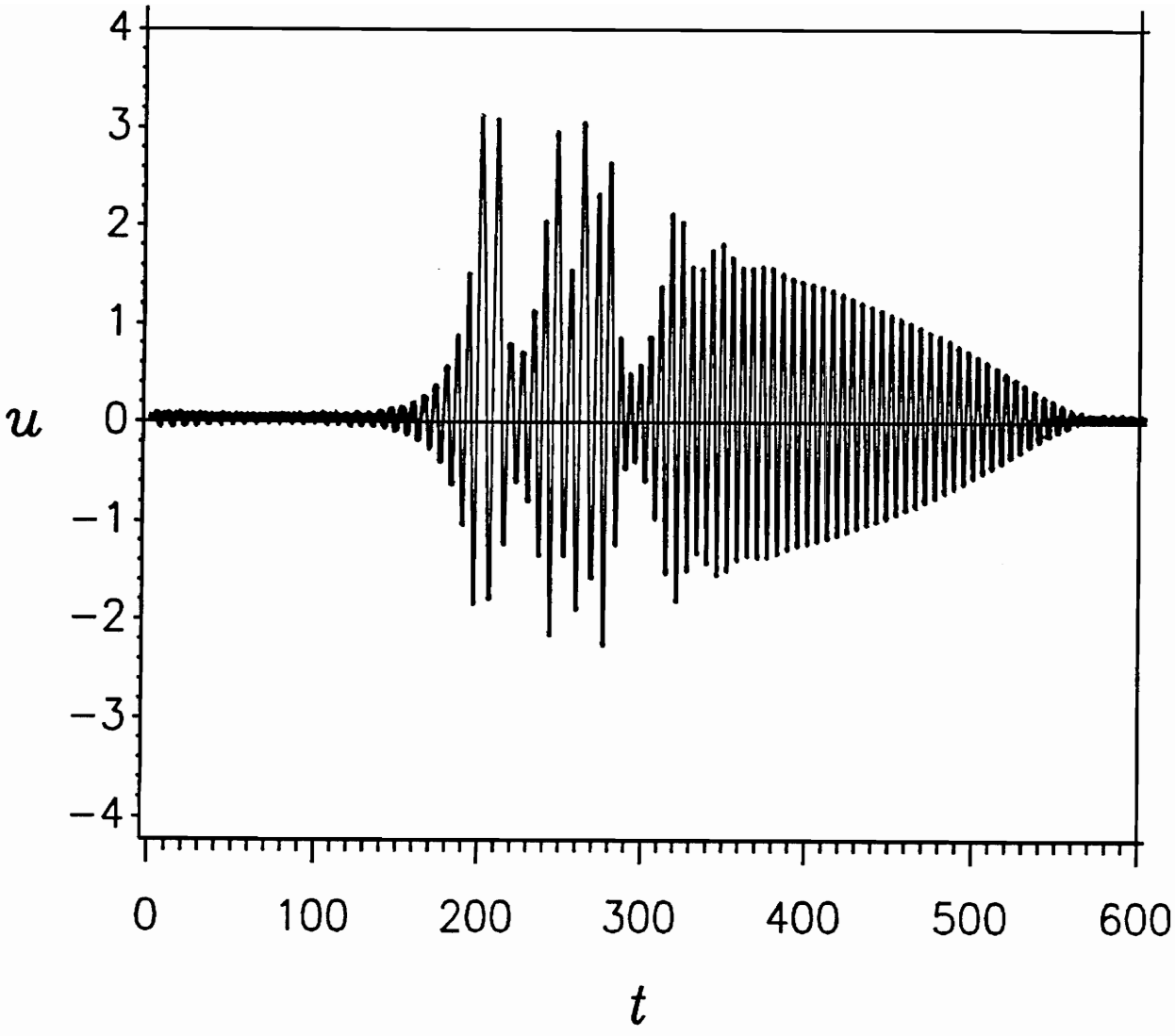

Figure 5.1 Analog computer response to a forward frequency sweep. $\alpha = 0.1$, $\mu = 0.05$, $\epsilon = 1.0$, $f = 0.5$, $r = 0.001$, and $\phi_0 = 1.7$.

In Figure 5.2, we plot the analog-computer results using the same sweep rate as in Figure 5.1. Because of the presence of different initial conditions and noise, the response penetrates farther before jumping up. The response continues to grow, and in a few cycles, it has become unbounded. As in the previous chapters, we see that changes in the initial conditions or noise can have catastrophic effects on a system under a nonstationary excitation.

In Figure 5.3, we plot the analog-computer results using the same sweep rate as in Figure 5.1, but this time, we stop the sweep after 300 seconds and hold the frequency at $\phi = 2$. The end of the sweep is marked with a vertical line. The response during the sweep is much like that in Figure 5.1. At the beginning of the stationary excitation, the amplitude is still oscillating as it did during the sweep, but soon after the solution converges to the stationary response.

In Figure 5.4, we plot the analog-computer results for a reverse sweep, with $r = -0.0005$. Here, the response penetrates, jumps up, oscillates, and converges to the stationary solution. Towards the end of the sweep, however, we see a distinct change in the behavior. The response undergoes a symmetry-breaking bifurcation and then a quasi-period-doubling bifurcation. The stationary response undergoes a period-doubling bifurcation at $\phi = 1.903$. In this sweep, the excitation frequency passes this value of ϕ at $t = 794$ seconds. Thus, for this sweep, the period-doubling behavior is delayed to a value of ϕ smaller than that in the stationary response. After several cycles of this

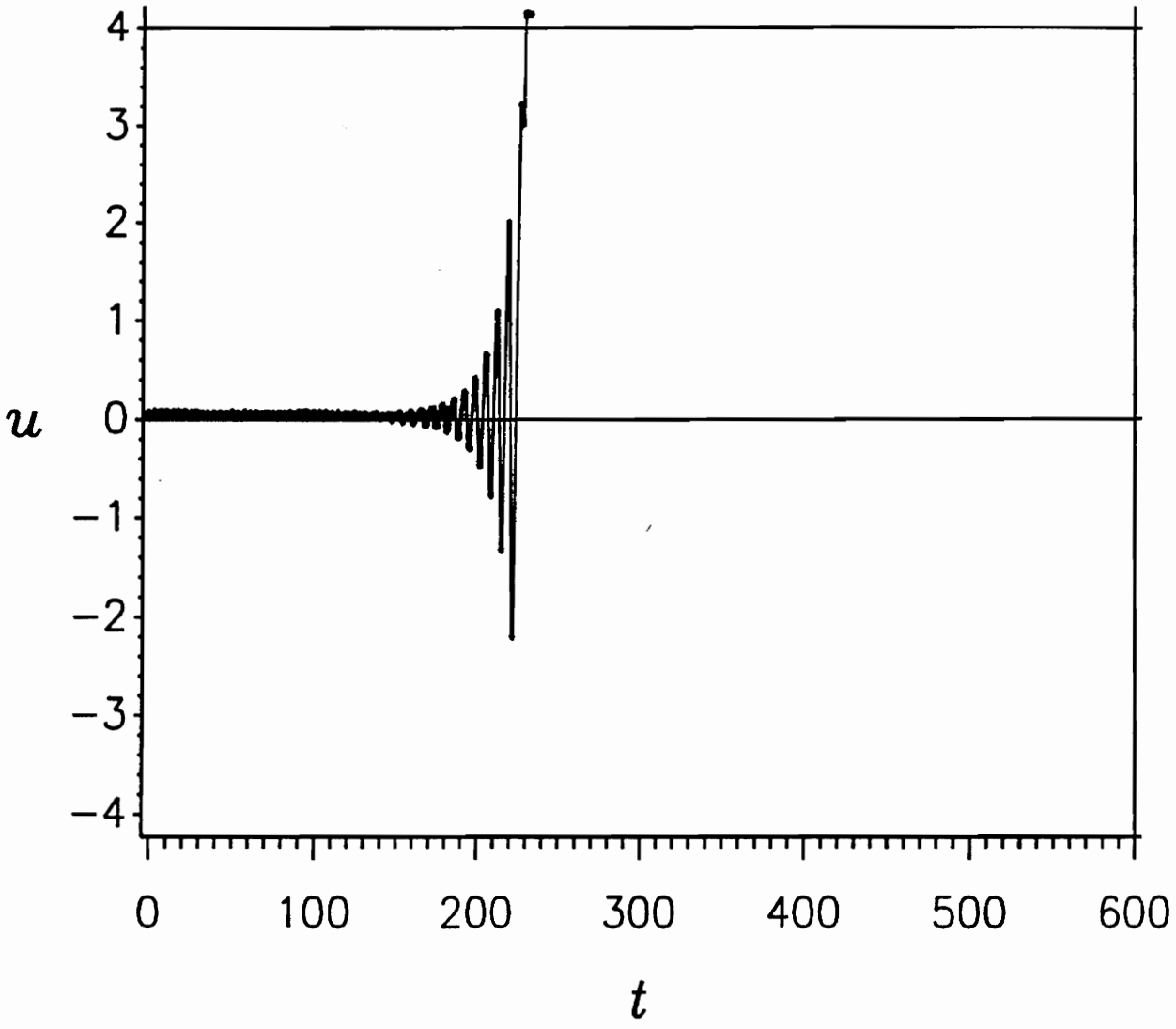

Figure 5.2 Analog computer response to a forward frequency sweep. $\alpha = 0.1$, $\mu = 0.05$, $\epsilon = 1.0$, $f = 0.5$, $r = 0.001$, and $\phi_0 = 1.7$.

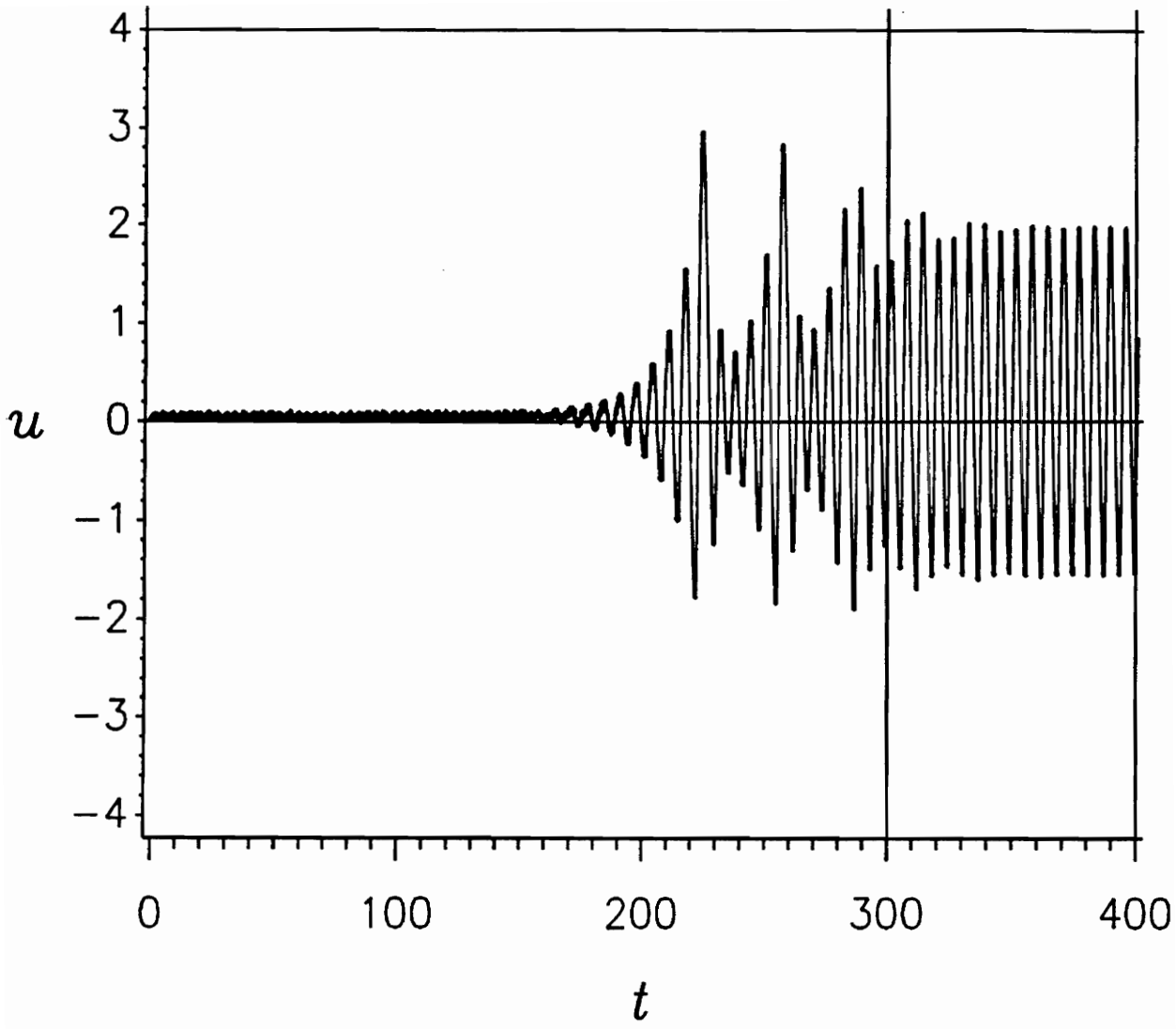

Figure 5.3 Analog computer response to a forward frequency sweep. After 300 seconds, the sweep is stopped at $\phi = 2$. $\alpha = 0.1$, $\mu = 0.05$, $\epsilon = 1.0$, $f = 0.5$, $r = 0.001$, and $\phi_0 = 1.7$.

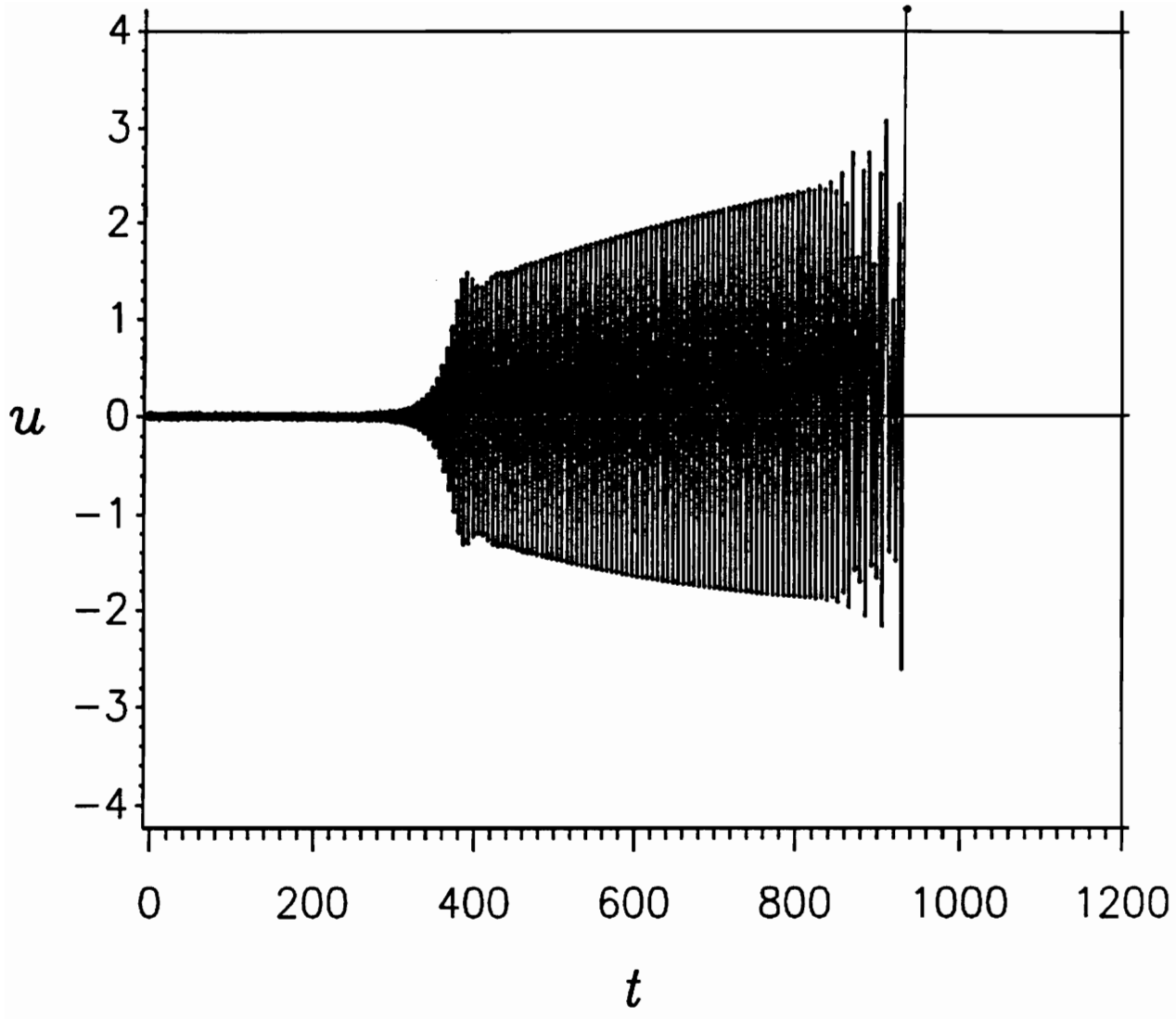

Figure 5.4 Analog computer response to a reverse frequency sweep. $\alpha = 0.1$, $\mu = 0.05$, $\epsilon = 1.0$, $f = 0.5$, $r = -0.0005$, and $\phi_0 = 2.3$.

behavior, the response becomes unbounded.

In Figure 5.5, we plot the analog-computer results for a reverse sweep with r = -0.001. The response behaves much like that shown in Figure 5.4. Because of the faster sweep rate, penetration is greater in this sweep. The excitation frequency passes ϕ = 1.903 at t = 397 seconds for this sweep. Again, the quasi-period-doubling bifurcation is delayed to a value of ϕ smaller than that in the stationary response. In fact, the quasi-period-doubling bifurcation is delayed even more than in the slower sweep of Figure 5.4. It is more difficult to identify the quasi-period-doubled behavior separately from the other response behaviors because it occurs for only a few cycles before the response becomes unbounded. The response becomes unbounded at a value of ϕ slightly smaller than that in the previous sweep.

In Figure 5.6, we plot the analog-computer results for a reverse sweep with r = -0.002. In this sweep, we see even deeper penetration. The response amplitude jumps up and begins to oscillate, but after a few cycles the response becomes unbounded. If a quasi-period-doubling bifurcation occurs, we cannot identify it because it occurs with all the other changes in the last few cycles of the response. The response becomes unbounded at a value of ϕ *higher* than that in the previous sweeps.

In Figure 5.7, we plot the results of a reverse sweep with r = -0.004. After 150 seconds, we stop the sweep and hold the frequency at ϕ = 1.7. When the sweep ends, the response is still bounded, unlike the sweeps of

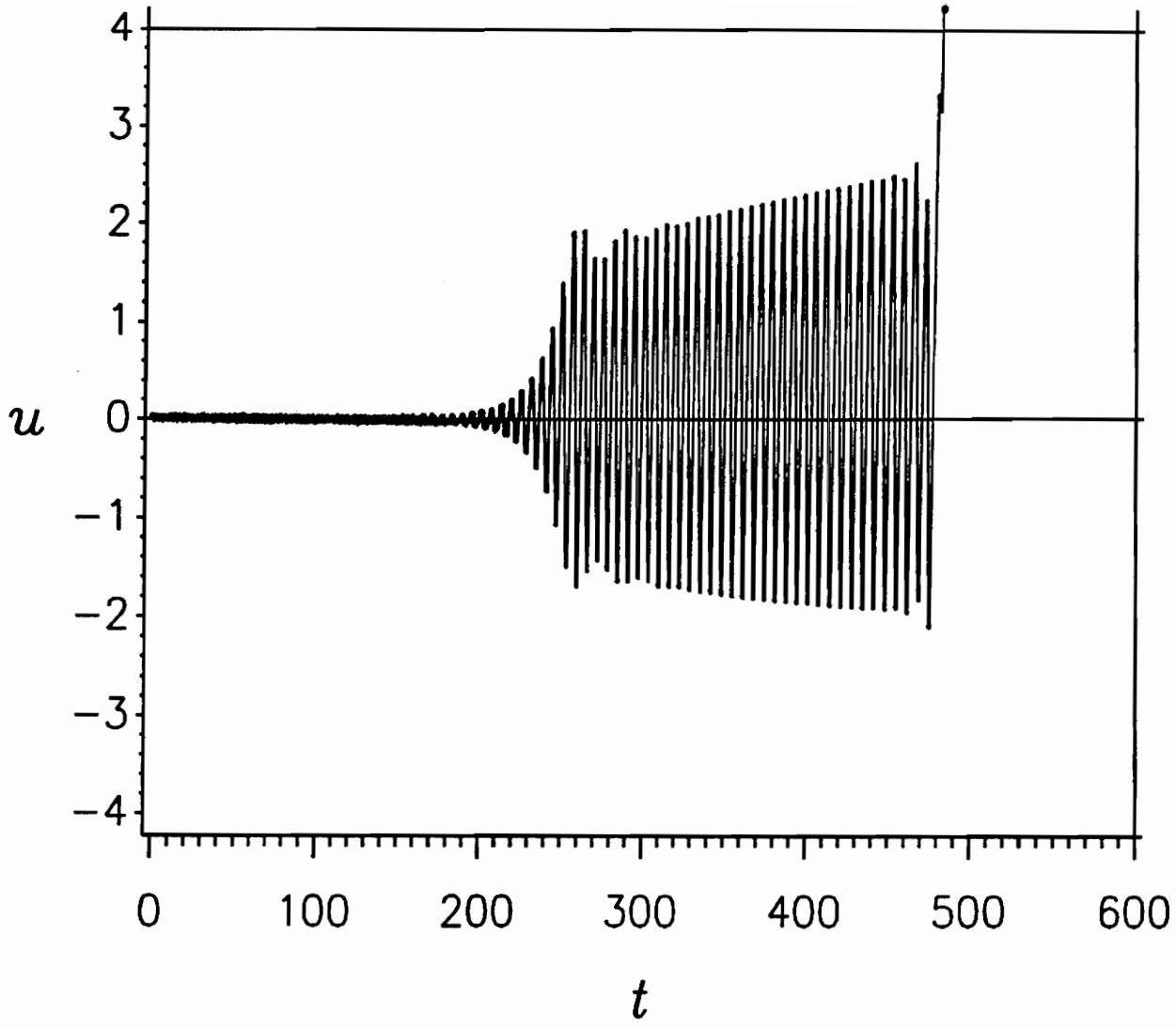

Figure 5.5 Analog computer response to a reverse frequency sweep. $\alpha = 0.1$, $\mu = 0.05$, $\epsilon = 1.0$, $f = 0.5$, $r = -0.001$, and $\phi_0 = 2.3$.

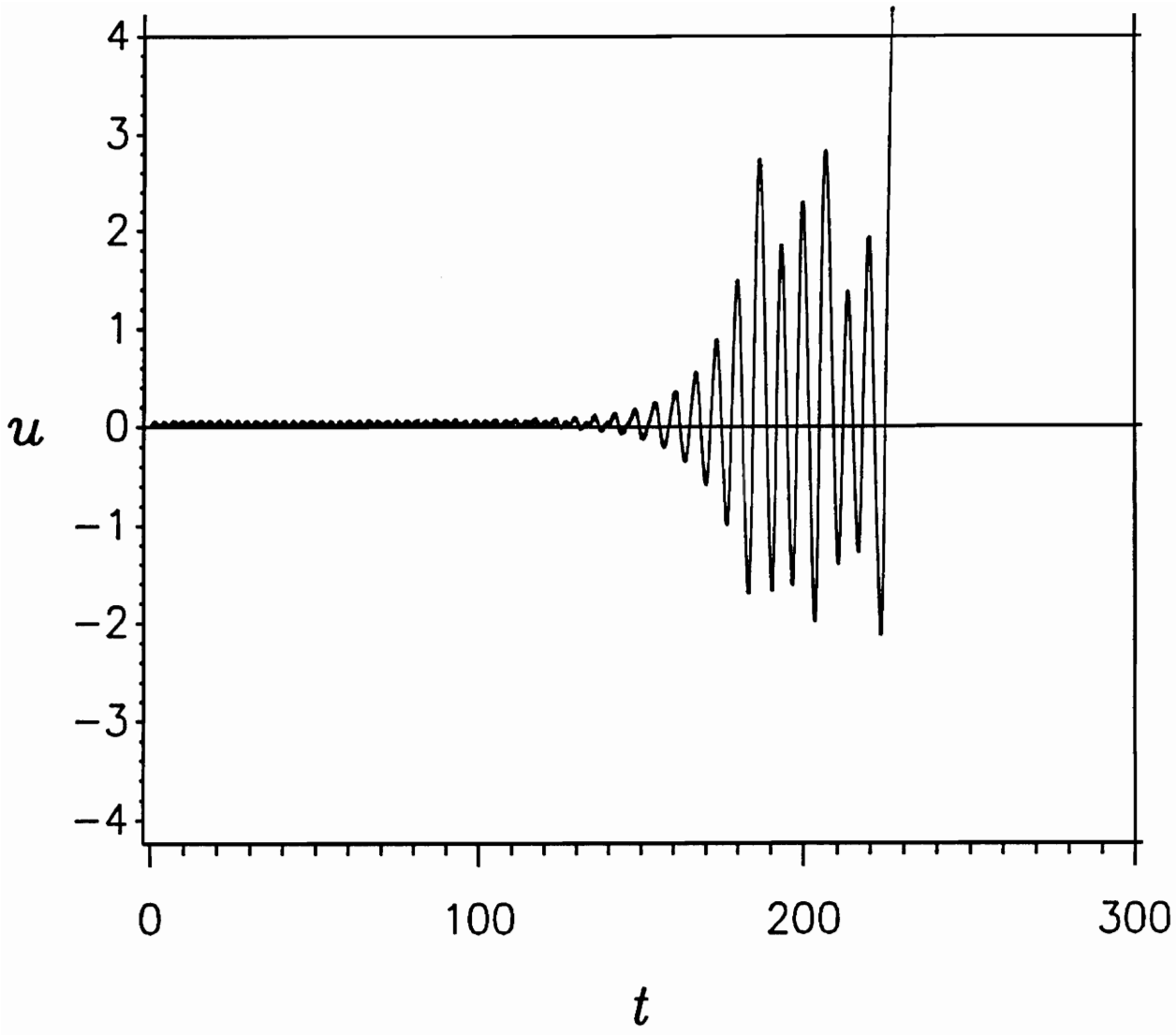

Figure 5.6 Analog computer response to a reverse frequency sweep. $\alpha = 0.1$, $\mu = 0.05$, $\epsilon = 1.0$, $f = 0.5$, $r = -0.002$, and $\phi_0 = 2.3$.

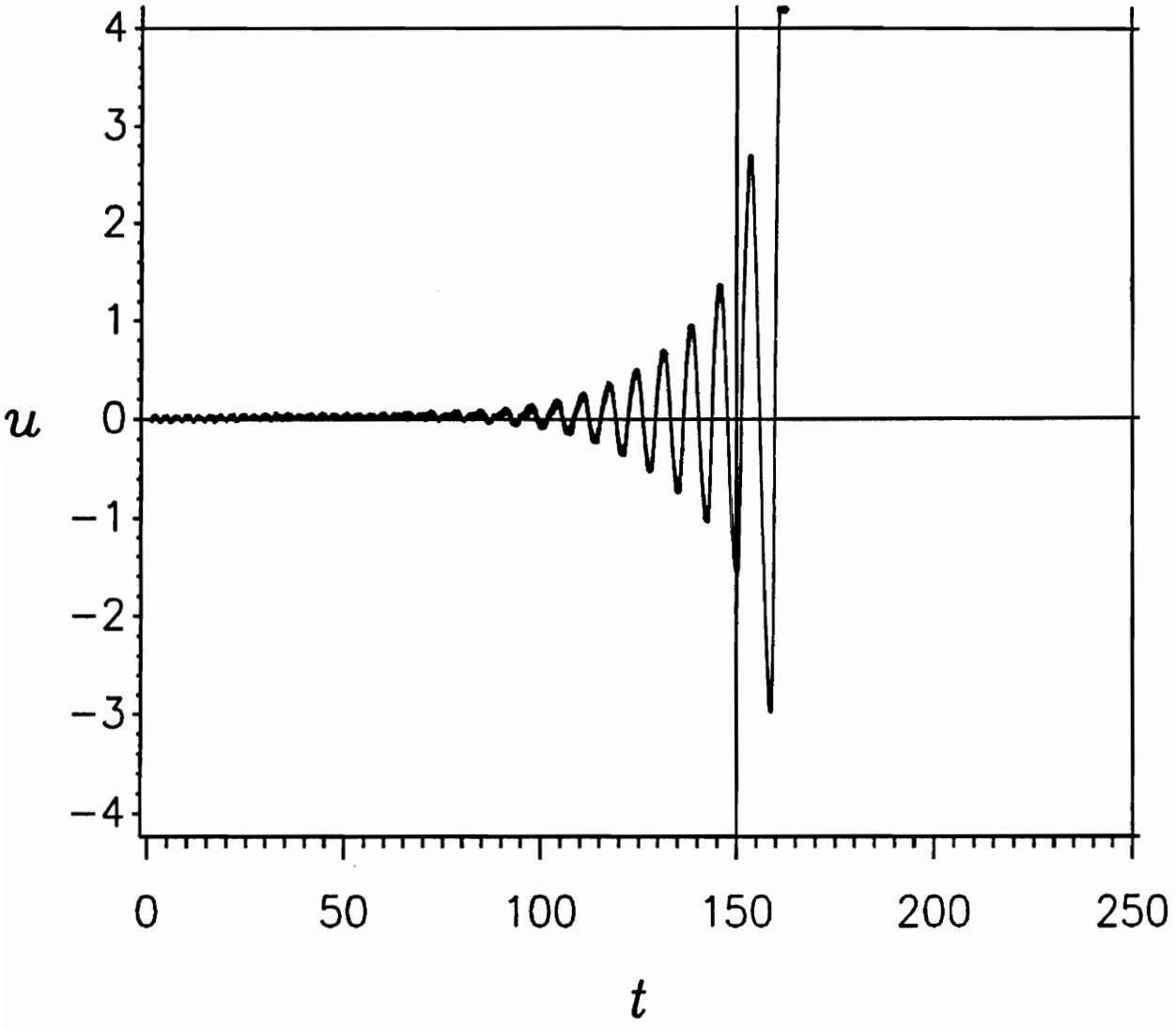

Figure 5.7 Analog computer response to a reverse frequency sweep. After 150 seconds, the sweep is stopped at $\phi = 1.7$. $\alpha = 0.1$, $\mu = 0.05$, $\epsilon = 1.0$, $f = 0.5$, $r = -0.004$, and $\phi_0 = 2.3$.

Figures 5.4-5.6. However, the oscillations are large enough so that the solution goes unbounded a few cycles later, *after* the sweep has ended and the excitation is stationary.

For some sweep rates, initial conditions, and noise levels, the response found from the analog computer *sweeps through*, just as it did in the digital-computer results. In such cases, the response never deviates significantly from the trivial response.

5.2 Amplitude Sweeps

In Figure 5.8, we show the results of an excitation-amplitude sweep on an analog computer with $s = 0.00208$. The results are very similar to those found on the digital computer. First, the response penetrates, jumps up, oscillates, and converges to the stationary solution. As the sweep continues, the response begins to change and no longer agrees with the stationary solution. After a few cycles, the response goes unbounded. The last few cycles of the response suggest the occurrence of a symmetry-breaking bifurcation and a quasi-period-doubling bifurcation that we found in the digital-computer simulations. The stationary solution undergoes a period-doubling bifurcation at $f = 1.002$. In this sweep, the excitation amplitude passes this value of f at $t = 480$ seconds. Thus, the period-doubling behavior in this

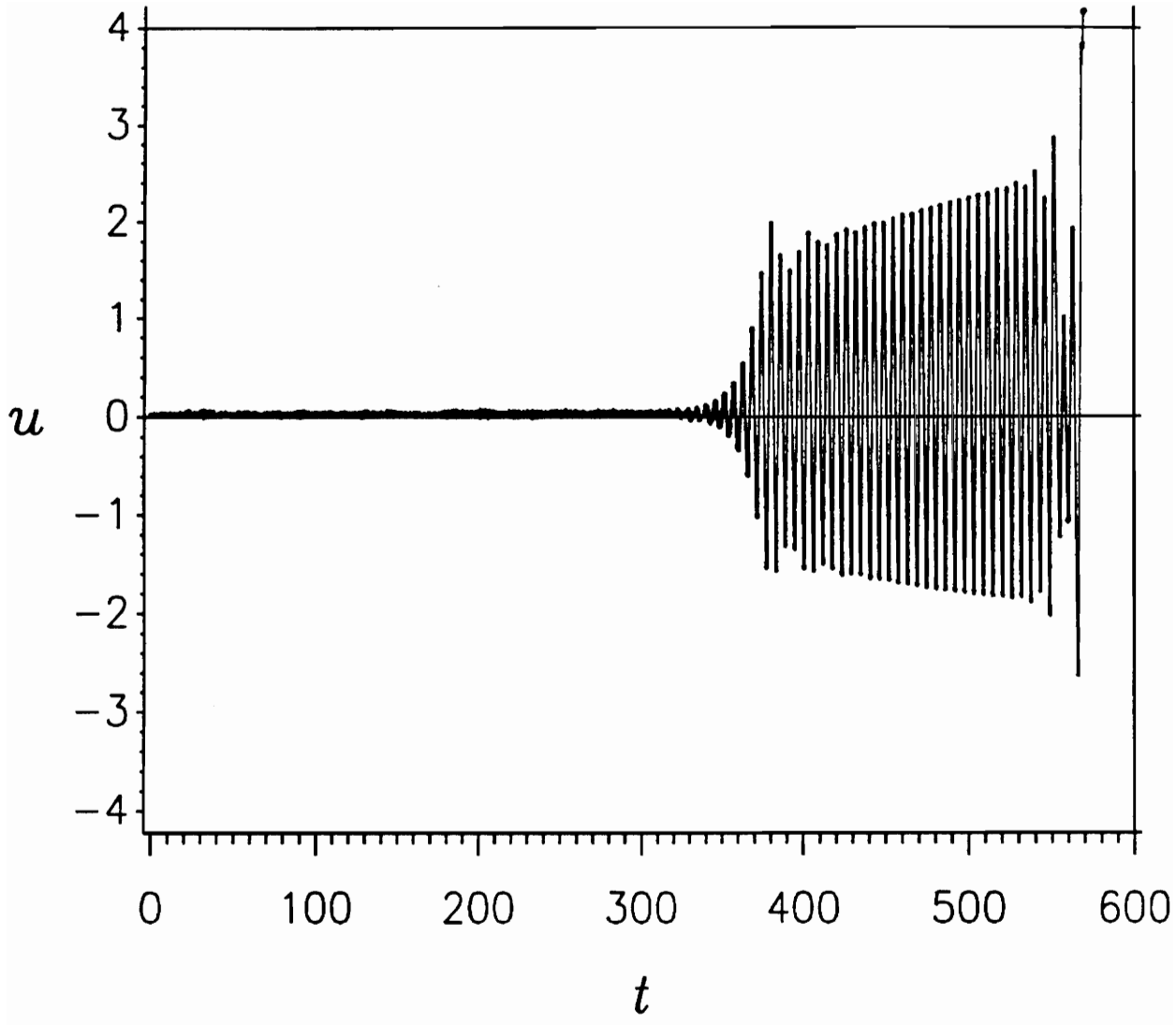

Figure 5.8 Analog computer response to a forward amplitude sweep. $\alpha = 0.1$, $\mu = 0.05$, $\epsilon = 1.0$, $\phi = 2.2$, $s = 0.00208$, and $f_0 = 0.0$.

sweep is delayed to a value of f higher than that in the stationary response.

In Figure 5.9, we show the results of a forward sweep with $s = 0.00167$. After 600 seconds, we stop the sweep and hold the excitation amplitude at $f = 1.0$. Again, we see penetration, jump up, oscillation, and convergence to the stationary solution. At the end of the sweep, the nonstationary response has already converged to the stationary response; therefore, there is no nonstationary behavior evident in the response once the sweep has ended.

In Figure 5.10, we show the results of sweeping the amplitude with $s = 0.0067$ for 150 seconds, and then holding the excitation amplitude at $f = 1.0$. The response penetrates farther than in the previous sweep because the sweep is faster, and only begins to grow at the end of the sweep. After the sweep is ended and the excitation is stationary, the response continues to grow and soon becomes unbounded. Again we see that the nonstationary behavior can have a critical effect on the response even after the excitation has become stationary.

In Figure 5.11, we show the results of a reverse amplitude sweep with $s = -0.00417$. After 150 seconds, we stop the sweep and hold the excitation amplitude at $f = 0$. The response jumps as soon as the sweep begins because the trivial solution is unstable at this level of excitation. The response soon converges to the stationary solution, but as the sweep continues, the response lingers. In fact, lingering is so great that the response is nontrivial even after

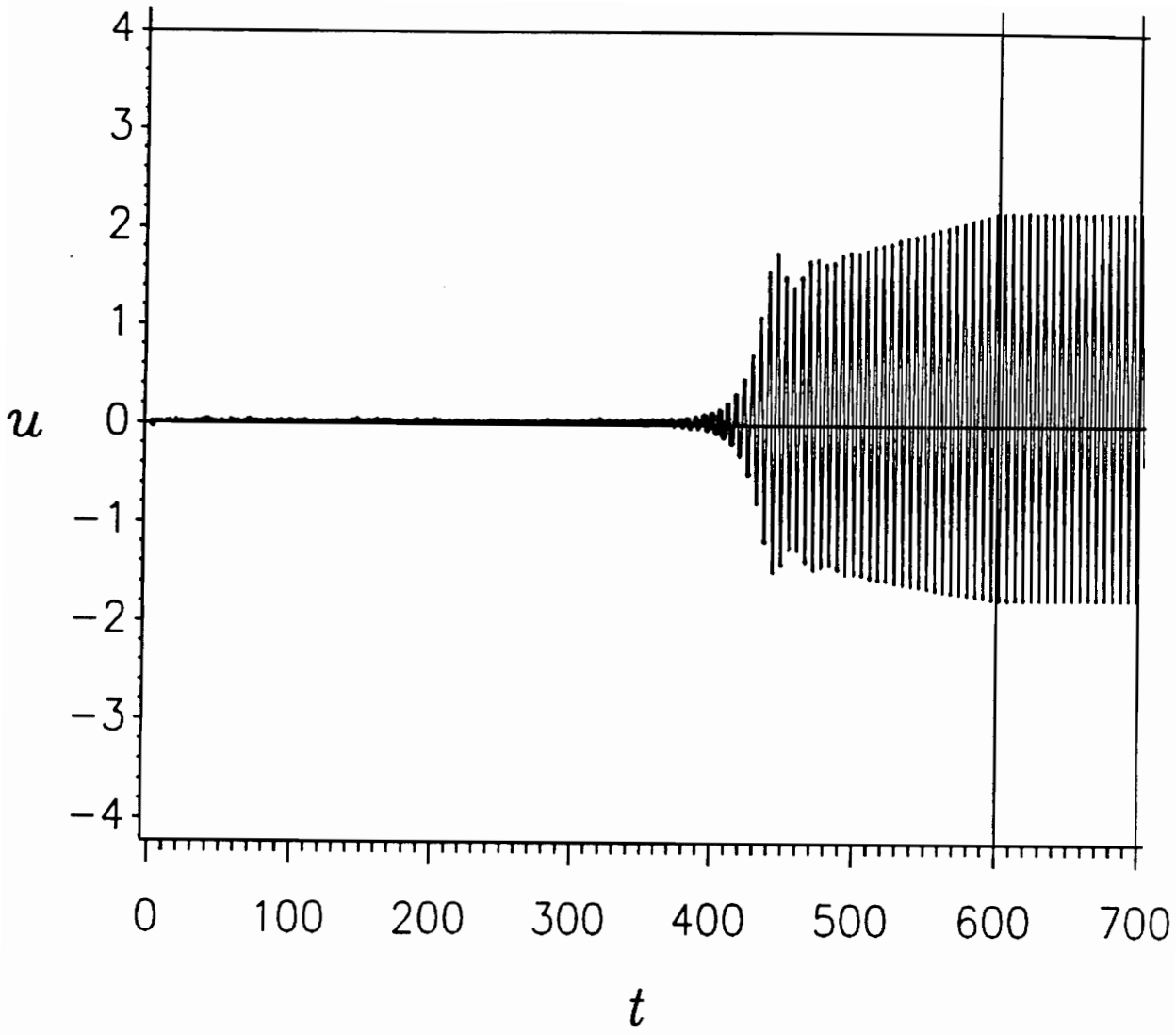

Figure 5.9 Analog computer response to a forward amplitude sweep. After 600 seconds, the sweep is stopped at $f = 1$. $\alpha = 0.1$, $\mu = 0.05$, $\epsilon = 1.0$, $\phi = 2.2$, $s = 0.00167$, and $f_0 = 0.0$.

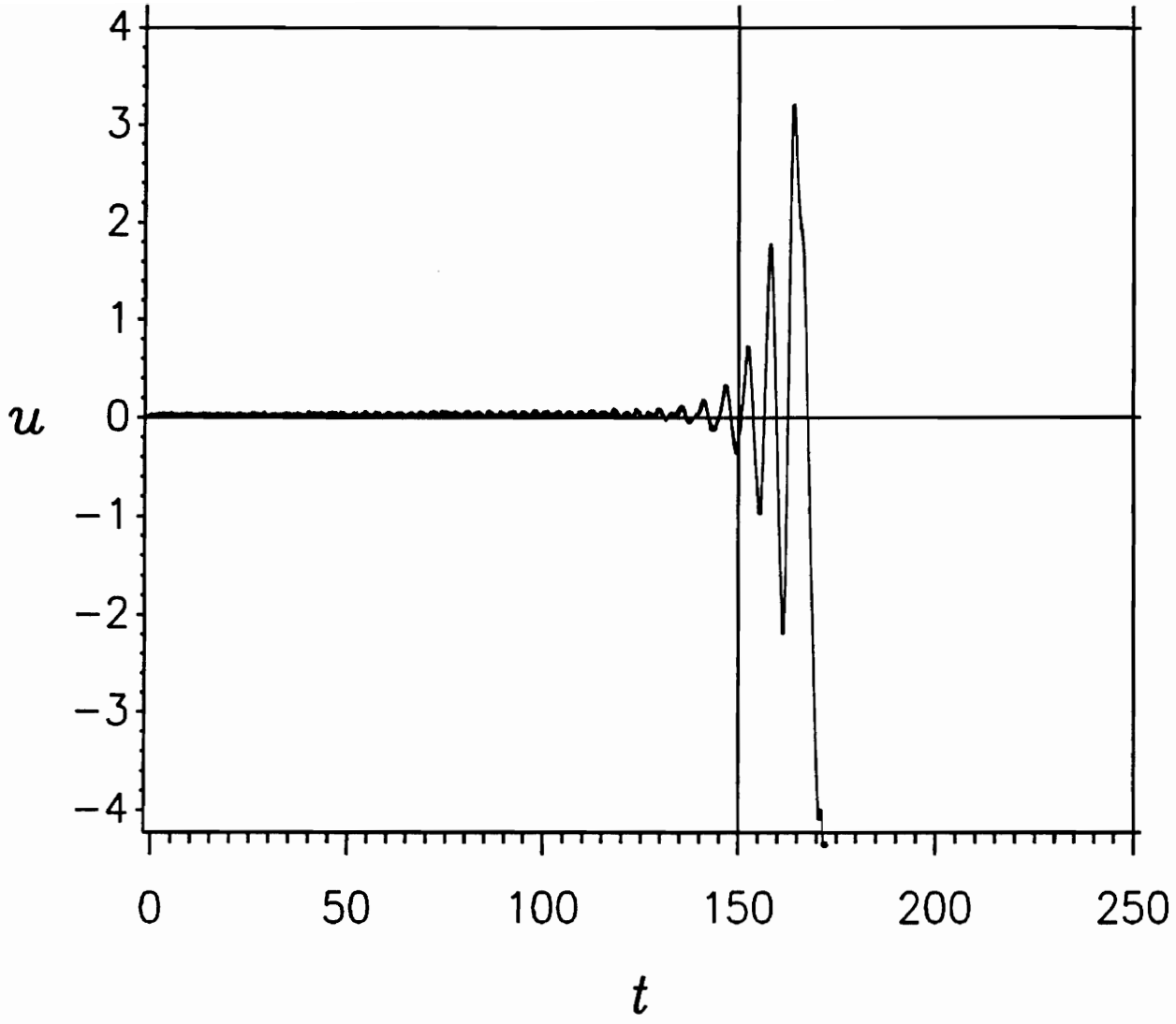

Figure 5.10 Analog computer response to a forward amplitude sweep. After 150 seconds, the sweep is stopped at $f = 1$. $\alpha = 0.1$, $\mu = 0.05$, $\epsilon = 1.0$, $\phi = 2.2$, $s = 0.0067$, and $f_0 = 0.0$.

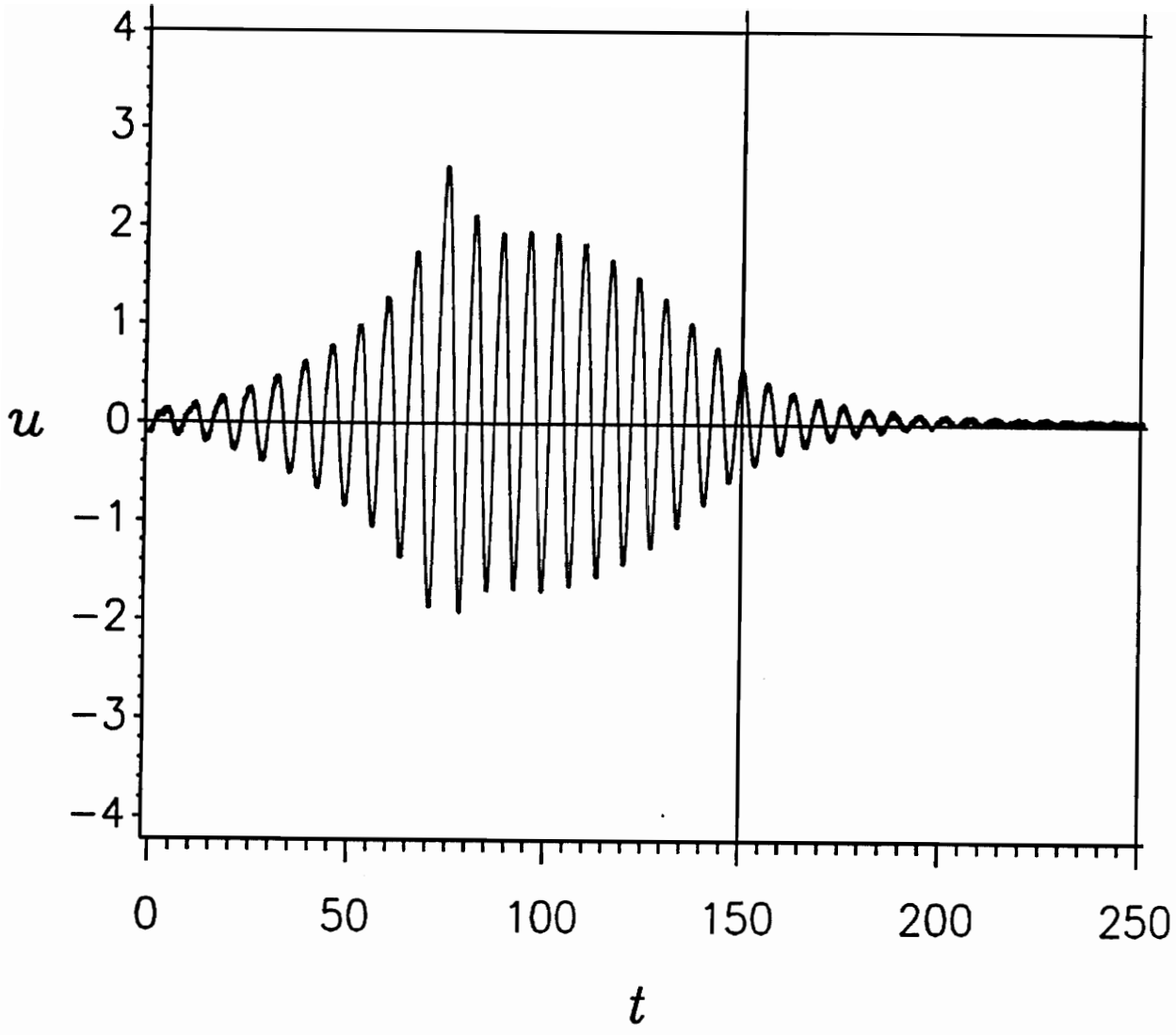

Figure 5.11 Analog computer response to a reverse amplitude sweep. After 150 seconds, the sweep is stopped at $f = 0$. $\alpha = 0.1$, $\mu = 0.05$, $\epsilon = 1.0$, $\phi = 1.8$, $s = -0.00417$, and $f_0 = 0.625$.

the excitation is trivial. However, the response decays after the sweep has ended and becomes trivial.

CHAPTER 6

Conclusions

We have considered a parametrically-excited one-degree-of-freedom system with nonstationary excitation. The excitation has either a frequency or an amplitude that is a linear function of time. Using the method of multiple scales, we determined equations governing the amplitude and phase of the response. From these, we found the stationary response of the system to a stationary excitation. We considered the stability of these solutions, and also examined the stability of stationary solutions to the original governing equation through a Floquet analysis. We found the nonstationary response to nonstationary excitation by (a) digital computer integration of the original governing equations; (b) digital computer integration of the equations found by applying the method of multiple scales; and (c) analog computer simulation of the original governing equation. We found good agreement between the responses found through digital computer simulation. The analog computer

simulations verified the digital computer results. We also found the maximum amplitude of the response as a function of sweep rate and the value of excitation amplitude or frequency at which the response goes unbounded as a function of sweep rate. We also examined the effect of initial conditions and noise on the response to nonstationary excitation.

For sweeps of the excitation amplitude or frequency, there are many characteristics which separate the nonstationary response to nonstationary excitation from the stationary response to stationary excitation. The nonstationary response remains trivial and *penetrates* into a range of parameters where the stationary trivial response is unstable. Then, the response *jumps up* and *oscillates* about the stationary response curve, and then *converges* to the stationary response. These characteristics vary with sweep rate in a complex manner, although we can identify trends in the variation. In addition to the sweep rate, initial conditions or noise in the system can greatly affect the response to nonstationary excitation.

For some sweeps, there are response behaviors analogous to symmetry-breaking bifurcations, period-doubling bifurcations, and chaos in the responses to nonstationary excitation found from the analog computer simulations and the digital computer simulations of the original governing equation. There is evidence that these bifurcations involve a structure similar to that of the basic nonstationary characteristics. For instance, the symmetric nonstationary response penetrates into the range of parameters where the stationary response

is asymmetric. The degree of asymmetry then changes in a way that suggests jump up, oscillation and convergence.

Future work in deterministic nonstationary excitations must proceed in two directions. First, different types and combinations of nonstationary variations need to be examined. Rather than the linear variations of excitation amplitude and frequency considered here, sinusoid variations might be considered, or the excitation amplitude and frequency could be varied at the same time. Secondly, the responses of different and more complex systems to nonstationary excitation must be considered. This will allow study of the interaction between nonstationary excitation and many dynamic behaviors.

References

Agrawal, B. J., and Evan-Iwanowski, R. M., 1973, "Resonances in Nonstationary, Nonlinear, Multidegree-of-Freedom Systems," *AAIA Journal*, Vol. 11, pp. 907-912.

Arya, J. C., Bojadziev, G. N., and Farooqui, A. S., 1975, "Response of a Nonlinear Vibrator Under the Influence of a Time-Dependent External Force," *IEEE Transactions on Automatic Control*, Vol. 20, pp. 232-234.

Baker, J. G., 1939, "Mathematical-Machine Determination of the Vibration of Accelerated Unbalanced Rotor," *Journal of Applied Mechanics*, Vol. 61, pp. A145-A150.

Collinge, I. R., and Ockendon, J. R., 1979, "Transition Through Resonance of a Duffing Oscillator," *SIAM Journal of Applied Mathematics*, Vol. 37, pp. 350-357.

Davies, H. G., and Nandall, D., 1990, "The Response of a van der Pol Oscillator to a Modulated Amplitude Sinusoidal Input," *Journal of Sound and Vibration*, Vol. 140, pp. 499-512.

Evan-Iwanowski, R. M., 1969, "Nonstationary Vibrations of Mechanical Systems," *Applied Mechanics Review*, Vol. 22, pp. 213-219.

Hok, G., 1948, "Response of Linear Resonant Systems to Excitation of a Frequency Varying Linearly with Time," *Journal of Applied Physics*, Vol. 19, pp. 242-250.

Howitt, F., 1961, "Accelerating a Rotor through a Critical Speed," *The Engineer*, Vol. 212, pp. 691-692.

Ishida, Y., Ikeda, T., and Yamamoto, T., 1987, "Transient Vibration of a Rotating Shaft with Nonlinear Spring Characteristics during Acceleration through a Major Critical Speed," *JSME International Journal*, Vol. 30, Series III, pp. 458-466.

Ishida, Y., Ikeda, T., Yamamoto, T., and Murakami, S., 1989, "Nonstationary Vibration of a Rotating Shaft with Nonlinear Spring Characteristics During Acceleration Through a Critical Speed," *JSME Internationarl Journal*, Vol. 32, Series III, pp. 575-584.

Kevorkian, J., 1971, "Passage through Resonance for a One-Dimensional Oscillator with Slowly Varying Frequency," *SIAM Journal of Applied Mathematics*, Vol. 20, pp. 364-373.

Lewis, F. M., 1932, "Vibration During Acceleration Through a Critical Speed," *Transactions of the ASME*, Vol. 54, pp. 253-261.

McCann, Jr., G. D., and Bennett, R. R., 1949, "Vibration of Multifrequency Systems During Acceleration Through Critical Speeds," *Transactions of the ASME*, Vol. 71, pp. 375-382.

Moslehy, F. A., and Evan-Iwanowski, R. M., 1991, "The Effects of Non-stationary Processes on Chaotic and Regular Responses of the Duffing Oscillator," *International Journal of Non-linear Mechanics*, Vol. 26, pp. 61-71.

Nayfeh, A. H., 1973, *Perturbation Techniques*, Wiley-Interscience, New York.

Nayfeh, A. H., 1981, *Interduction to Perturbation Techniques*, Wiley-Interscience, New York.

Nayfeh, A. H., and Asfar, K. R., 1988, "Non-stationary Parametric Oscillations," *Journal of Sound and Vibration*, Vol. 124, pp. 529-537.

Nayfeh, A. H. and Mook, D. T., 1979, *Nonlinear Oscillations*, Wiley-Interscience, New York.

Neal, H. L. and Nayfeh, A. H., 1990, "Response of a Single-Degree-of-Freedom System to a Non-stationary Principal Parametric Excitation," *International Journal of Non-linear Mechanics*, Vol. 25, pp. 275-284.

Qazi, A. S., and McFarlane, A. G. J., 1967, "The Controlled Transition of a Rotating Shaft Through its Critical Speed," *International Journal of Control*, Vol. 6, pp. 301-315.

Sanchez, N. E., and Nayfeh, A. H., 1990, "Prediction of Bifurcations in a Parametrically Excited Duffing Oscillator," *International Journal of Non-Linear Mechanics*, Vol. 25, pp.163-176.

Zavodney, L. D., and Nayfeh, A. H., 1989, "The Non-linear Response of a Slender Beam Carrying a Lumped Mass to a Principal Parametric Excitation: Theory and Experiment," *International Journal of Non-Linear Mechanics*, Vol. 24, pp. 105-125.

APPENDIX

Finding Initial Conditions on a Solution

In order to use the Floquet stability analysis, we first need a way to compute the solution to the equation we are considering. We could use the solution found from the method of multiple scales. But since we will be using computer integration in the Floquet analysis, we also will use computer integration to find the solution.

To do so, however, we must find initial conditions that place us on the solution that we wish to consider. We employ the following method to find such initial conditions.

We wish to find initial conditions $u_1(0) = \eta$ and $u_2(0) = \gamma$ such that the solution of the governing equations is periodic. We define the function $\theta_i(\eta,\gamma,t)$ to be the computed value of $u_i(t)$ after we have integrated the system of differential equations with those initial conditions. If the choice of η and γ is on a periodic solution, then after one period τ of the response, the system will

be back at its starting point; that is

$$\theta_1(\eta,\gamma,\tau)=\eta \qquad \theta_2(\eta,\gamma,\tau)=\gamma \tag{A.1}$$

This will not in general be true, because we must make a guess for η and γ. So we use a Newton-Raphson technique to refine our guess for η and γ. Assume that

$$\eta=\eta_0+\eta_1 \qquad \gamma=\gamma_0+\gamma_1 \tag{A.2}$$

where η_0 and γ_0 are the guesses for η and γ, and η_1 and γ_1 are the corrections to the guesses. Combining (A.1) and (A.2) we get

$$\begin{aligned}\theta_1(\eta_0+\eta_1,\gamma_0+\gamma_1,\tau)-\eta_0-\eta_1=0 \\ \theta_2(\eta_0+\eta_1,\gamma_0+\gamma_1,\tau)-\gamma_0-\gamma_1=0\end{aligned} \tag{A.3}$$

We expand θ_1 and θ_2 using Taylor series and rearrange to get

$$\begin{bmatrix} \frac{\partial\theta_1}{\partial\eta}-1 & \frac{\partial\theta_1}{\partial\gamma} \\ \frac{\partial\theta_2}{\partial\eta} & \frac{\partial\theta_2}{\partial\gamma}-1 \end{bmatrix} \begin{bmatrix}\eta_1 \\ \gamma_1\end{bmatrix} = \begin{bmatrix}\eta_0-\theta_1 \\ \gamma_0-\theta_2\end{bmatrix} \tag{A.4}$$

Once we have the left side matrix in (A.4), we can solve for the corrections γ_1 and γ_1. Using these corrections, we obtain a new guess. The process can be continued until an acceptable tolerance is met. We note that this process is very dependent on the original guess. We must use much trial and error just to find a guess that is close enough to the solution so that the method will work.

In order to solve for the matrix in (A.4), we use the equations (2.66)

derived in our application of the Floquet analysis. Replacing u_i with θ_i and differentiating the result with respect to η and γ, we get

$$\frac{\partial}{\partial t}\left[\frac{\partial \theta_1}{\partial \eta}\right] = \frac{\partial \theta_2}{\partial \eta}$$

$$\frac{\partial}{\partial t}\left[\frac{\partial \theta_1}{\partial \gamma}\right] = \frac{\partial \theta_2}{\partial \gamma}$$

$$\frac{\partial}{\partial t}\left[\frac{\partial \theta_2}{\partial \eta}\right] = -\frac{\partial \theta_1}{\partial \eta} - 2\epsilon\mu\frac{\partial \theta_2}{\partial \eta} + 3\epsilon\alpha\theta_1^2\frac{\partial \theta_1}{\partial \eta} + \epsilon f\cos\phi t\frac{\partial \theta_1}{\partial \eta} \tag{A.5}$$

$$\frac{\partial}{\partial t}\left[\frac{\partial \theta_2}{\partial \gamma}\right] = -\frac{\partial \theta_1}{\partial \gamma} - 2\epsilon\mu\frac{\partial \theta_2}{\partial \gamma} + 3\epsilon\alpha\theta_1^2\frac{\partial \theta_1}{\partial \gamma} + \epsilon f\cos\phi t\frac{\partial \theta_1}{\partial \gamma}$$

We also differentiate (A.1) with respect to η and γ to get the initial conditions

$$\begin{aligned} &\frac{\partial \theta_1}{\partial \eta}(\eta,\gamma,0)=1 \qquad \frac{\partial \theta_1}{\partial \gamma}(\eta,\gamma,0)=0 \\ &\frac{\partial \theta_2}{\partial \eta}(\eta,\gamma,0)=0 \qquad \frac{\partial \theta_2}{\partial \gamma}(\eta,\gamma,0)=1 \end{aligned} \tag{A.6}$$

So now we have a set of six equations (2.66) and (A.5) that we integrate to find the response of the system and to compute the correction to our guess for initial conditions.

There is a nice side benefit to this method. Note that equations (2.67) and their initial conditions are the same as (A.5) and their initial conditions. Therefore, in finding initial conditions for a stationary solution, we have also performed the calculations to compute the monodromy matrix.

Vita

The author was born in Clifton Forge, Virginia on September 21, 1966. He lived in Rainelle, West Virginia until entering Virginia Tech in September 1984. He graduated Summa Cum Laude with a Bachelor of Science in Engineering Science and Mechanics in May 1988, and received his Master of Science in Engineering Mechanics in December 1992. He is continuing his education at Virginia Tech in pursuit of a Ph.D.

Harold Lewis Neal, Jr.